The Palmitoyltransferase hZDHHC3 as a Lipid Raft Associated Protein in its Cell Physiological Context

Von der naturwissenschaftlichen Fakultät
der Gottfried Wilhelm Leibniz Universität Hannover
zur Erlangung des Grades
Doktors der Naturwissenschaften
Dr. rer. nat.
genehmigte Dissertation
von

Dipl. Biol. Arndt Rohwedder
geboren am 25.03.1969 in Bremen

2009

Referent/in: Prof. Dr. H.Y. Naim
Korreferent/in: Prof. Dr. G. Bicker
Tag der Promotion: 30. Juni 2009

The Palmitoyltransferase hZDHHC3 as a Lipid Raft Associated Protein in its Cell Physiological Context

Von der naturwissenschaftlichen Fakultät
der Gottfried Wilhelm Leibniz Universität Hannover
zur Erlangung des Grades
Doktors der Naturwissenschaften
Dr. rer. nat.
genehmigte Dissertation
von
Dipl. Biol. Arndt Rohwedder
geboren am 25.03.1969 in Bremen
2009

Für Uwe Glockenthör

Contents

Zusammenfassung

Detergent resistente Membranen (DRMs) sind Membranbereiche die durch ihre einzigartige Zusammensetzung unlöslicher Lipide definiert sind. Diese Bereiche sind ungleichmäßig lateral und horizontal über Biomembranen verteilt. Hoch geordnete, oft auch als Lipid Raft bezeichnete, Regionen in Membranen sind reich an Cholesterol und Phospholipiden mit gesättigten Fettsäure Seitenketten (Simons and Ikonen, 1997). Die Assoziation mit diesen Regionen erfordert vielfach eine posttranslationale Modifikation der betreffenden Proteine. Eine Form dieser Modifikation ist die kovalente Bindung von Palmitinsäure an ein Cystein mit hilfe einer Protein Acyl Transferase (PAT) (Pechlivanis and Kuhlmann, 2006). Typischerweise teilen solche Transmembranproteine das zinkbindende DHHC Motiv und werden daher als ZDHHC Proteine bezeichnet.

In der vorliegenden Arbeit wird die Identifizierung einer in Caco-2 Zellen hoch exprimierten intestinalen PAT (iPAT) beschrieben, die über ein ZDHHC Motiv verfügt und an der Regulation der intrazellulären Fettsäurezusammensetzung sowie den damit verbundenen Signalwegen beteiligt ist. Die Verwendung stabil exprimierter siRNA gegen die bisher nicht charakterisierte iPAT (ZDHHC3) in einer Caco-2 Zelllinie ermöglichte einen Einblick in ein verwobenes System von DRM Intigrität und Fettsäure Gleichgewicht, notwendig für die Signaltransduktion und Nahrungsaufnahme.

Aus den Daten kann geschlossen werden, daß die Regulation der intrazellulär verfügbaren Fettsäuren, insbesondere der Palmitinsäure, ein schlagkräftiges Instrument für die Feineinstellung in der Kontrolle der intestinalen Barriere sowohl unter normalen Bedingungen, wie auch in der Krankheit darstellt.

Schlagwörter: Palmitoylierung, ZDHHC3, iPAT, Lipid Raft, Detergent resistente Membranen

Abstract

Detergent resistant membranes (DRMs) are membrane regions defined by a unique composition of insoluble lipids. These regions are inequally distributed over biomembranes both laterally and horizontally. Theses ordered regions within membranes are rich in cholesterol and phospholipids with saturated fatty acid chains and are often termed as lipid rafts (Simons and Ikonen, 1997). Association with those regions in many cases require a posttranslational modification of regarding proteins. One class of those modifications is the covalent binding of palmitoic acid to a cysteine residue by protein acyl transferases (PATs) (Pechlivanis and Kuhlmann, 2006). Typically those transmembrane proteins feature a common zink binding DHHC motif and are generally designated as ZDHHC proteins.

In this thesis a highly expressed intestinal PAT (iPAT) owing a ZDHHC motif in Caco-2 cells with the ability to regulate intracellular fatty acid composition and connected signalling pathways was identified. The usage of a stable expressing siRNA against the formerly not characterized iPAT (ZDHHC3) Caco-2 cell line provided insight to an interconnected system of DRM integrity and fatty acid maintenance for signal transduction and nutritional uptake.

It is concluded that the regulation of the intracellular fatty acid availabilty, in particular palmitate, is a powerful cellular fine tuning instrument for controlling the intestinal barrier in health and disease.

Keywords: Palmitoylation, ZDHHC3, iPAT, lipid raft, detergent resistant membrane

1.Introduction

1.1 Structure of Lipid Rafts

Detergent resistant membranes (DRMs) or lipid rafts are membrane regions defined by a unique composition of insoluble lipids. These regions are inequally distributed over biomembranes both laterally and horizontally (fig. 1). Lipids in this regions reveal a high ordered structure within cellular membranes and are rich in cholesterol and other lipids with saturated fatty acid chains. Often sphingolipids, phosphatdylinositols and glycolipids can be found enriched within those DRMs (Simons and Ikonen, 1997). Size and compostion of these structures vary depending on cell type (Schuck et al., 2003), nutrition conditions (Peretti et al., 2005) and differentiation stage of the cell as reported in the formation of myelin (Fitzner et al., 2006).

Even the mentioned lipids exist in numerous variations. Sphingolipids for example provide hundreds of different types sharing only the spingosine backbone structure (Merrill et al., 2008). Phosphatidylinositol and its oligophosphorylated derivates are frequently found parts of the intracellular messenging system (Jones et al., 1979). Glycolipids are early found determinants of the blood groups (Koscielak, 1963).
The properties of the lipids strongly depend on the associated fatty acids. Long chained saturated fatty acids like palmitate tend to allocate proteins to structures that are highly hydrophobic and tend to concentrate together with cholesterol. This structural aggregation finally leads to the function of the lipid rafts/DRMs, when proteins take part (Sengupta et al., 2007).

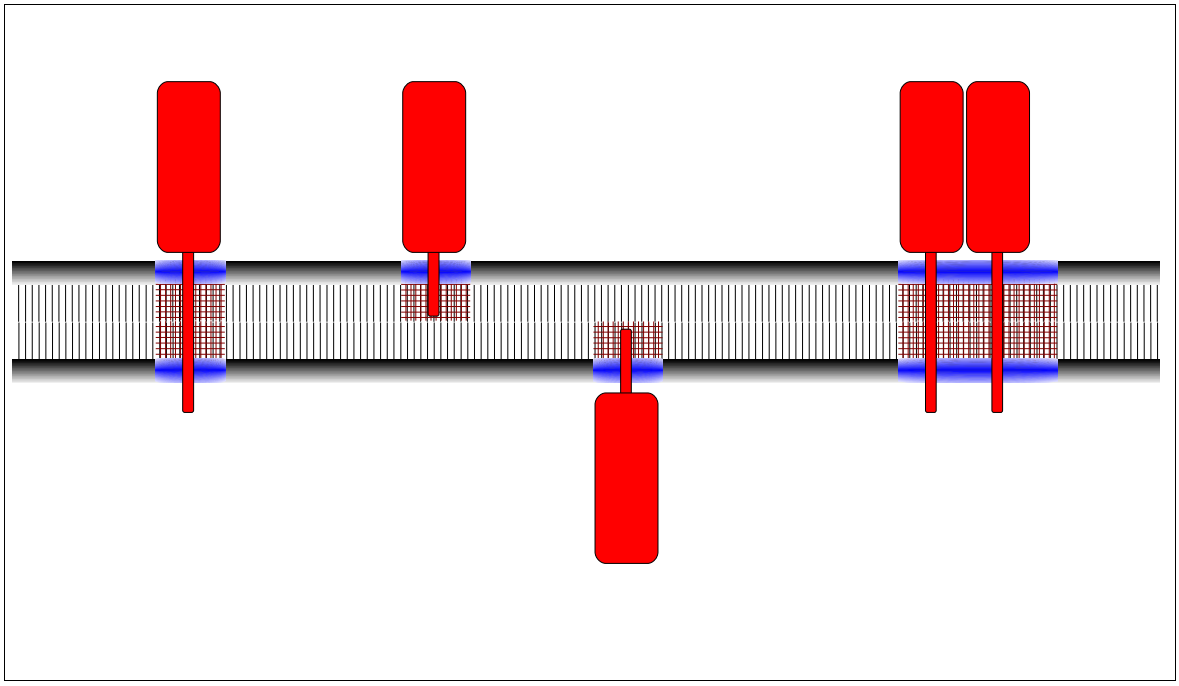

Figure 1: Detergent resistant membrane (DRM). Cartoon of different type of lipid rafts (DRMs) and protein association. From the left: DRM associated protein crossing both layers of the membrane; Unilayer DRM with a associated towards outside of the cell; the same as before with an inside orientation; aggregation of DRM associated proteins.

Whether there is a general kind of lipid raft or a definition relying on the used type of detergent has to be made still is a matter of discussion. Considering the different characteristics like ionic or neutral detergents, a general valid definition of DRMs for all kind of detergents is improbable (Seddon et al., 2004). An unique composition of lipids soluble by a certain detergent already has been characterized (Alfalah et al., 2005).

1.2 Applying FRET

The tendency to accumulate certain types of proteins and lipids turns those structures to excellent platforms for the interaction of proteins (Bromley et al., 2001). Beside the opportunity to use specific detergents to isolate DRMs biochemically/biophysically the high proximity of the proteins offers the alternative to apply the fluorescence resonance energy transfer between tagged transfected proteins (fig. 2).

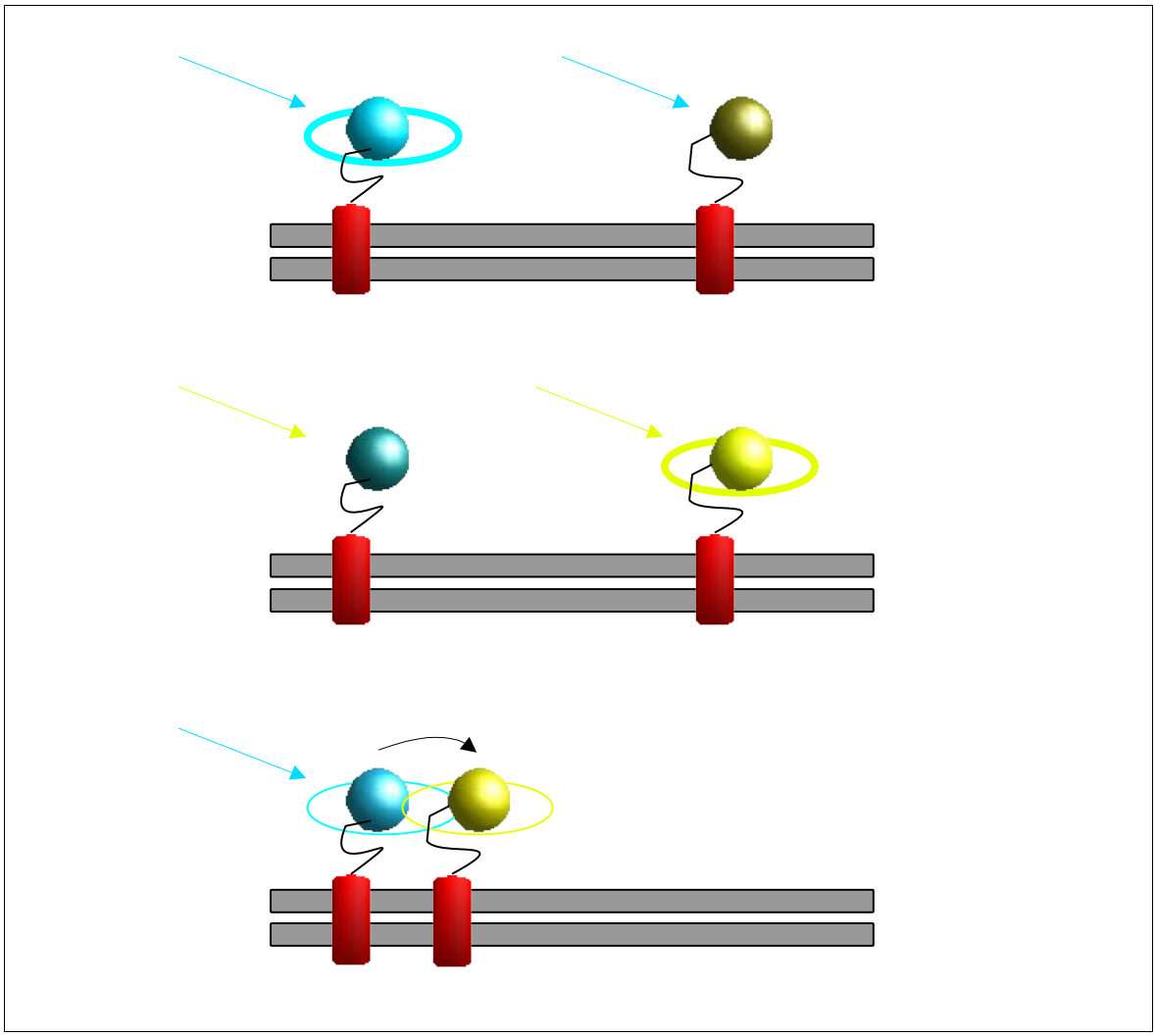

Figure 2: Fluorescence Resonance Energy Transfer (FRET): This technique is based on the phenomenon, that energy from on fluorescent protein (e.g. CFP) can be transmitted to another fluorescent protein (e.g. YFP).
It is possible to exploit this phenomenon for protein interaction studies as presented in the cartoon on the right. The upper two images show the reaction of non-interacting proteins when exited with a wavelength specific for one of both (coded by colour): only the specific fluorescent protein will emit light. When fluorescent tagged proteins are interacting energy can be transmitted from one partner to the other after excitation with the lower wavelength (lower image). This results in an emission of both partners in their specific wavelength, which can be measured and used for protein interaction studies.

1.3 Function of Lipid Rafts

A number of cellular processes correlate with DRMs and depend on the correct localization within those membrane regions. DRMs have been shown to be platforms for intracellular transport. The human intestinal sucrase-isomaltase in epithelial cells depends in its transport on the association with DRMs (Alfalah et al., 1999), turning this protein into an excellent marker for lipid rafts. Proteins of the intracellular transportation system, like caveolin are subject of regulation by DRMs themselves. The caveolin trafficking is strongly regulated by the composition of regarding microdomains as cholesterol depletion experiments recently were able to demonstrate (Pol et al., 2005).

Signalling events underlie the same restrictions like FRET. The regulation of the activity of PI3K-Akt signalling takes place at those platforms (Arcaro et al., 2006) to provide the necessary proximity of the participants delivering also the phosphoinositol. Again aggregative effects are the key for the functional assembly of the phagocyte NADPH oxidase which also depends on intact DRMs (Vilhardt and van Deurs, 2004).

Often posttranslational modifications of proteins are necessary to associate them with lipid rafts. A well studied modification of this kind is an attachement of a glycosyl phosphatidylinositol (GPI) anchor to proteins in polarized cells for apical transport (Hooper and Bashir, 1991; Polishchuk et al., 2004; Delacour et al., 2006).

1.4 Lipid Anchors

Other modifications are covalent but reversible attachments of fatty acid residues like myristolate, farnesylate or palmitate (see fig. 3). Myristoylation occurs during the translation process and causes a nonselective membrane association of the protein, not depending on certain membranous structures like DRMs (Basu, 2004). It could be observed, that the binding of ARFs to their inhibitor arfaptin is influenced by the myristoylation state of the ARFs (Tsai et al., 1998). For preferred DRM association other acylation events have to take place. Prenylation is a posttranslational process that often promotes further modification like palmitoylation, a modification that clearly promotes association to DRMs. Proteins of the Ras and Rab family are often subjected to this kind of modification which is necessary for the efficient function by placement of those proteins (Pechlivanis and Kuhlmann, 2006).

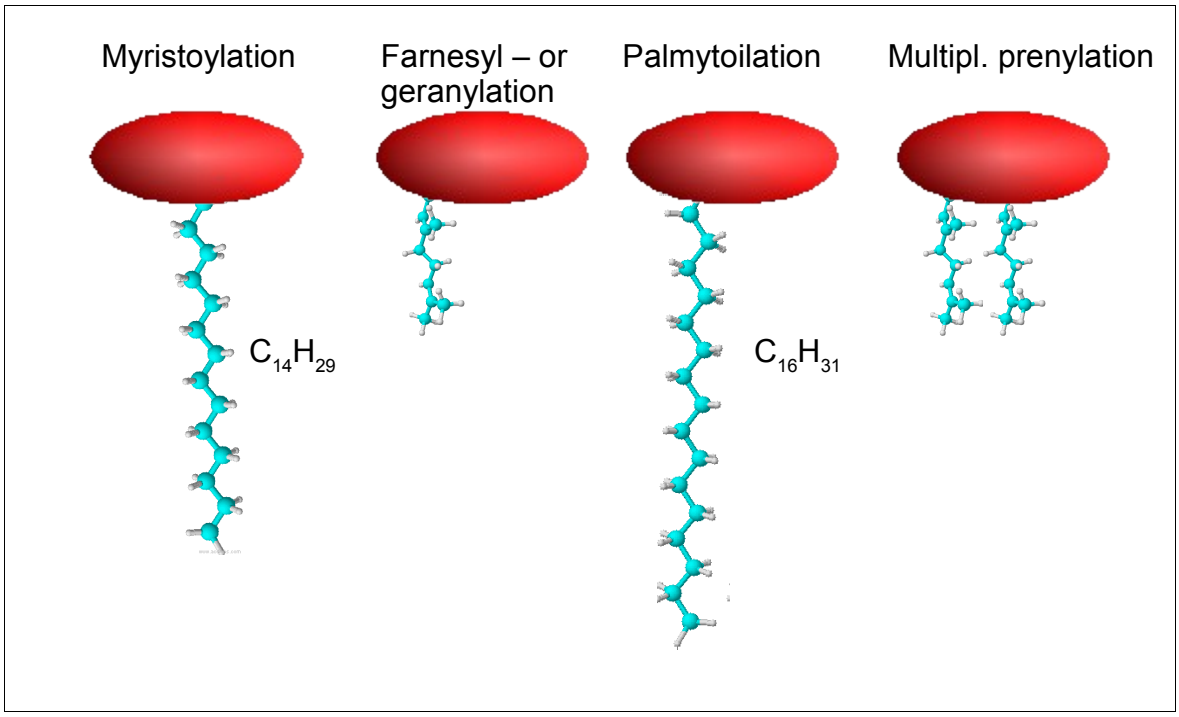

Figure 3: Types of lipid modifications. From the left: Myristoylation provides 14 saturated carbon residues, Farnesyl- or geranylation provides a number of unsaturated carbon residues, Palmytoilation contains 16 saturated carbon residues, example for multiple prenylation.

For palmitoylation a differentiation between serine and cysteine acylation has to be done. Since palmitate is the final step in the fatty acid synthesis by the fatty acid synthase complex (FAS) it is the starting point for a number of synthesis steps (Zakim & Herman, 1969). Serine palmitoylation characterizes the first step in the biogenesis of sphingolipids and takes place in the ER. Using the same substrates like cysteine palmitoyltransferases, palmitoyl-CoA, serine palmitoyltransferases (SPTs) are involved in the condensation of L-serine and palmitoyl-CoA to 3-ketodihydrosphingosine (KDS) (Yard et al., 2007). Deficiencies in the activity or expression of SPTs can be brought into context with neuronal defects like hereditary sensory neuropathy type I (HSN1). A complete loss of SPTs is considered to be embryonic lethal (Hanada, 2003).

Palmitoylation of cysteine residues of proteins is a postranslational modification that enables the recruitment of cytosolic proteins to ordered structure membranes or lipid rafts. These events may take place spontaneously *in vitro* or *in vivo* under the control of palmitoyltransferase, which transfers a palmitoic acid (C16:0) group using an acyl-CoA-palmitate substrate via a thioester binding to cysteins of certain proteins. Spontaneous palmitoylation only could be observed in *in vitro* experiments and the affected cysteine residues are the same like *in vivo* (Basu, 2004). Due to a pKa of 8.5 cysteine it is unlikely that a spontaneous palmitoylation emerges in isolated cysteines. An environment of a much lower pH is necessary to induce palmitoylation. Observed *in vivo* autoacylation events may be possible due to pH reducing compartments of the regarding proteins or or other non-proteineous constitutents (Dietrich and Ungermann, 2004).

In the yeast it has been demonstrated that palmitoylation at the cysteine residues of the CHS-3 protein is necessary for the ER-export pointing thus to a role of palmitoylation in the quality control in the ER (Lam et al., 2006). Palmitoylation modifications can take place in the Golgi or ER compartment. This highly hydrophobic attachment permits an association with highly ordered cholesterol rich membrane regions often associated with cell recognition elements like glycolipids or -proteins and receptors (Fischer et al., 2006, Liang et al., 2007, Palmer et al.

2007). It is known that the spike glycoprotein of the SARS coronavirus binds to raft domains in the cellular membrane after being palmitoylated. This palmitoylation enhances the cell fusion of the virus (Petit et al., 2006).

The effect of palmitoylation on cellular processes can not be always assigned to the effector directly but operate through a mediator protein. The intestinal sodium-dependent glucose transporter is positively controlled by HSP70 (Ikari et al., 2002), that binds to the cysteine-string protein isoform beta (Cspβ), a membrane bound protein existing in a palmitoylated and nonpalmitoylated form. The non palmitoylated form is mainly found in the trans Golgi presenting the palmitoylation as a tool for plasma membrane recruitment of HSP70 (Boal et al., 2007).

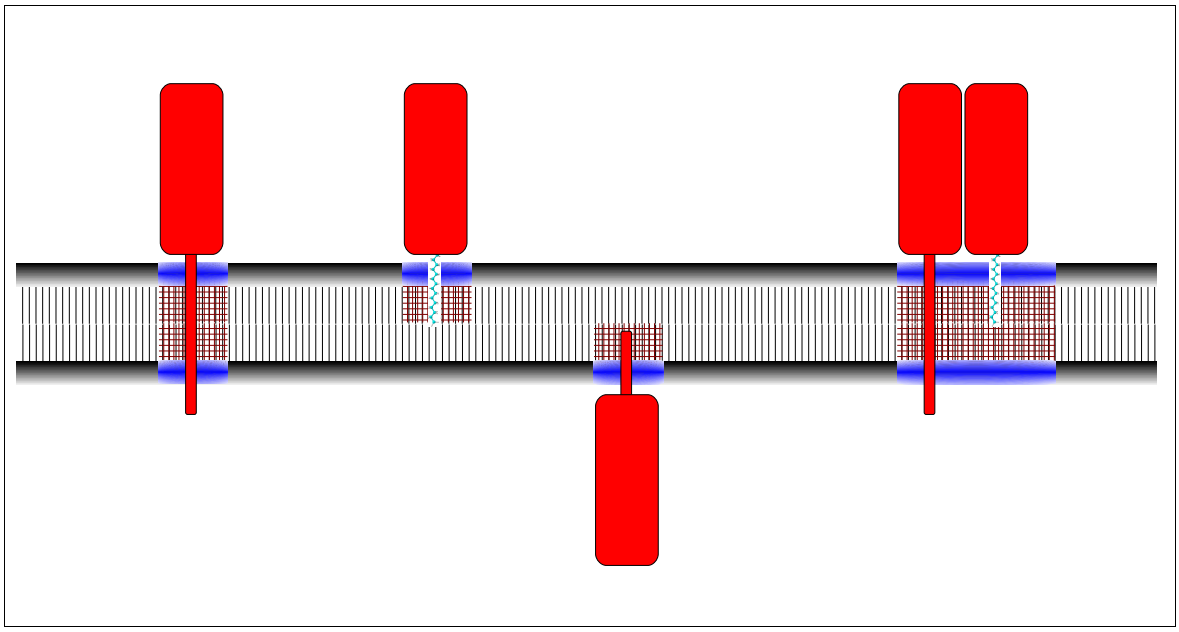

Figure 4: Palmitoylation dependent DRM association. The figure resembles figure 1 with the difference that palmitoylation fullfills the anchorage of the protein in the DRM.

Increasing evidence suggests a potential role of palmitoylation is involved in protein sorting (Greaves and Chamberlain, 2007). This feature of the above kind of acylation especially affects highly polarized cells. Neuronal dysfunctions could be observed in cases of a loss of function of cysteine palmitoyltransferases. It could be shown that a genetic X-linked defect in the human palmitoyltransferase ZDHHC9 is responsible for a familiar marfanoid mental retardation phenotype (Raymond et al., 2007).

An important class of polarized cells often associated with health and disease are the intestinal cells. Apically exposed to the intestinal microflora those cells are frequent targets of pathogens. As a consequence the integrity of apical membranes are necessary for healthy intestinal conditions. Recent studies have shown an attenuating effect of applied poly unsaturated fatty acids (PUFAs) like docohexanoic acid in induced colitis, which is characterized by an disintegration of the intestinal brush border (Li et al., 2008). This points to a crucial impact of the fatty acid metabolism in the regulation of the brush border barrier function.

Using Caco-2 cells as a valid model for intestinal brush border cells (Vincent et al. 1985) we present a mechanism in which the loss of storage for saturated fatty acids, the palmitoyltransferase iPAT, causes an increase of PUFAs in the membrane of Caco-2 cells. A possible explanation may be the limited resources of palmitoyl-CoA in the cell and its utilization by palmitoyltransferases as exemplified by the human palmitoyltransferase iPAT highly expressed in Caco-2 cells.

2.Material and Methods

All solutions, buffers and plasticware used for cell culture were autoclaved (121°C, 1 bar, 20 min) before usage. Glasware was sterilized (250°C, 1h). Reagents were at least of p.a. quality.

2.1 RT-PCR

For mRNA extraction the Rneasy kit from Qiagen has been used following the distributers protocols. RT-PCR was performed with the RevertAid® First Strand RT-PCR Kit from Fermentas as described in the protocol from the distributor using following primers:

hZDHHC3:	5'-GCGAGATCTAAAATGATGCTTATCCCCACC-3'
	5'-CGCGTCGACTTTTCAGACCACATACTGGTA-3',
hgage1:	5'-GCGCTCGAGAAAATGAGTTGGCGAGGAAGA-3'
	5'-CGCAAGCTTTTTTCAAGGTTTCCGTGGGGA-3'
hmyl6:	5'-GCGCTCGAGAAAATGTGTGACTTCACCGAA-3'
	5'-CGCAAGCTTTTTTCAGCCATTCAGCACCAT-3'
hsyt3:	5'-GCGCTCGAGAAAATGTCAGGAGACTACGAG-3'
	5'-CGCAAGCTTTTTTCACTCGGAGTTCTCTTT-3'
hsytl4:	5'-GCGCCGCGGAAAATGTCGGAGTTACTGGAC-3'
	5'-CGCGGGCCCTTTTCATAAACCCAGCTTCTG-3'
htppc:	5'-GCGAGATCTAAATGTCTGGAAGCTTCTAT-3'
	5'-CGCGTCGACTTTTCAGCTTAAAAGGTGTTT-3'
beta - actin:	5'-GGACTTCGAGCAAGAGATGG-3'
	5'-AGCACTGTGTTGGCGTACAG-3'

Ligation in pECFP-C1 vector was performed as described before. In brief: cut out cDNA and closed pECFP-C1 vector DNA were treated with BglII (MBI) and SalI (MBI) to produce sticky ends. Digested DNA was seqareted in a 0.8% Agarose gel electrophoresis, lanes were excised and DNA extracted as before. Ligation was performed using T4 – Ligase from MBI in an insert to vector ratio of 3/1 over night at 20°C. For amplification competent E.Coli gold strain was used. For siRNA design the PolII MiR RNAi Expression Vector Kit with EmGFP-Kit from Invitrogen was applied using following primers:

ZDHHC3:

5'-TGCTGTGACAAAGAGGACCACGAACTGTTTTGGCCACTGACTGACAGTTC GTGCCTCTTTGTCA-3'

5'-CCTGTGACAAAGAGGCACGAACTGTCAGTCAGTGGCCAAAACAGTTCGTG GTCCTCTTTGTCAC-3'

2.2 Microscopy techniques

Cells grown on coverslips were fixated as described before. Confokal Microskopy: Images were taken with a Leica DM IRB/E TCS SP2 confokal microscope from fluorescent tagged proteins in cotransfected COS-1 cells. For CFP-tagged proteins an excitation wavelength of 454 nm and a detection wavelength of 490 nm has been used. 3D-reconstruction was performed with the aid of the Volume Viewer plugin under ImageJ (Rasband 1997-2008, Abramoff et al., 2004).

For analysis of morphology phase contrast images were taken from a Zeiss Axiovert 25 microscope with a Canon PowerShot A640 digital camera and subsequent image analysis using ImageJ analysis tools.

2.3 Raft preparation and 2D Gelelectrophoresis

Triton – X 100, TWEEN-20 and Lubrol DRM preparation: 50 µl of PSMF were diluted in 100 µl protease inhibitor solution. 40 µl of the resulting inhibitor mix were added to 1 ml of 1% regarding detergent in PBS. 10 cm Dishes with 5 days confluent Caco-2 cells were washed twice with PBS and 1 ml TX was dispensed on the dishes. Cells were scrapped off the dishes and the resulting solution was transfered in 2 ml reaction tubes. Cells were homegenized 20 time with 0.8 mm and 15 times with a 0.45 mm cannula using a 1 ml injection. To achieve constant degree of lysis homogenates were left over night rocking at 4°C. Lysate was centrifugated for 1.5 h at 100,000 g. The resulting pellet was washed with washbuffer I and two times with washbuffer II. Pellets were dissolved with 600 µl of lysis buffer (0.5% deoxycolate, 0.5% Triton-X 100 + 40 µl PI) for at least one hour at 4°C. After 10' centrifugation protein of supernatant was quantified. Proteins were precipitated with absolute ethanol over night at -20°C, pelleted with 3000 rpm, washed once with 96% ethanol and two times with 70% ethanol. The resulting pellet was rehydrated with RH buffer depending on the protein concentration to achieve a 100 µg of protein final concentration over night at 4°C under gentle rocking. Before applying samples to isoelectic (IE) -strips pH 3-10 (IPG) 0.2 µl of ampholytes (Bio-Lyte 3/10, BioRad) were added. Isoelectric focusing was performed on Protean ® IEF Cell (BioRad) with 12 h of equilibration, followed by an gradient with 4,000 V at 20°C.

For the second dimension a 12% PAGE was accomplished after washing the strips 2 times 10' in equilibration buffer with additional 0.05 g / ml DTT followed by a washing step of equilibrium buffer with additional 0.05 g / ml iodacetamide. The proteins were visualized by silverstaining of the gel.

2.4 Growth rate, glucose uptake and transepithelial resistance

Coverage of culture dishes was estimated using a raster overlay und light microscopy every 24 hours. For 2 – bromo palmitate treatment Caco-2 cells were grown for 24 h in 10 ml DMEM High Glucose at 37°C, 5% CO_2 with 100 µM and 10 µM 2-bromo palmitate respectively. Glucose uptake measurements were performed using samples taken from cells cultured as described with 1 h time steps for eight hours. 100 µl of the sample were mixed with 24 mg p-ABS, 500 µl DMSO/ice cold acetate, 10 mg Na-CBH and incubated for 15' at 60°C. After a dilution of 1:10 in the fluid phase (10 mM $NaPO_4$ buffer pH 2.0, 20 mM $TBAHSO_4$) samples were measured in HPLC with a synergie-fusion-RP 80 column (Phenomenex). Detection was accomplished by fluorescence detection of emission wavelength of 358 nm with excitation wavelength 313 nm.
For measurements of transepithelial resistance cells were grown on transwell culture dishes (Corning Inc., Acton, MA) and after confluence for at least four days resistance was measured with a Millicell-ERS (Millipore). After each performed measurement cells were trypsinated and counted using with a hemocytometer.

2.5 Measurement of cholesterole and phospholipids and fatty acids

Lipidextraction was performed following Bligh & Dyer (A rapid method of total lipid extraction and purification. Can J Biochem Physiol. 1959 Aug;37(8):911-7). Cholersterole was applied to HPLC following Takadate, 1985. Briefly 400 µl of the sample soluted in CH_2Cl_2 was mixed with 100 µl internal standard (1,5 mg/ml 1 – eicosanol) and 7-methoxycoumarin-3-carbonylacide (MCCA) was added to a final concentration of 20 nMol. Samples were then dried at 110°C and resoluted in 50 µl CH_2Cl_2 with 200 µl methanol. 50 µl of this solution were injected on a Microsorb-MV 100-5 C18 column (Varian). For analysis of phospholipids samples were dried

at roomtemperature und N_2 gas and resoluted in 0.5 ml $CHCl_3$:Methanol (2:1 v/v). 50 µl were injected on a Lichrospher Si 100 (Merck) column and subjected to gradient of flux agent A ($CHCl_3$:Methanol:30% NH_3; 80:19.5:0.5 v/v) to flux agent B ($CHCl_3$:Methanol:H_2O:30% NH_3; 60:34:5.5:0.5 v/v) of 100% A / 0% B, 8' 45% A / 55% B, 15' 40% A / 60% B, until end 0% A / 100% B. Detection was performed with Sedex 55 light scatter detector (S.E.D.E.R.E)

Esterification of fatty acids from lipids: 15 ml reaction tubes have been precleaned with n-hexane. Samples of in chloroform dissolved lipids were dried under N_2 at room temperature. Together with the internal standard (37,3 ng/µl C17:0) samples were dissolved in 2 ml methanol and 0,5 ml n-hexane. 200 µl acetylchloride were carefully added and the samples were left for 1 hour at 100°C. After 5 minutes of cooling on ice 4 ml 6% K_2CO_3 were applied. Samples were centrifuged for 1 minute at 1500 rpm (~10000 G) and 10°C. The upper phases were transferred into a new reaction tube and evaporated until 50-60 µl were left. Those were applied to GC (Varian 3400) on a supelcowax-10 column.

2.6 Brush border preparation and western blot

Brush border preparation: Cells were washed two time in sterile PBS and homogenized in 2 ml buffer containing 2 mM tris-HCl, 50 mM mannitol 40 µl PI. $CaCl_2$ solution was added dropwise to a final concentration of 10 mM while the samples were gently stirred on ice. Another 30 minutes the samples were stirred on ice. In the first centrifugation step samples were centrifuged for 20 minutes at 2000 g, 4°C. The pellet (P1) containing basolateral and intracellular membranes was stored at 4°C until use. Supernatant was centrifugated at 25000 g for 30 minutes at 4°C. The second pellet (P2) containing the brushborder membrane was used together with P1 for westernblot. The supernatant containing the cytosol was discarded.

Immunoblotting employed polyvinylidene difluoride membranes (Millipore,

Germany) and horseradish peroxidase-conjugated secondary antibodies, which were visualized by ECL (Amersham Biosciences). Primary monoclonal antibodies were Annexin 2 (HH7), kindly provided by Prof. Dr. Gerke, Münster, SI (705) by Prof. Dr. Columbatti, Verona Flotilin-2 (B-6), Santa Cruz BT (SC, Cal.), EEA1 by ABR, Golden (Co).

2.7 Confocal Microscopy, FRET and Colocalization Analysis

Confocal microscopy: Images were taken with a Leica DM IRB/E TCS SP2 confocal microscope from fluorescent tagged proteins in cotransfected COS 1 cells. For CFP-tagged proteins an excitation wavelength of 454 nm and a detection wavelength of 490 nm and for YFP-tagged proteins an excitation wavelength of 510 nm and a detection wavelength of 535 nm has been used. Additionally images were taken 454 nm excitation wavelength and 535 nm detection wavelength for FRET analysis.

Colocalization Analysis: Colocalized pixels were superimposed using the colocalization finder plugin (C. Laummonerie, J.Mutterer, Institut de Biologie Moleculaire des Plantes, Stasbourg, France) under ImageJ (Rasband, 1997-2006, Abramoff et al., 2004). For calculation of the releative amount of colocalized pixels cotransfected cells were digitally isolated with the threshold function under ImageJ. Pixel values of colocalized versus CFP signal values were calculated and treated as areas.

FRET Analysis: Determination of FRET values was performed via the PixFRET plugin (Feige et al., 2005) under ImageJ with $\frac{FRET}{(Donor \times Acceptor)}$. Relative FRET values were obtained the same way as in the colocalization analysis with CFP as donor and YFP as acceptor. Background subtraction was performed using

exponential fitting: ax^e+b .

2.8 Electronmicroscopy

For fixation of the cells 30 minutes incubated with 1% glutaraldehyd in 100mM cacodylatbuffer. The samples were rinsed in cacodylatbuffer followed by 1.5 h of incubation with 2% OsO_4 in H_2O. Next the samples were washed twice with H_2O and over night incubated with 0.5% uranylacetate in H_2O.
The following steps were performed in Gießen at the group of Prof. H.P. Zimmer
The next day the samples were washed twice with H2O followed by a graded series of ethanol:

2 x 15 min. 50%, 70% and 90% ethanol
4 x 10 min. 100% ethanol
1 x 5 min. propylenoxide

Embedding in epon:

2 x 30 min. 1 +1 epon with propyleneoxide
2 x 60 min. pure epon

Samples were transferred to flat embedding mould or beam capsule.
Electromicrographs were taken on an electronmicroscope Philips EM 208 (Eindhoven, Niederlande) with photographs by Kodak electronmicroscope film 4489 (Rochester, New York, USA).

2.9 Glycolipidpreparation and Lectin Screening

For the isolation of glycolipids two TLC (Glass, Si-60, Phenomenex) of dried isolated lipids (see lipid extraction) were performed. The fluid phase consisted of chloroforme; methanol; aqeous 0,2% $CaCl_2$ solution (60/35/8). The process took place in a glass chamber. After drying one plate was stained with 2µg/ml orcinol in 70% H_2SO_4 and developed at 110°C. Using this template targeted glycolipids were

isolated on the other plate by carfully scrapping out previously defined areas with a scalpell. After the incubation of the fragments in chloroforme/methanol (50/50) a centrifugation separated the lipids from the solid phase. The pellet was discarded. The supernatant was dried under N_2 gas and soluted in methanol.
For lectin screening methanol dissolved samples were transferred into a methanol resistant 96-well plate and dried again. The treated plates were incubated with BSA to reduce any possible background. 15 µl of lectins in lectin buffer (300 mM NaCl, 100 µM $CaCl_2$ in 10 mM HEPES, pH 7.5) were applied to each well. After washing 3x with PBS samples were stained using streptavidine Cy-3 conjugates (Sigma), dissolved 1:250 in PBS for 1 h at room temperature. For quantification a Fluorimeter (Tecan) with 552 nm excitation and 565 nm emission was used.

2.10 Used Chemicals

Acrylamide	Rotiphorese Gel30, Roth, Karlsruhe, Deutschland
Agarose	Gibco, Eggenstein, Deutschland
Ammoniumchlorid (NH_4Cl)	Fluka, Steinheim, Schweiz
Ammoniumperoxosulfate (APS)	Merck, Darmstadt, Deutschland
Ampicilin	Sigma, Taufkirchen, Deutschland
Bacto Yeast Extract	BD Biosciences
Bacto-Tryptone	BD Biosciences
Bovine Serumalbumine (BSA)	PAA
Brij	Sigma
Chloroforme	Roth
Dithiolthreitol (DTT)	Sigma
Dimithylsulfoxide (DMSO)	Fluka
Ethanol	Roth
Ethylendiamintetraacetate (EDTA)	Roth
Ethidiumbromid	Merck

Fetal calfserum (FCS)	Gibco
Glycerole	Sigma
Glycine	Roth
Lubrol	Merck
Magnesiumchloride (Mg_2Cl)	Merck
Moviol	Molecular Probes
N,N,N',N'-Tetramethlethylendiamine (TEMED)	Roth
Nonidet P40 (NP40)	Fluka
Paraformaldhyde	Merck
Peniciline-Streptomycine	Gibco
Phenole	Roth
Tris-HCl	Roth
Sodium hydroxide (NaOH)	Merck
Di-sodiumhydrogenphosphate-dihydrate ($Na_2HPO_4x\ 2H_2O$)	Merck
sodium dodecyl sulfate (SDS)	Roth
Triton-X-100	Sigma
Tween-20	Roth

2.11 Used Enzymes

Ligase T4	MBI Fermentas
Protease inhibitors	Roche Diagnostics
1mM PMSF:	
1µg/ml pepstatine A	
1µg/ml antipain	
5µg/ml leupeptin	
5µg/ml aprotinin	
50µg/ml trypsine-chymotrypsine-inhibitor	

Restriction enzymes and buffer	MBI Fermentas
Rnase A	Roche
RNAse inhibitor	MBI Fermentas

3.Results

3.1 A set of proteins can be found in several kinds of detergent resistant membranes.

A series of 2D-gel electrophoresis images has been produced out of detergent insoluble fractions from Caco-2 cells to investigate the protein composition of four types of detergent resistant membranes (DRM), defined by their susceptibility against different detergents. The used detergents were Triton X-100, Tween-20, lubrol and brij. Triton X-100 is the typical detergent for the generation of DRMs or lipid-rafts. Tween-20 is a detergent recently (Alfalah et al., 2005) identified as capable for the isolation of early, ER/Golgi rafts. Lubrol and brij are weak detergents with not yet clearly defined specificity for membrane compartments. Although a number of proteins seemed to vary in concentration and appearance, a few spots remained comparatively stable expressed (fig. 1 A). Using free available image analysis software and software based pI and molecular mass estimation a careful internet based search using the ExPASy TagIdent tool revealed five proteins. The most promising identified protein with this method was the presumptive palmitoyltransferase ZDHHC3 or intenstinal protein acyl transferase (iPAT), a 37 KD transmembrane protein (fig. 1 A, lowest arrow).

Although this method of identification bears a comparative high risk of errors, it could be used for proteins like the iPAT. Prerequisites for the application of the *in silico* identification of spots in 2D-gels is the comparative isolated situation of the spot and the exclusion of proteins that are known to undergo secondary procession like glycosylation or extensive phosphorylation. Those kinds of intracellular secondary protein procession are known to change the protein pI and,

in many cases (especially in the case of glycosylation), the protein mass. The spot for the invariable iPAT satisfied the initial prerequisites by standing comparatively isolated and producing a strong signal. Exclusion of all proteins with a high degree known possible secondary processed domains left only one protein, the iPAT as candidate.

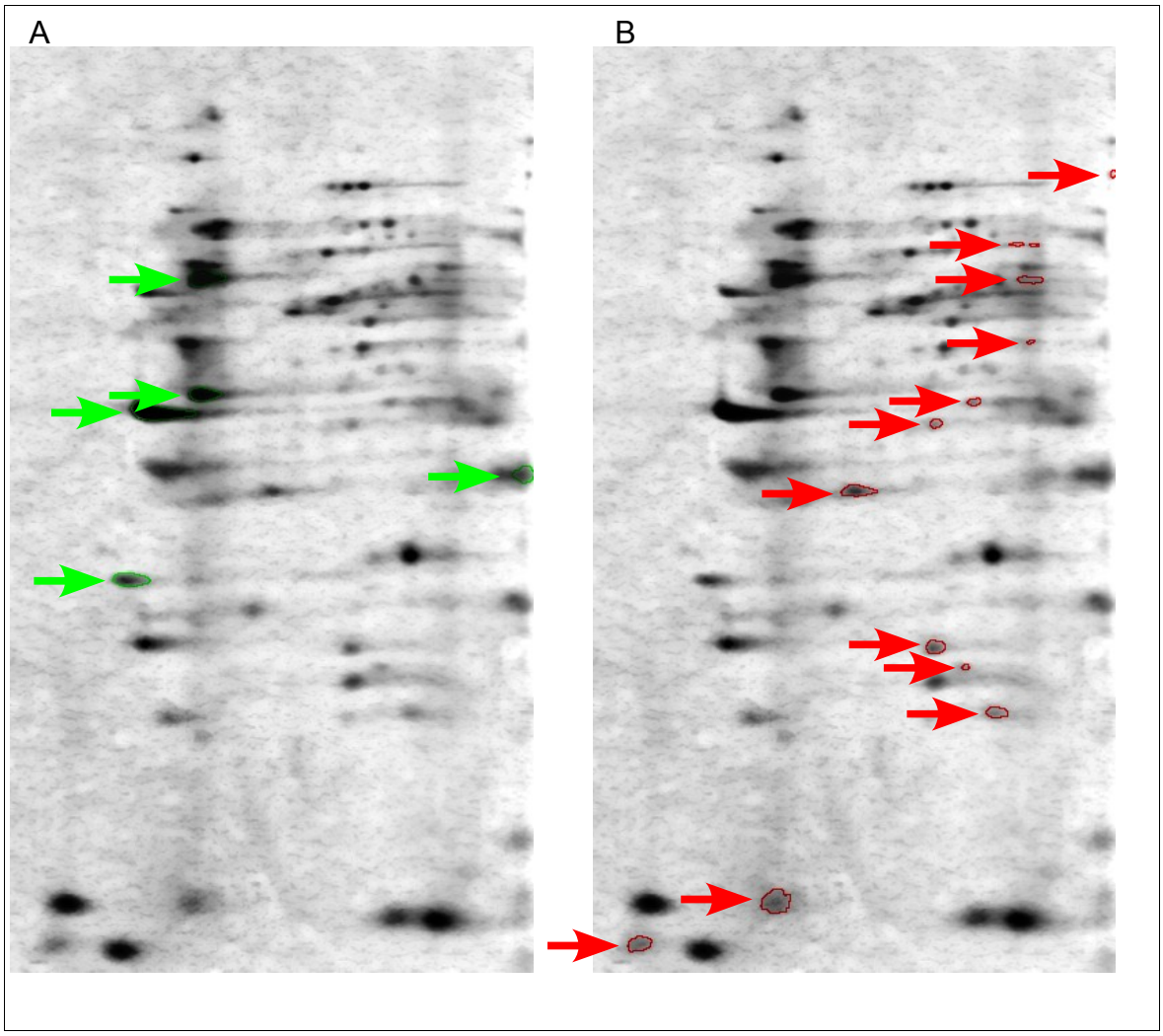

Figure 1: 2D Gel of Tween-20 DRMs. Example of a typical 2D-gel resulting from the preparation of Tween-20 derived DRMs. For better distinguish between variable and invariable spots the same image has be been used.
A: invariable or spots with a low alteration rate between different types of DRMs marked by green arrows.
B: variable or spots with a high alteration rate between different types of DRMs marked by red arrows.

3.2 iPAT is expressed in Caco-2 cells and is located in the Golgi membrane

To test the expression rate of the human palmitoyltransferase iPAT a semi-quantitative RT-PCR for a number of proteins with different expression rates has been used. Four proteins are known to work at Caco-2 cells as a positive control and two proteins that should produce no or only weak signals as a negative control were chosen. The positive control proteins have been myosin light polypeptide 6 (Myl6), a widely expressed regulatory non muscular myosin, synaptotagmin like protein 4 (SytL4), a protein associated with exocytosis, MBP-1 interacting protein 2A (TPPC) a protein supposed to take part in the vesicular transport between ER and Golgi and beta actin. The TPPC was detectable only at a faintl level while the rest presented sufficient signals (fig. 2). For negative controls the G antigene 1 (GAGE1), which only can be found in testis tissue and synaptotagmin III (Syt3), a SytL4 related protein highly expressed in the neuronal system but not in intestinal cells were used. None of the negative controls did show any signal.

The scaffold protein beta actin presented the highest level of expression. Compared to beta-actin the iPAT a high degree of expression presented (fig. 2). Quantification of the intensity revealed a comparative intensity to actin of about 72%. Considerable less intensity could be detected of Myl6 with about 30% of actin and SytL4 with 11% presented an even lower signal of the positive controls.
Since none of the used negative controls did produce any signal, providing evidence for the specificity of the RT-PCR.

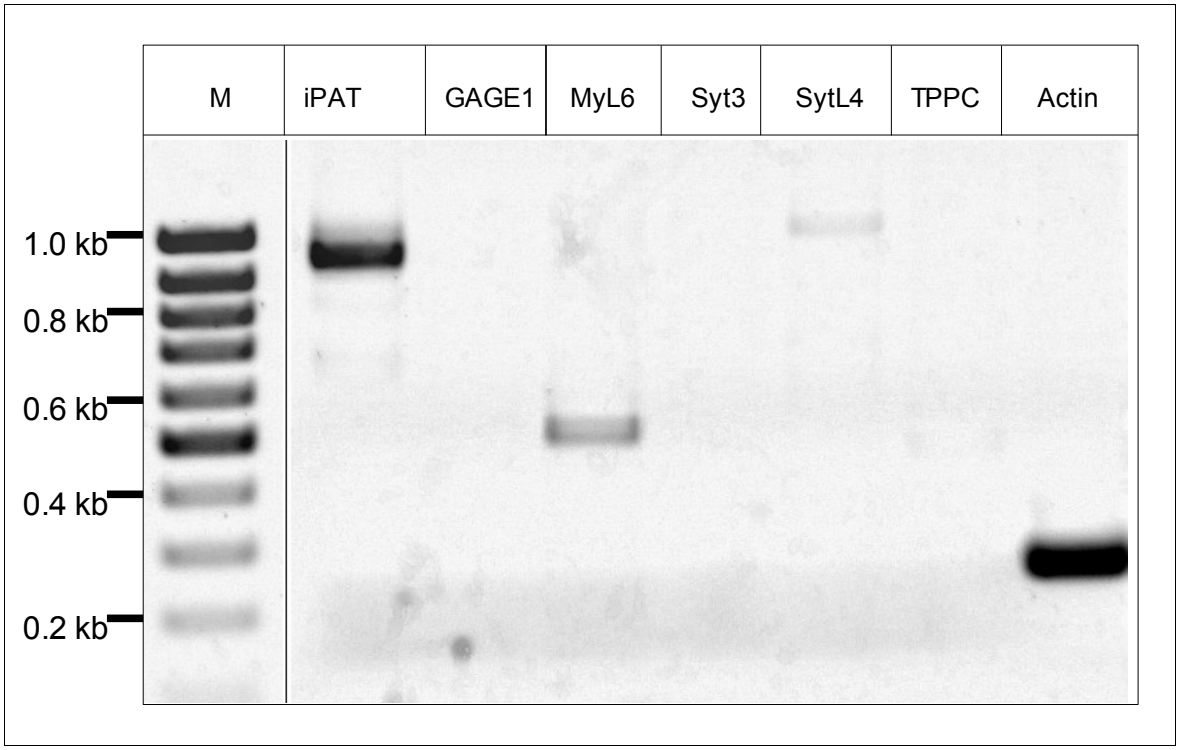

Figure 2: Agarose Gel of RT-PCR. cDNA resulting of mRNA RT-PCR was applied to a 0.8% agarose gel. Used primers were iPAT for the human palmitoyltransferase ZDHHC3, GAGE1 for the human G antigene 1, MyL6 for myosine light polypeptide 6, Syt3 for synaptotagmin III, SytL4 for synaptotagmin-like protein 4 (granuphilin a), TPPC for MBP-1 interacting protein 2A, and finally actin for a fraction of beta-actin. For detailed information about the primers see methods.

Further analysis of the iPAT sequence data allowed a presumptive view on the iPAT topology (Fig. 3). For this purpose the specialized software TMRPres2D (Spyropoulos et al., 2004) had been used, that is able to extract predicted transmembrane data out of sequence and to display resulting topology in 2D graphical representation of regarding proteins. The DHHC type zinc finger domain had been identified to be located between the amino acids 127 and 177. This resembles in the graphical representation of fig. 3 the second as extracellular characterized loop of the protein. This domain is the region hold responsible for a palmitoylation activity of proteins belonging to the ZDHHC family.
Isolated cDNA was subsequently used for cloning iPAT in a pECFP vector.

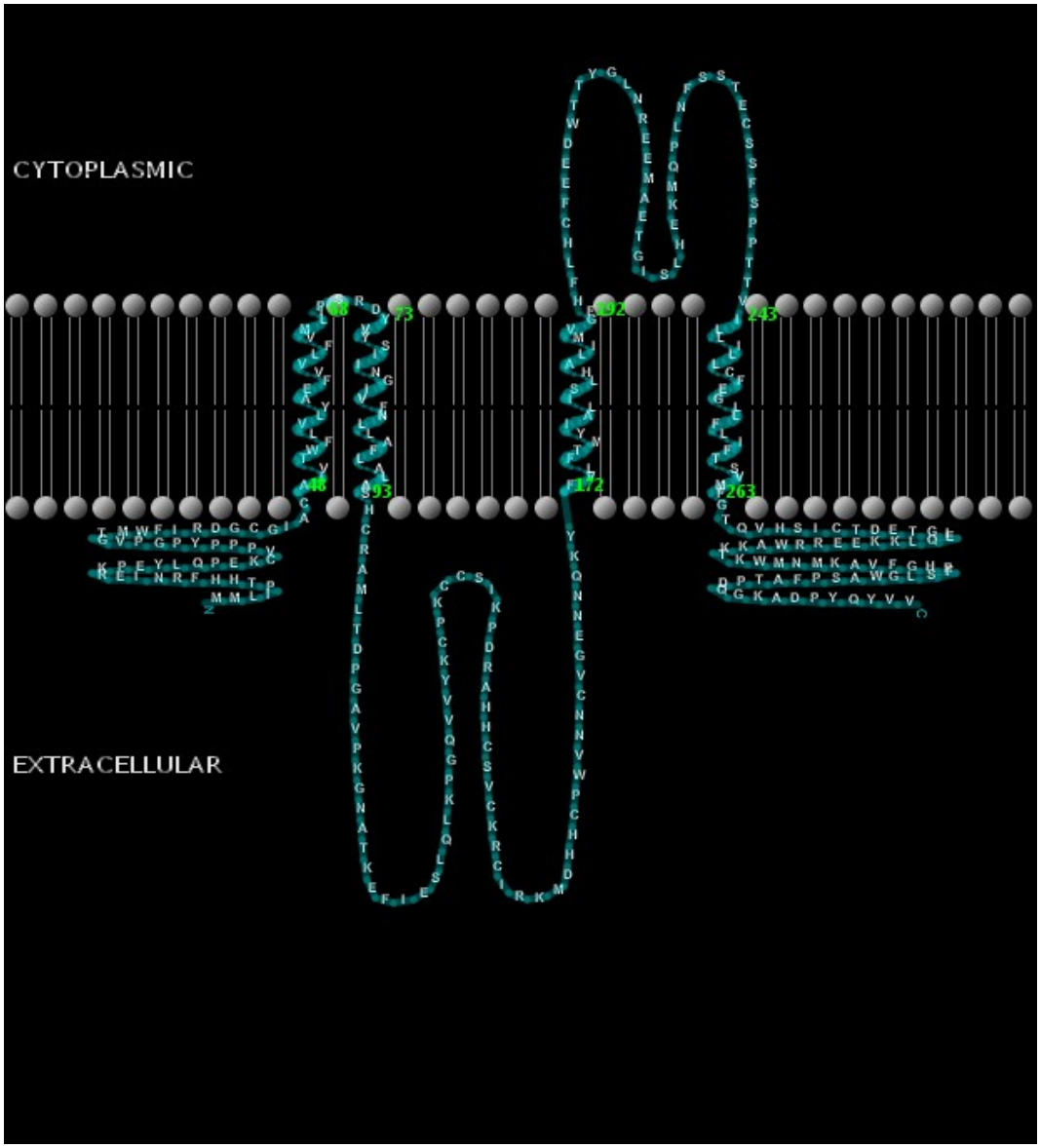

Figure 3: iPAT localization in the membrane. Cartoon image of putative membrane resident iPAT constructed out of sequence data with TMRPres2D (Spyropoulos et al., 2004).

Transfection in COS-1 cells showed a clear localization in the perinuclear region of the cells which is presumably the Golgi region (fig. 4 A and B) of the cells. This has been predicted before with the aid of sequence similarity analysis in the uniprot database system (uniprot entry: Q9NYG2) and hence the second name GODZ (Golgi apparatus – specific protein with the DHHC zinc finger domain) (Uemura et al., 2002). Additionally a vesicular association could be detected in some cases together with a compact perinuclear signal, indicating an apoptotic situation with a disintegrating Golgi apparatus (fig 4 C and D).

A BLAST search of protein sequence on NCBI with subsequent alignment (see appendix) revealed that iPAT is a highly conserved protein, found in all classes of animals. This has been visualized using a tree chart for relatedness of species (see appendix). Even distant related species are included with the identifier ZDHHC3 including isoforms of iPAT. This indicates a low degree of variability (fig. 5), which could be strengthened by the comparatively short amino acid sequence (327 aa) and the high number of membrane passages. Thus together with the pure alignment data (see appendix) the tree representation indicate a high functional dependence on the amino acid sequence.

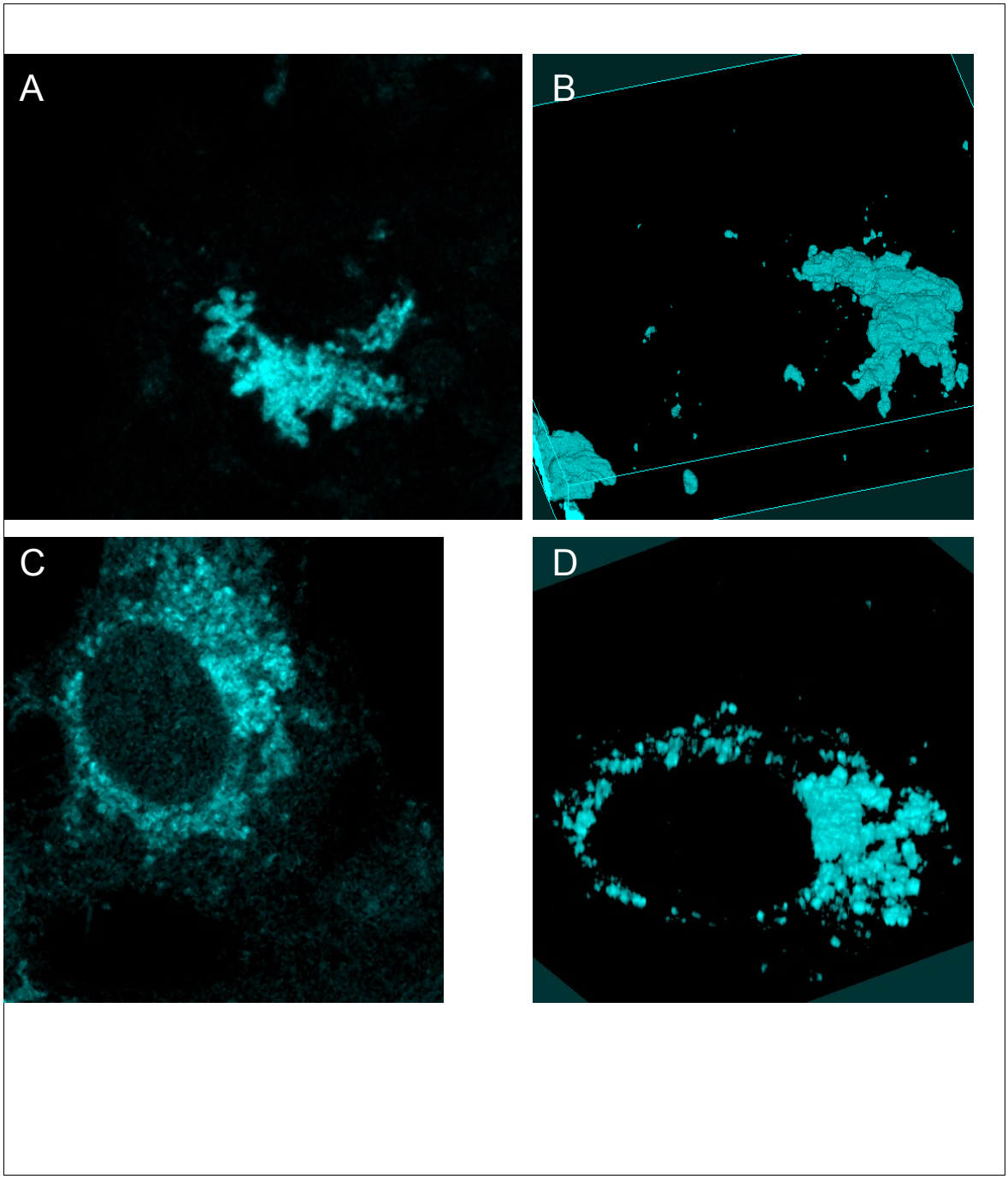

Figure 4: Confocal images of iPAT. Left side: iPAT cloned in pECFP transfected into Cos-7 cells. On the right: 3D-reconstruction produced with the Volume Viewer ImageJ plugin Two types of distribution could be observed. A and B show a strong compact perinuclear association. C and D present a vesicular view with a compact centre.

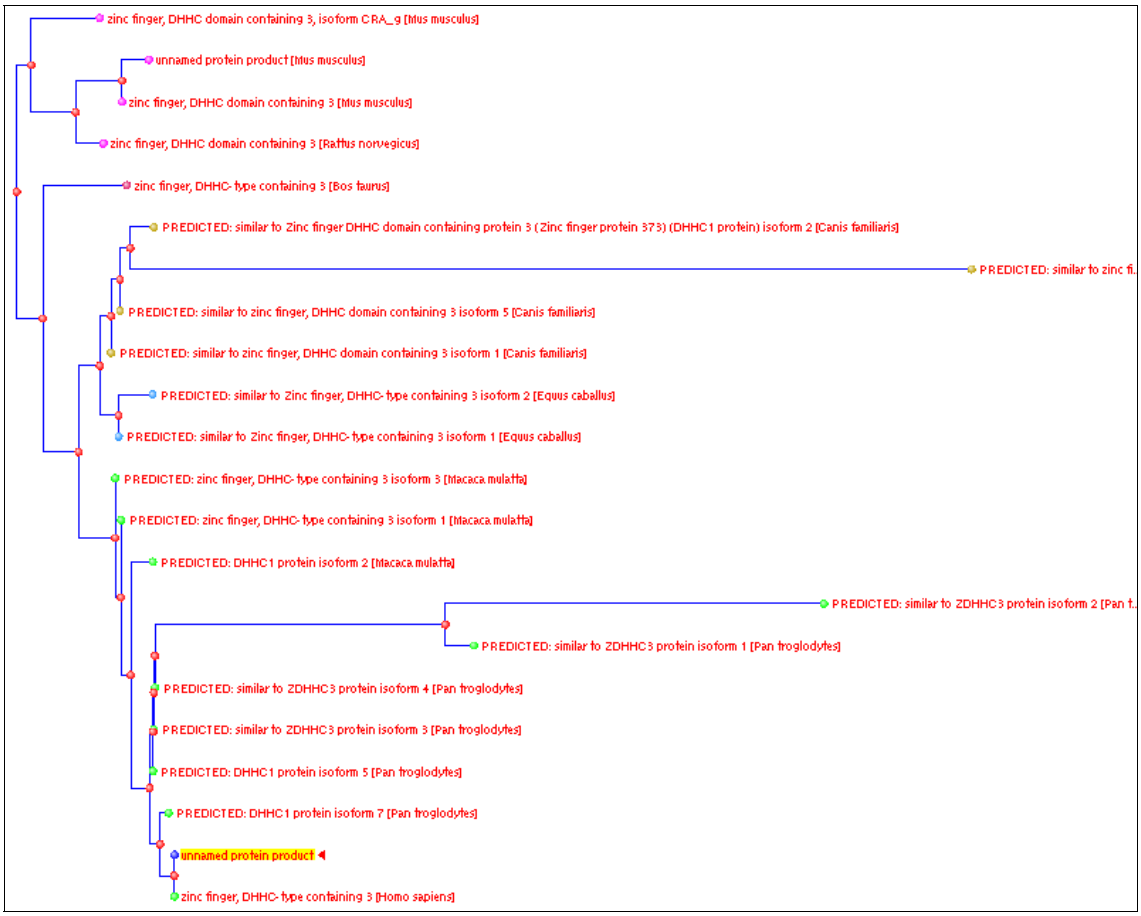

Figure 5: Phylogenetic tree of the iPAT. This images is an excerpt of the complete tree in the appendix. Rooted on the input sequence (last entry at the bottom; DHHC type containing 3). Apart from the yellow marked unnamed protein product all identified sequences are DHHC – type proteins with little variations throughout all species.

3.3 siRNA against iPAT changes morphology and cell growth characteristics

To learn about the function of the identified protein iPAT, a siRNA against iPAT was introduced into Caco-2 cells. A stable cell line with reduced iPAT (fig. 6) was produced to perform reliable tests. To control the efficiency of the introduced siRNA 2D-gel electrophoresis and biosynthetic labelling with S^{35}-methionine were performed, since no reliable antibody against iPAT does exist. Although a higher protein concentration lead to a general over staining in the 2D-gels derived from the wild type cells, relatively high intensity of the iPAT spot allowed the detection of the corresponding position and the comparison in the treated clone. The stable expressed siRNA caused a marked reduction of iPAT signals (fig. 6 red circle). Using radioactive labelling of proteins with S^{35} labelled methionine revealed in the one dimensional SDS gel electrophoresis a marked reduction of a protein with a size where the iPAT is expected to be found (Fig. 6b). Both data strongly implicate the successful and functional application of siRNA.

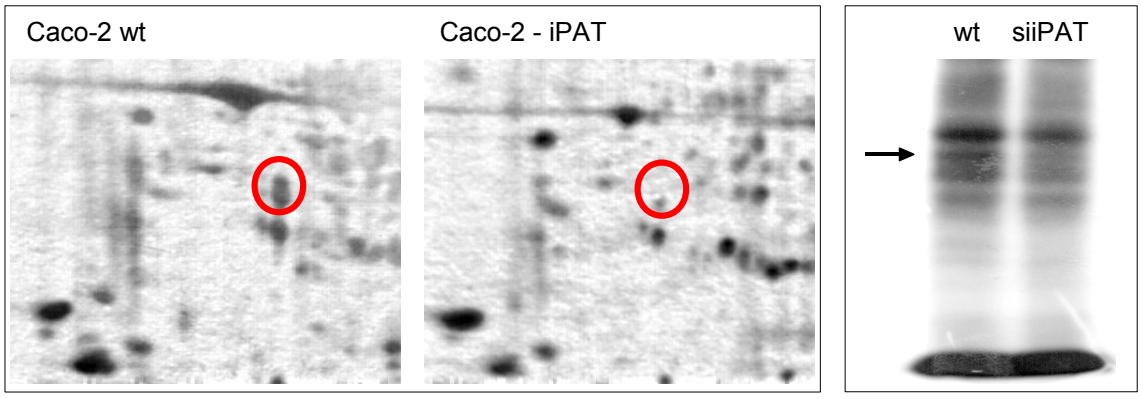

Figure 6: Test of iPAT reduction by siRNA.
A) Excerpt of silver stained 2D gel showing the difference of wild type (left) compared to siRNA treated Caco-2 clones (right). The red circle indicates the position of the palmitoyltransferase ZDHHC3 (iPAT).
B) Biosynthetic labelled proteins of Caco-2 wild type and Caco-2 stable expressing siRNA against iPAT. Approximate position of iPAT is indicated by the arrow.

Analysis of cell growth showed a considerable decrease in the growth rate of the Caco iPAT siRNA treated (siiPAT) clone compared to Caco-2 wild type. Starting with 2 x 10^6 cells, wild type Caco-2 cultures reached confluence after 48 h whereas siiPAT cultures did not show complete confluence after 72 h (fig. 7A) although finally the confluence at about 100 h is reached by the siiPAT cells. A regression analysis of the growth rates showed a significant difference (p-value 0.011) in the slope. A partial linearisation of the growth curves allowed a reliable assessment of the differences between the wild type and siiPAT Caco-2 cells.

The growth of the siiPAT clone starts with a delay of approximately 20% compared to the wild type at the time point of the first measurement (fig. 7B). Since the first time point of the petri dish coverage has been 12 h after seeding, the slope can be expected to be linear from this point. This implies not only a reduced growth rate of the siiPAT clone, which was also about 20% lower (data not shown) of the cultured Caco siiPAT clones but also a delayed inset of the growth or settlement on the petridish surface compared to wild type cultures.

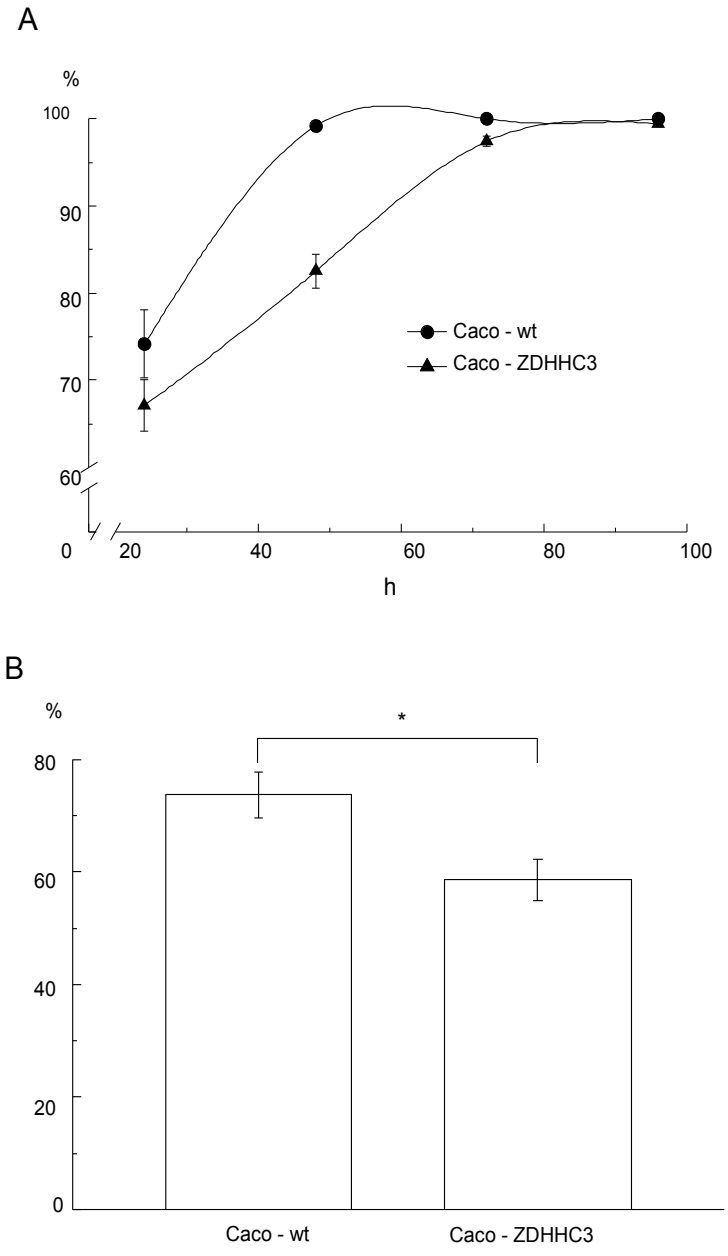

Figure 7: Cell growth of Caco-2 wild type and Caco-2 siiPAT. 2 x 10^6 cells were plated on 10 cm petri dishes and the occupied area was estimated under the microscope every 24 h. The growth curve (A) of the Caco-siiPAT (triangles) clone compared to the Caco-2 wild type (black dots) presents a slower growth rate. A more precise view can be achieved in the consideration of the intercept (B). The slope of the Caco-siiPAT clone growth rate is significantly reduced.

Out of this data it could be expected that the morphology of the cultured cells is altered too. In fact quantification of phasecontrast micrographs (fig. 8A and B) delivered a significant decrease in cell size of about 35% in the siiPAT clone compared to Caco-2 wild type cells (fig. 8C). To avoid effects due to ageing of the cell culture the maximal time of confluence was not used.

An observed gain of circularity of about 1% (fig. 8 D) may mainly be due to this decrease in size. This indicates a more dense growth of the stable transfected cell line, which can also be observed in the corresponding micrographs (fig. 8 A and B). If those data are adopted to the growth rate data (fig. 8) general reduction in the growth rate has to be relativised because this reduced measured growth rate may be due to the reduced size of the cells which are needing more time to cover the same area like the wild type cells.

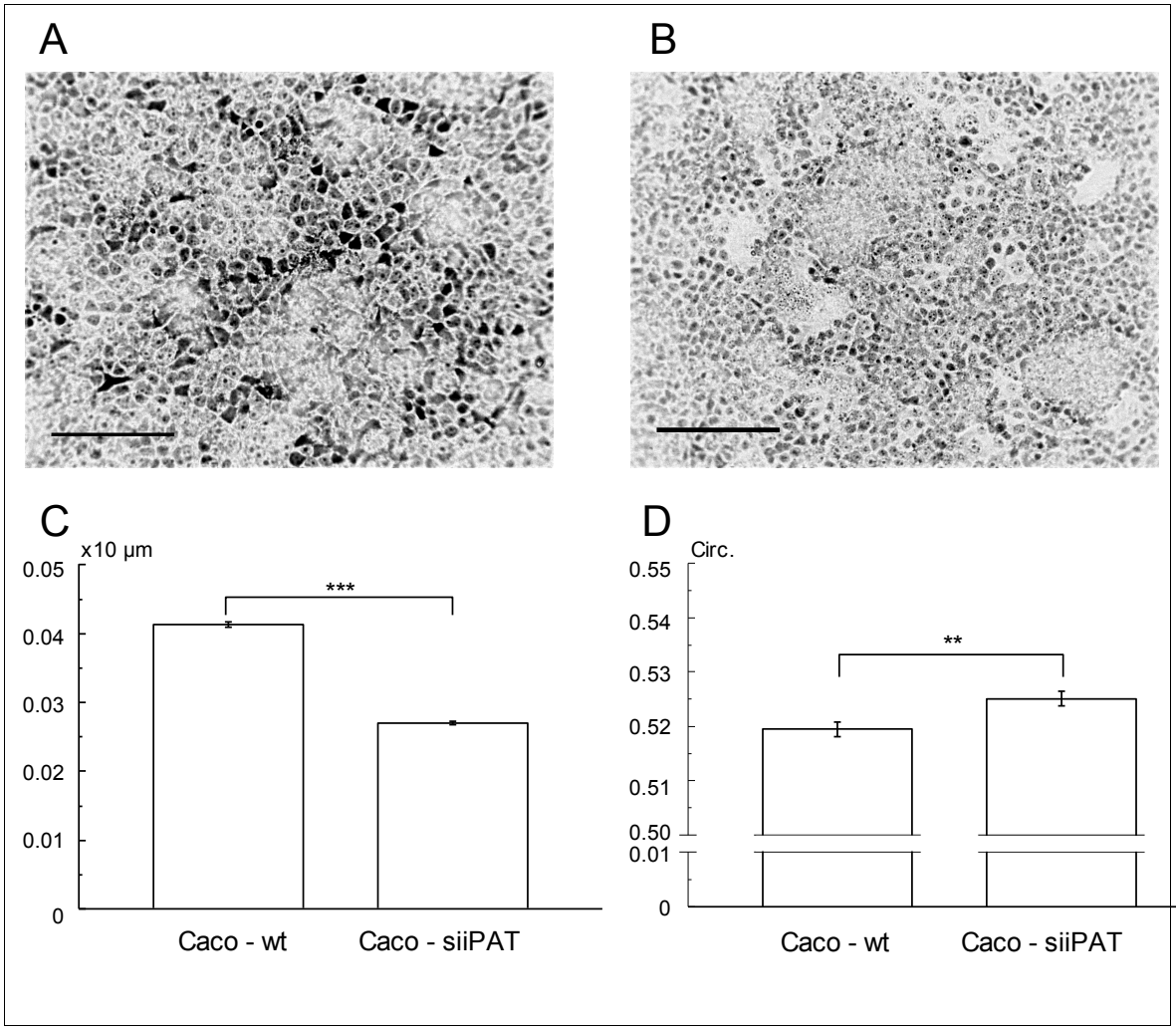

Figure 8: Exemplary phasecontrast micrographs of confluent cultures of Caco – 2 wild type (A) and iPAT siRNA treated Caco cells (B) and quantification (C,D) of wild type Caco – 2 cells compared to iPAT siRNA treated Caco cells. Scale bar in figures A and B represent 100 µm. iPAT siRNA treated Caco cells are significantly smaller than Caco – 2 wild type cells (C). The circularity of iPAT siRNA treated Caco cells is significantly higher than of the wild type (D).

The phasecontrast micrographs implied a change in the morphology of the siRNA treated cells compared to the wild type cells. To receive a closer look at the ultra structure of treated and untreated Caco-2 cells transmission electron microscopy with a uranylacetate staining for membranes had been applied (fig. 9).

Noticeable differences appears to exist at the immediate brush border membrane, where a loss of ordered villi in size and direction could be detected (fig. 9 A and B, red arrows). Also the cytoskeleton in this apical region seems to be affected, showing a loss of order where the actin meshwork usually can be found (fig. 9 A and B, blue arrows).

An analysis of the recognized organelles inside of the cells revealed a striking difference in the numbers of larger compartments like multivesicular bodies (MVB) between wild type Caco – 2 cells and iPAT siRNA treated Caco – 2 cells. Whereas the number of MVBs (fig. 9c, inlet) in wild type Caco – 2 cells outbalance the siiPAT cells by about 2 times (2.03), siiPAT cells clearly dominate in the case of lamellar bodies over the wild type cells by 38 times (fig. 9d, inlet).

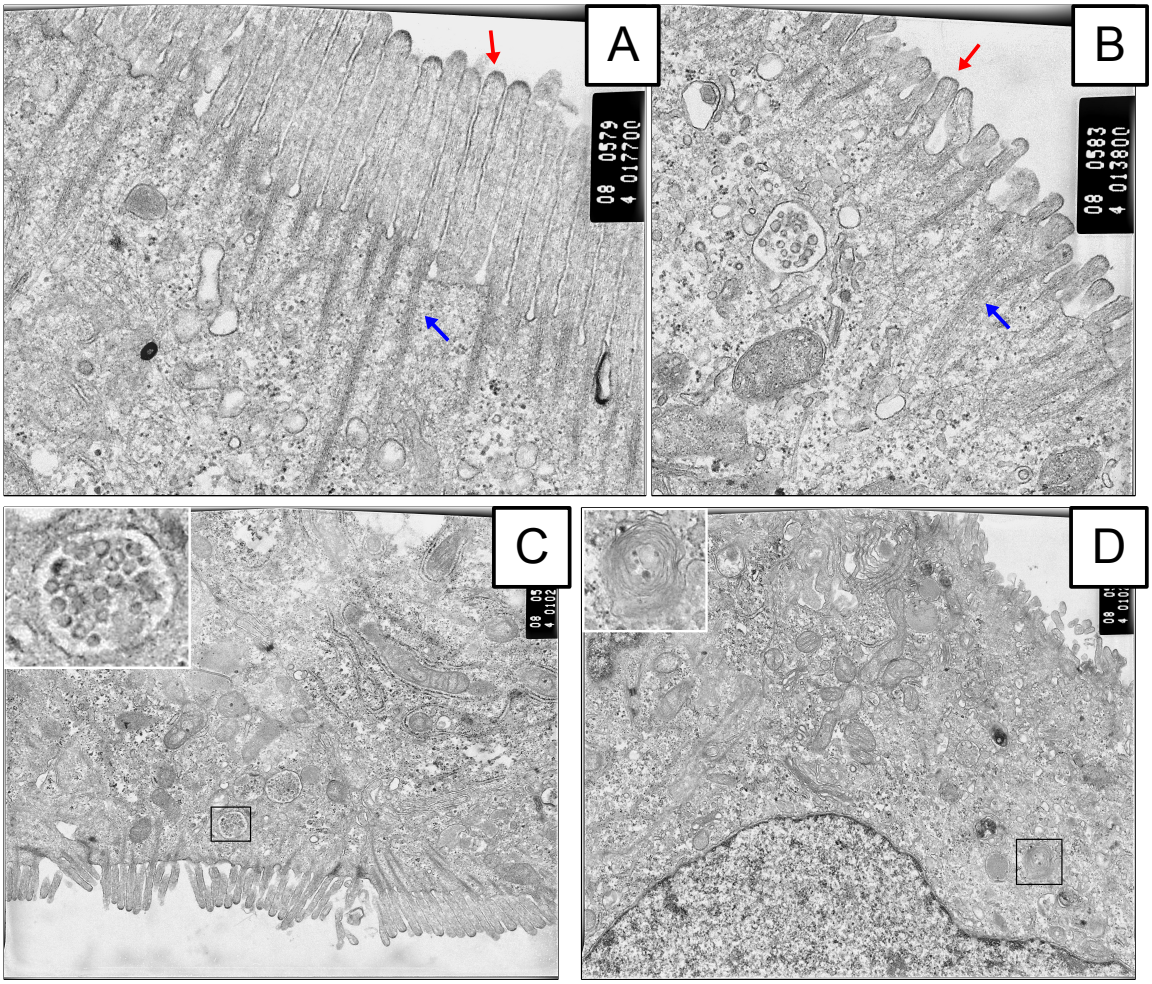

Figure 9: Transmission electron micrographs of Caco – 2 wild type (A,C) and iPAT siRNA treated Caco – 2 cells (B, D). Images A and B emphasize the difference of the brush border membrane. C and D are representatives for the intracellular organelle aberrations. Inlet in C shows a magnification of a mulitivesicular body. Inlet in D represents magnification of a typical lamellar body found in siiPAT Caco – 2 cells.

3.4 The iPAT Influences the Cellular Physiology

It is probable that those growth characteristics also may influence the permeability of the cell layer.

Indeed, measurements of transepithelial resistance (TER) presented an increase compared to wildtype culture. The significant ($p = 0.02$) increase of about 20% in TER was detectable even at the cellular level (Fig 10). A more compact growth behaviour of the the cells may account for this increase (see Fig. 8).

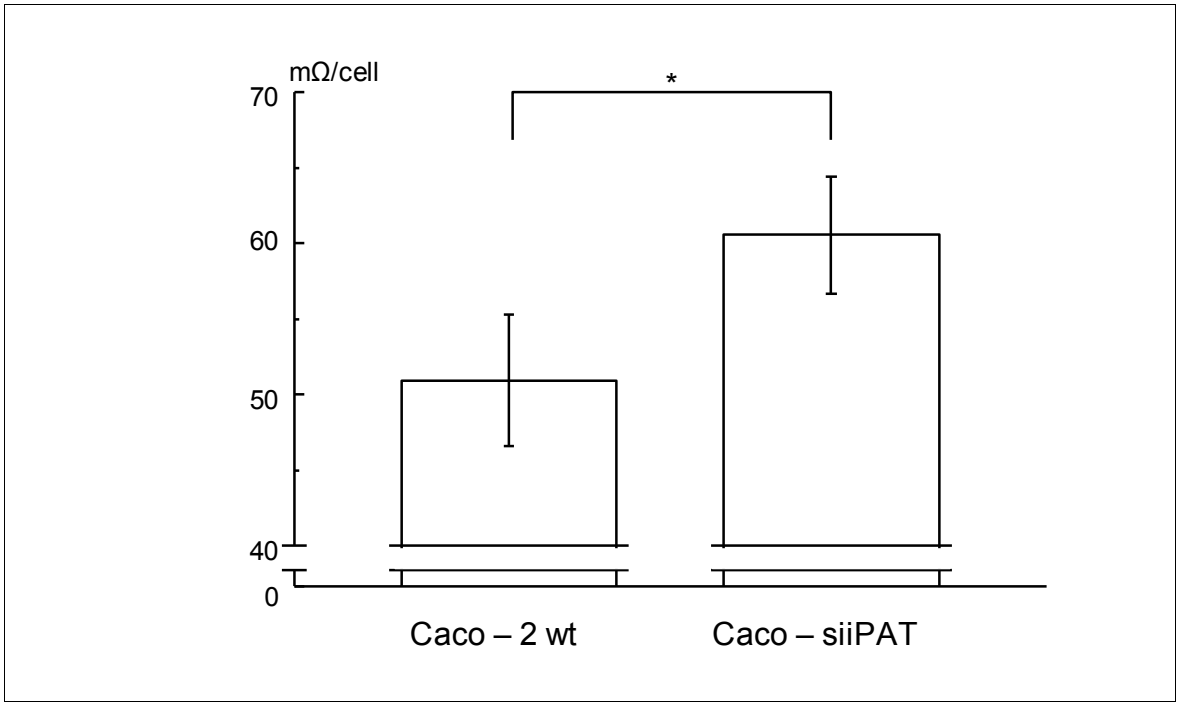

Figure 10: Cell number corrected transepithelial resistance of confluent cell cultures of Caco – 2 wildtype and iPAT siRNA treated stable cell line. The transepithelial resistance has been measured in mΩ.

Marked differences in growth rates, morphology and TER suggest a change of overall metabolic conditions within the cells. To estimate whether a change in the metabolism of the siiPAT cells emerges, the consumed glucose in confluent cell lines from the medium has been measured by periodically taking samples of the medium and the quantification of remaining glucose in those. Figure 11A illustrates a decreasing concentration of glucose in the medium in all cultured cell lines. The strongest decrease of glucose in medium can be observed in the siiPAT cells (Fig. 11A, solid diamonds) compared to the wild type cells (Fig. 11A, solid circles). As a control for a dependence between glucose consumption and palmitoylation events 2-bromopalmitate was applied as a general inhibitor of cellular palmitoylation in two different concentrations (Fig. 11). 2-bromopalmitate caused a concentration dependent decrease in the uptake of glucose from medium, with a marked effect when 100µM (Fig. 11A, solid squares) was applied.

A more detailed view can be achieved considering only the values of the slopes of the linear regression of the time series (Fig. 11B). Significant differences ($p = 0.04$) of about 40% exist between wild type cells and iPAT reduced Caco-2 cells, with a stronger negative slope in the iPAT reduced Caco-2 cells. This implies a much faster consumption of glucose than in the wild type cells. A significant ($p = 0.04$) lower reduction of glucose concentration in medium than in the wild type cells of about 40% could be found in cells treated with 100 µM 2-bromopalmitate, supporting a dependence of glucose uptake and palmitoylation events.

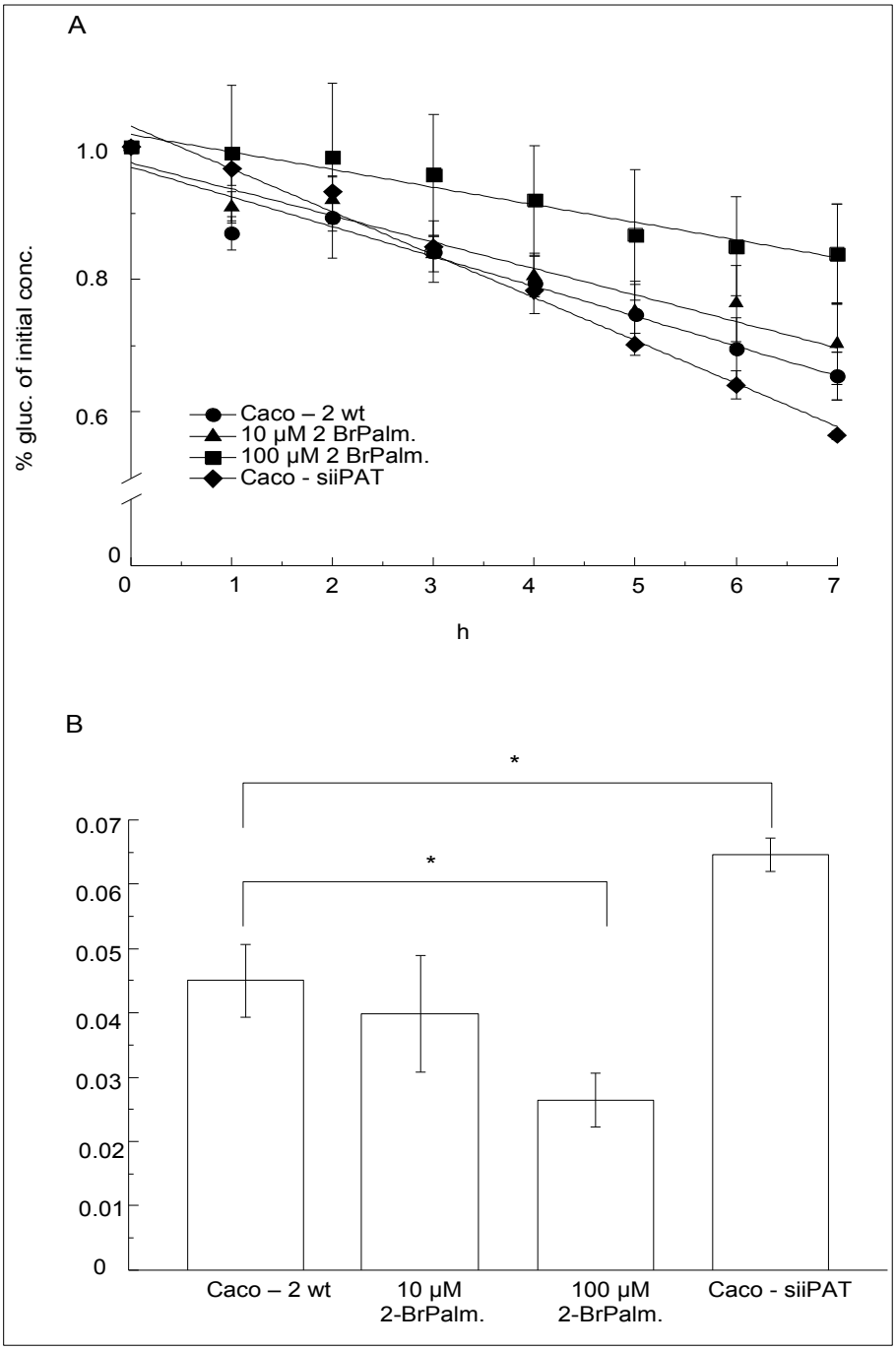

Figure 11: Glucose uptake from medium. Decrease of glucose concentration in medium has been measured in one hour steps by HPLC and normalized by the starting concentration (A). To measure the degree of decrease a linear regression (A, solid lines) was applied to the raw data and the resulting slopes were compared (B). Significant differences between Caco-2 wild type (●, A) and 100 µM 2-bromopalmitate (■, A) and Caco – siiPAT (♦, A) respectively, could be detected.

3.5 Lipid and Fatty acid composition is altered in siiPAT cells.

The previous results suggested an impact of the iPAT on intracellular metabolism, barrier function and membrane morphology in Caco-2 cells. Keeping in mind the fact that palmitoyltransferases utilize intracellular produced palmitate, this ability is expected to have consequences for the composition of lipids in the cell to explain the physiological effects.

To test this issue we isolated and compared lipids out of wild type cells and siiPAT cells (Fig. 12). In fact a redistribution of the lipid composition could be observed: Surprisingly the relative distribution of the lipids in wild type cells present a concentration in the more hydrophobic lipids, whereas in iPAT reduced cells the distribution tends to the more hydrophilic lipids. Definite differences were found with ca. 60% in low glycosylated glycolipids ($p = 0.03$), 25% in phosphatidyl glycerole ($p = 0.04$) and 12% in phosphatidyl ethanolamine ($p = 0.04$) respectively for the wild type cells. For siiPAT cells noticeable differences are found with 20% in phosphatidyl insositole ($p= 0.04$), 10% in phosphatidyl serine ($p= 0.04$) and 9% in phophatidyl choline ($p = 0.04$) respectively.

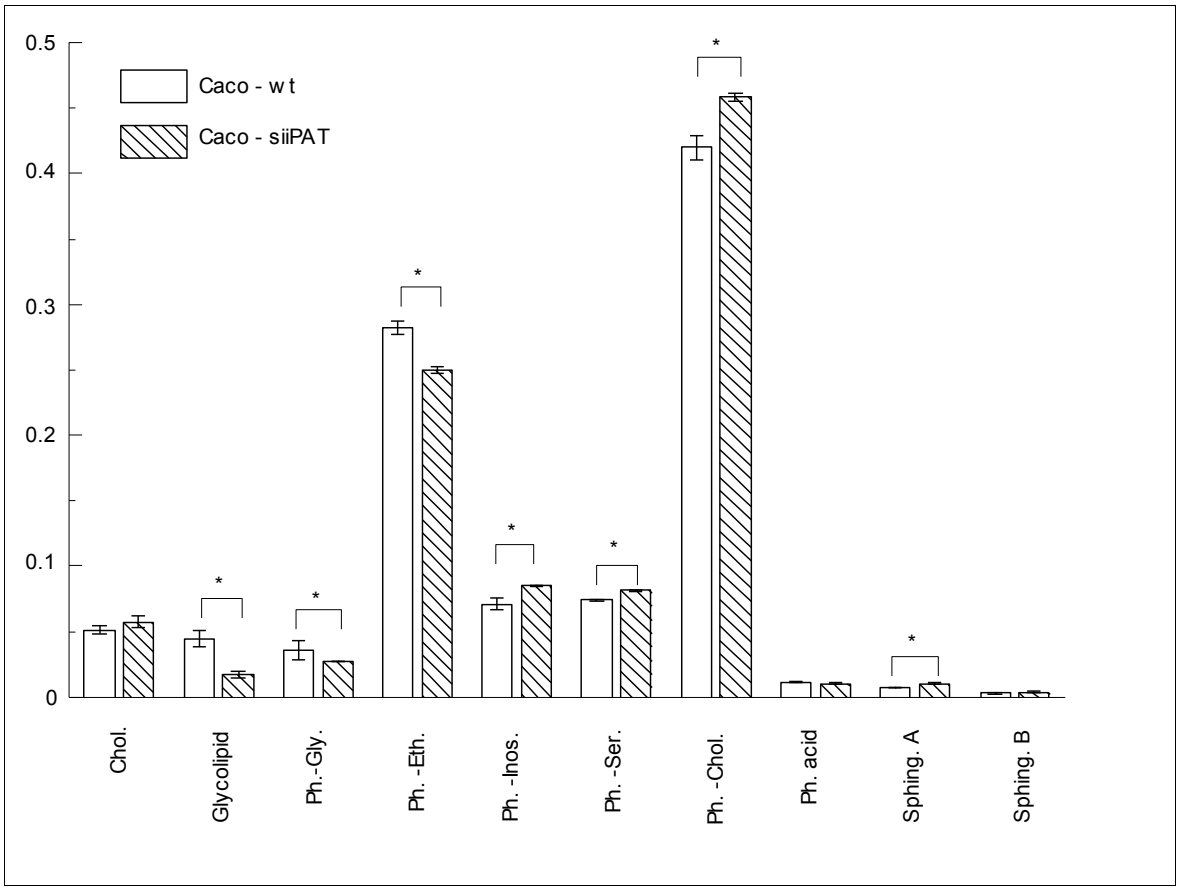

Figure 12: Lipid composition of Caco-2 wild type cells compared with -siiPAT cells. Relative values of the measured lipid concentration have been compared and significant differences are marked. From left to right a decrease in hydrophobicity can be adopted. Abbreviations: Chol., cholesterole; Ph.-Gly., phosphatidyl glycerole; Ph.-Eth., phosphatidyl ethanolamine; Ph.-Inos., phosphatydil inositole; Ph.-Ser., phosphatidyl serine; Ph.-Chol., phosphatidyl choline; Ph. acid, phosphatic acid; Sphing. A, sphingomyeline peak A; Sphing. B, sphingomyeline peak B.

It could be expected that the increase in unused palmitate (C16:0) by the reduced expression of iPAT should lead to an enhanced synthesis of lipids bearing long chain saturated fatty acids. This seemed not to be the case. To resolve the cellular composition of the lipids an analysis of the complete fatty acids was performed. In fig. 13 actually an increase of the long chain fatty acids (C18 and longer) in the siiPAT cells compared to the Caco-2 wild type can be observed. But this increase focuses in the unsaturated fatty acids (right half of the figure), pointing to an accumulation in processed derivatives of palmitate.

The key enzymes of palmitate procession include the elongation of palmitoyl – CoA by acetyl – CoA carboxylase to stearic acid (C18:0) (Kim et al., 1989) or an introduction of double bindings by the stearoyl – CoA desaturase (Brett et al., 1971, Fulco, 1974, Jones et al., 1998) to palmitoleic acid (C16:1 Ω 7). The subsequent derivates are increasing depending on the procession step less hydrophobic than the initially saturated forms, that were found in higher concentrations in the wild type cells with only two exceptions: the C16:1 Ω 7 (palmitoleic acid) and C18:1 Ω 9 (oleic acid). The consequence for the resulting lipid composition is a shift towards the decrease of hydrophobicity observed in fig. 13.

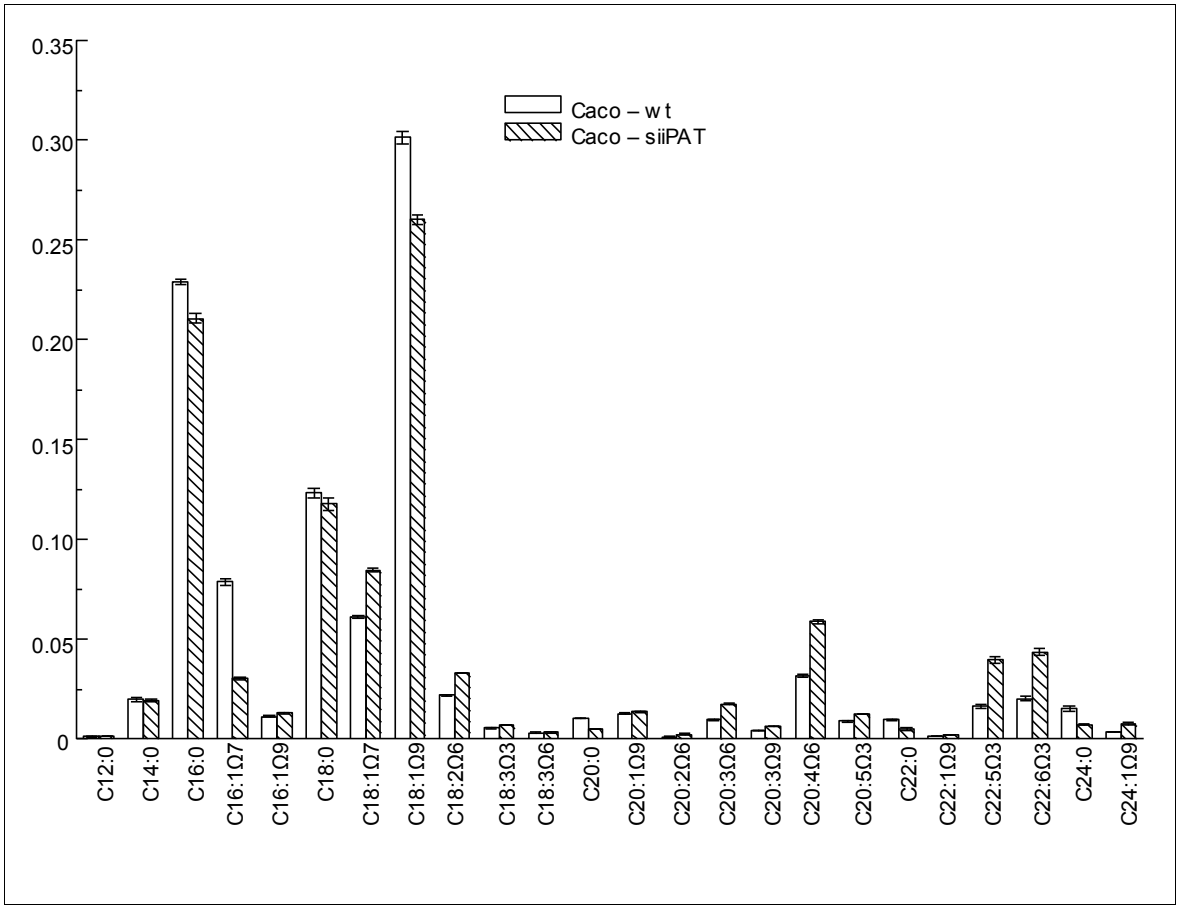

Figure 13: Relative values of fatty acid composition of Caco – 2 cells compared to siiPAT Fatty acids are sorted depending on their chain length. All differences are significant except for C12:0, C14:0, C18:0 and C18:3Ω6.

3.6 Differences in the palmitoylation pattern of proteins can be detected

The results of the fatty acid analysis did not provide sufficient evidence for the remaining palmitate. Thus a association with proteins was to be expected. To test this hypothesis a analysis of the “palmitome” together with a control of general protein biosynthesis was performed.

While the general expression pattern of the proteins was not strongly altered, the palmitoylation of proteins was changed. Using two different kinds of radioactive labelling, S^{35} labelled methionine for biosynthetic protein labelling and H^{3} labelled palmitate for palmitoylation, differences of palmitoylation at three positions could be detected. One nearly vanished in the siiPAT clone compared to the wild type caco-2 cells (fig. 14 A) .

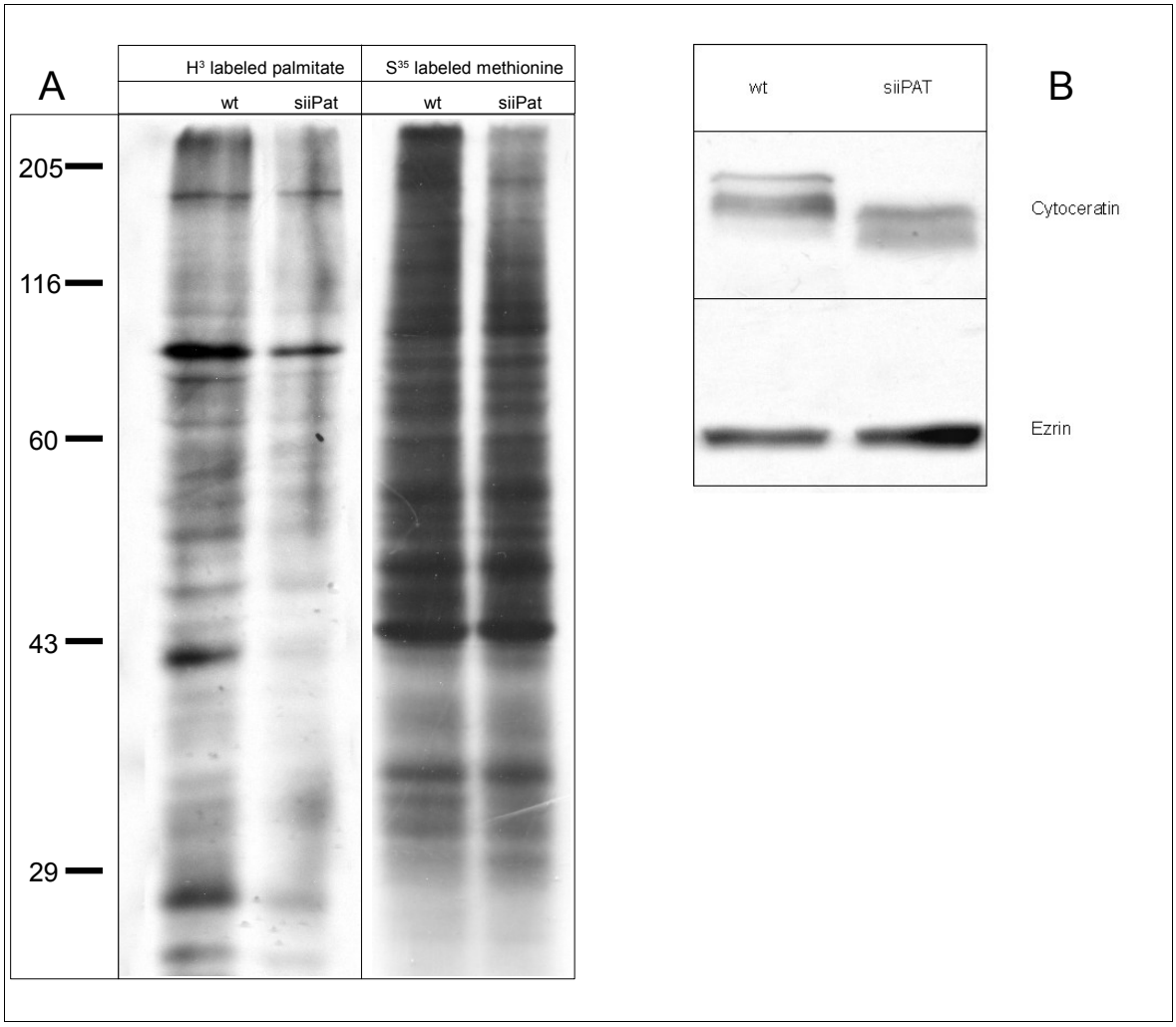

Figure 14: Proteine differences in wildtype and siiPAT treated cells. A) Radioactive tritium labeled palmitate (left) compared to S^{35} labeled methionine (biosynthetic labeling of proteins within 2 h). B) Westernblotting of the cytosceletal proteins cyclokeratin and ezrin.

3.7 Cytoskeletal implications

A change in the morphology of the cytoskeleton due to the reduction of iPAT has already been noted in the electromicrographs in fig. 9 A and B. The comparison of cytoskeletal proteins with respect to the modified ultrastructural morphology (see fig. 9 A and B) of the brushborder membrane in the siiPAT cell line revealed no differences in ezrin in westernblot (fig. 14 B). Ezrin plays a critical role in the organization of apikal brushborder membrane and influences the junctions between the cells of the brushborder (Saotome et al., 2004).

Cytokeratin presented a pattern of different sizes that could not be explained in the course of the experiments, but may be due to deviating maturation or phosphorylation levels of this kind of intermedial filamental proteins. This cytoskeletal protein has recently been associated with cellular polarity in Caco – 2 cells (Oriolo et al., 2007).

Using phalloidin – Alexafluor 543 staining of filamentous actin only subtle differences could be detected under confocal microscopy (Fig. 15). Compared to the wild type the siiPAT clone exhibited a reduction of stained vesicles, whereas the basal organization of the actin cytoskeleton remained unaltered. In the apical region of the cell a more diffuse pattern of the actin distribution is. Profiling the surface roughness of the apical staining revealed a higher number of large structures, detected by the broader and higher peaks in the profiles (Fig. 15, upper row first image) at the apical membrane in the wild type cells then in the siiPAT cell line (Fig. 15, profiles).The framing peaks illustrates the lateral plasmamembrane and thus the cell borders. This can be seen in the apical micrographs at the apical membrane. In the basal layer (fig. 15, images on the right) of the micrographs an clear assignment to the individual cell cannot be made but stress fibres are easy to identify.

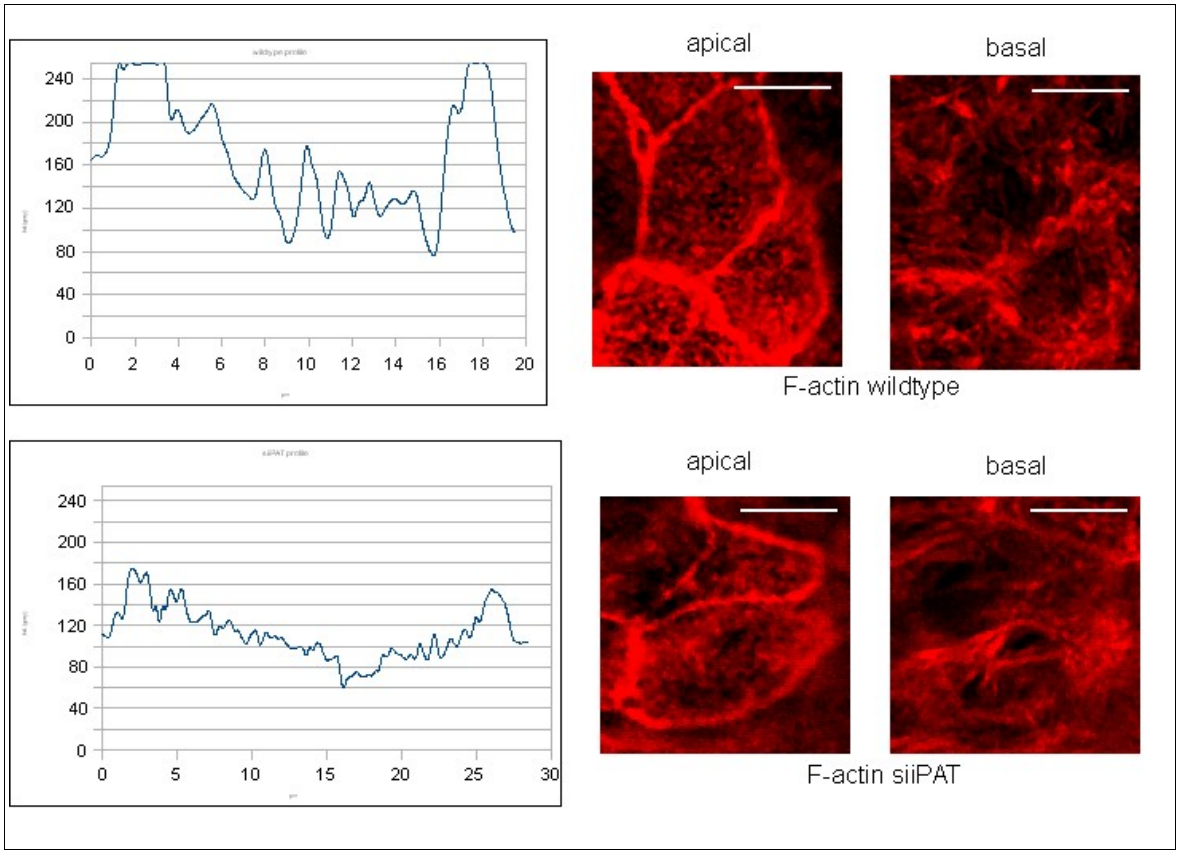

Figure 15: Comparison of the F-actin distribution in wild type (upper row) and siiPAT (lower row) treated cells. The profile over the length of a cell (X-axis) was taken from the apical layers of confocal images, indicating the intensity of the f-actin signals (Y-axis). Calibration bar is 15 µm.

3.8 DRM associated proteins are affected in siiPAT cells

We assumed an effect on proteins, that depend on their interaction with lipid domains. For that reason we tested whether the intestinal sucrosase-isomaltase (SI), a raft associated transmembrane protein of type II, presents a changed distribution throughout the cell. Analysis of sucrose step gradient centrifugation of triton-X 100 dissolved Caco-2 wild type and iPAT reduced cells revealed a distribution of the SI from floating fractions to fractions with higher sucrose content (fig. 16 A). The differences were more distinct on the low concentration partitions (fig. 16A right) than on the high concentration partitions (fig. 16A left).

To achieve a more polarity based two component system with a simple possibility of quantification a brush border membrane preparation was performed following Naim et al. (Naim et al., 1988a). In that case only brush border membrane enriched pellets (fig. 16 C, P2) and remaining membrane pellets (fig. 16 C P1) have to be quantified and compared. This provides SI distribution ratios bearing information about sorting effectiveness inside the cells. In fact the comparison of P2/P1 intensity based ratio of Caco-2 wild type and siiPAT cells revealed a striking difference ($p = 0.04$, fig 16 B).

The enrichment of the SI in the brush border membrane fraction in the iPAT reduced cells is nearly five times higher than in the Caco-2 wild type cells. All samples were normalized by means of the protein concentration allowing the conclusion of a generally lower expression of SI in iPAT reduced cells (fig. 16C). Relating to P1 more than 12 times more SI can be detected in the wild type cells, whereas P2 only a little more than 2 times more SI can be detected in the wild type.

Furthermore Annexin 2, a protein known to be associated with the transport of the SI (Jacob et al., 2004), also expose an altered distribution comparable to that of

the SI throughout the gradient (Fig. 16A). A test with a marker protein for rafts, Flotilin indicate a breakup of raft structures in the siiPAT cell line comparable to the situation in induced colitis in mice (Li et al., 2008).

As a control a sucrose gradient with subsequent westernbloting was performed to investigate a possible alteration of the distribution of DPP4 (dipeptidyl peptidase 4, CD26). In contrast to the SI, this protein is known to be transported independent of DRMs. If the affected membraneous parts of the cell are structures like the mentioned DRMs, DPP4 should remain unchanged in its distribution throughout the gradient. It could be shown that this is the case (fig. 16 A) what supports the correlation of DRMs and palmytoilation of proteins.

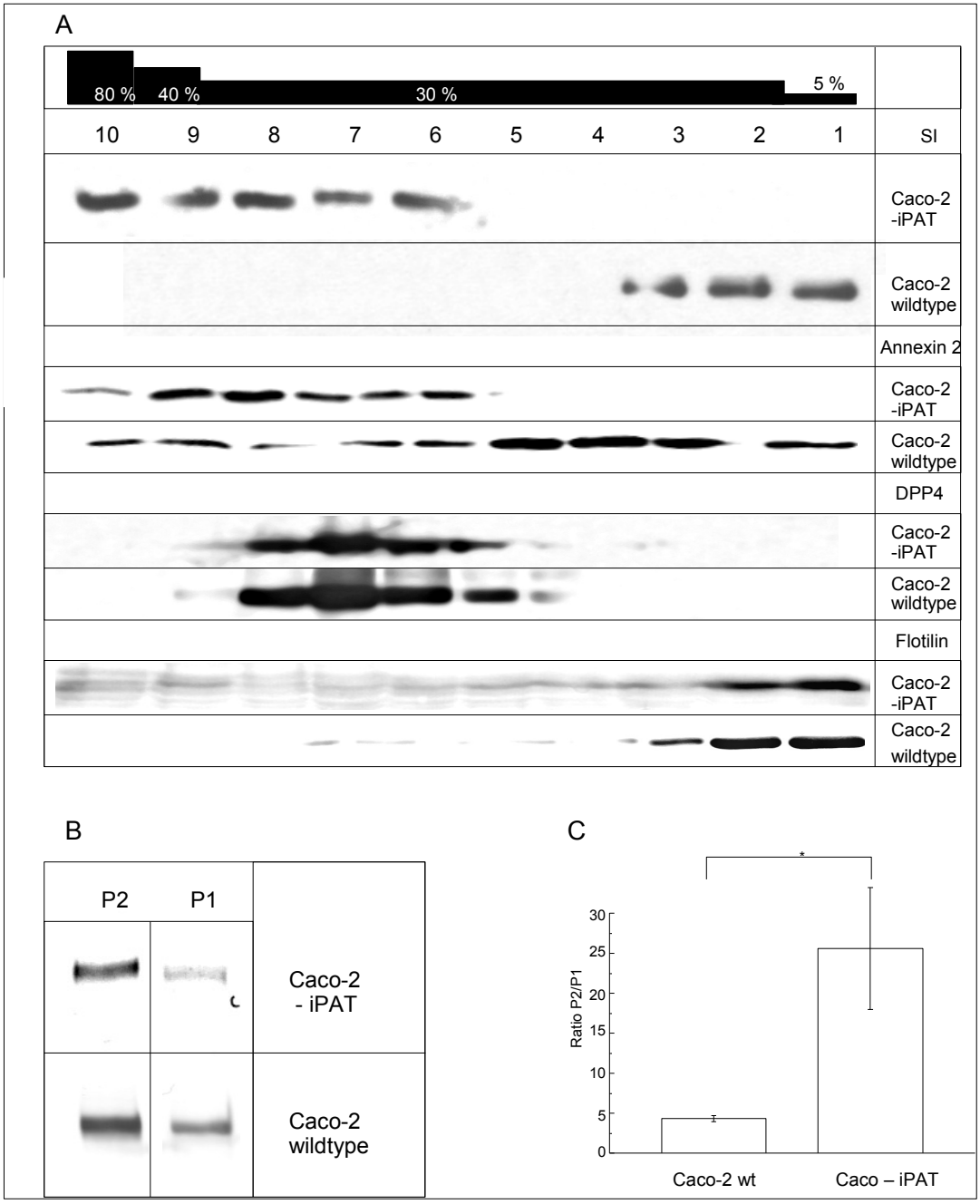

Figure 16: Distribution of the raft associated intestinal sucrase-isomaltase (SI) in Caco-2 wild type and Caco-siiPAT cells. (A) Sucrose step gradient centrifugation of triton-X100 dissolved cells, where the upper panel represents the concentration of the gradient, divided into ten steps. The brush border preparation (B, C) and subsequent western blotting is divided in P1 and P2, where P2 represents enriched brush border membranes and P1 remaining membrane components like Golgi, ER and nucleus. Quantification of western blot data reveal significant differences between the ratios of P2/P1 of treated to untreated cells (C).

3.9 Interacting Proteins

Out of database and FRET data a crude map of interacting proteins in the context of the palmitoyltransferase iPAT can be created. The basically used database for the identification of protein – protein interaction in this thesis has been the database IntAct from EBI (http://www.ebi.ac.uk/intact/site/index.jsf). The minor contribution resulted out of queries in the BOND database from Unleashed informatics (http://bond.unleashedinformatics.com/). This resulted in the complex interplay of the mentioned proteins found in the appendix. This representation was not very intuitive.

Subsequently applied filtering by concentrating on an iPAT, annexin 2, as a member of transport associated proteins, and major components of the cytoskeleton like tubulin and actin, used in the context of this thesis resulted in the interaction map of figure 17. This graph offers despite its reductive representation a number of interesting clues. Out of this data, no direct contact of the iPAT to any cytoskeletal element could be expected. Indirect contacts can only be established by either annexin 2 or myl 6 (myosin like polypeptide 6).

Whereas myl 6 only contacts the actin cytoskeleton, annexin 2 also provides possibilities to contact tubulin via secondary mediators. Although no direct interaction to annexin is established, via secondary mediators a number of binding situations are possible between iPAT and annexin 2. Focussing on the annexin 2 side of the graph (fig. 17 upper half), there is a clear tendency toward an actin interaction. For the consideration of intracellular transport systems, the possible constellation of iPAT – COPB – Glucose Transporter Type 4 – annexin 2 seems to be of special interest in view of the Glucose data in figure 11.

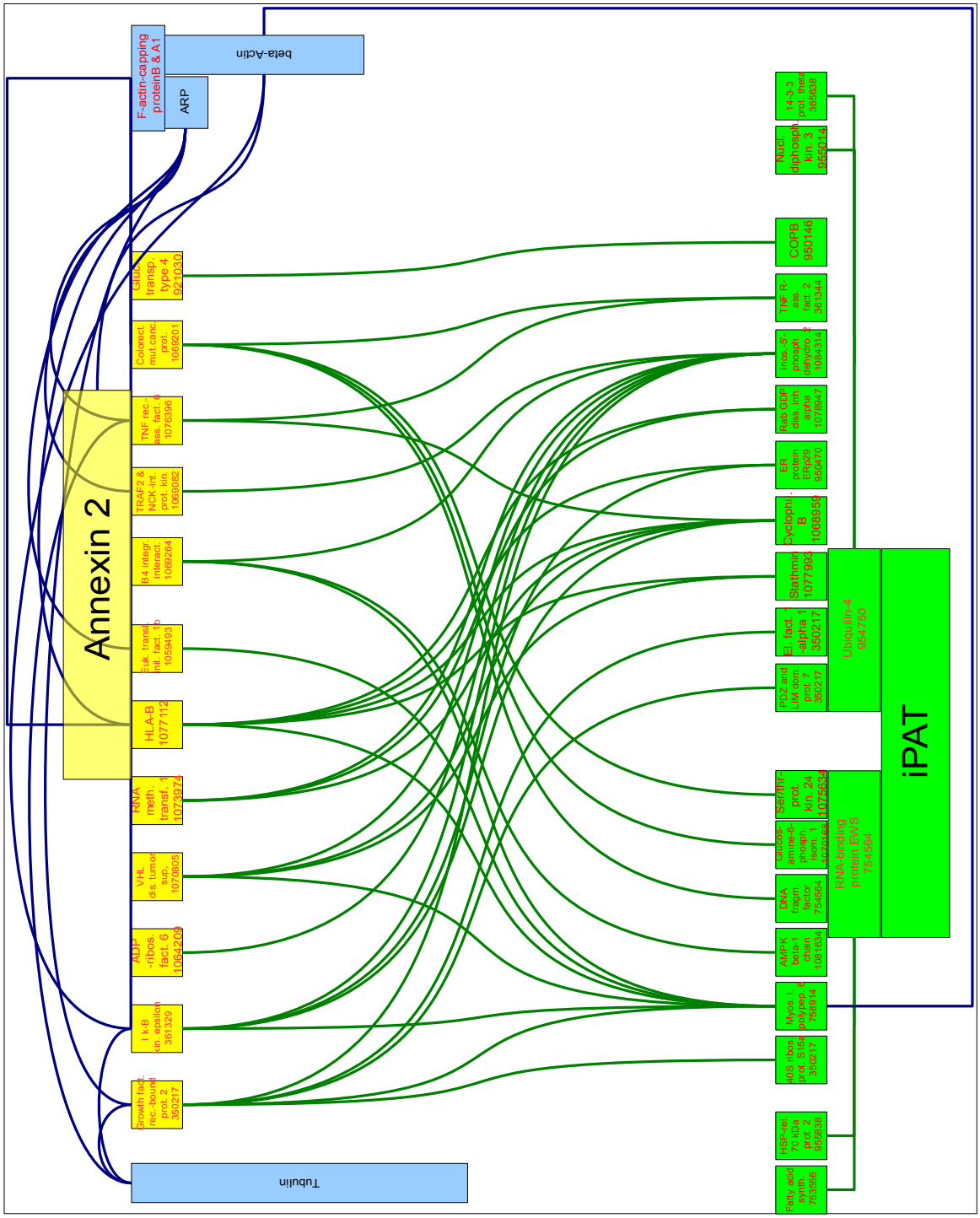

Figure 17: interaction map of iPAT in context with annexin 2 and immediate cytoskeletal elements like actin and tubulin. Data were derived from the databases BOND and IntAct. 3 instances were accepted between the central proteins iPAT and annexin. Blue codes for cytoskeletal elements and connections, green codes for iPAT specific interactors, yellow codes for annexin 2 specific interactors

Using the technique of FRET for the detection of interacting proteins which are tagged with fluorescent proteins, that are able to “communicate”, i.e. to transfer activation energy from one to the other if a minimum distance of 9 nm is granted a number of model proteins had been tested (fig. 18 A). The amount of FRET signals were quantified and normalized to achieve a map of comprehensive interactions (fig. 18 B). Even when determining a FRET signal of 10% of complete fluorescence as threshold (fig. 18 B, red circle), annexin 2 turns out to be a potent binding partner for all tested proteins with a strong affinity for cytoskeletal elements (actin, myosin1a).

In the context of the apically sorted SI very similar FRET values could be found, suggesting a actin dependent transport mechanism mediated by annexin 2. This is not the case with the LPH, which could be shown not to be transported over the actin cytoskeleton (Jacob et al., 2003).

Derived out of the FRET data the components and connections for the correct transport of the SI in view of the tested proteins can be drawn (fig. 19 B). Since the secondary connections (painted in red in fig. 19 B) are considered to be enforcements of established connections the distance of the participating proteins have been shortened. This leads to a complex of annexin 2, actin, myosin 1a and SI with more distant elements like LPH, DPP4 or APN.

FRET measurements could also be performed using a fluorimeter. In this case dissolved transfected Cos – 7 cells were used to produce sufficient amounts of pEYFP – iPAT. As a negative control pECFP and pEYFP vectors were used (fig. 19 A, upper graph). After the subtraction of background fluorescence the only clear signal of an interacting protein could be measured has been a glycosyl transferase (fig 19 A, lower graph).

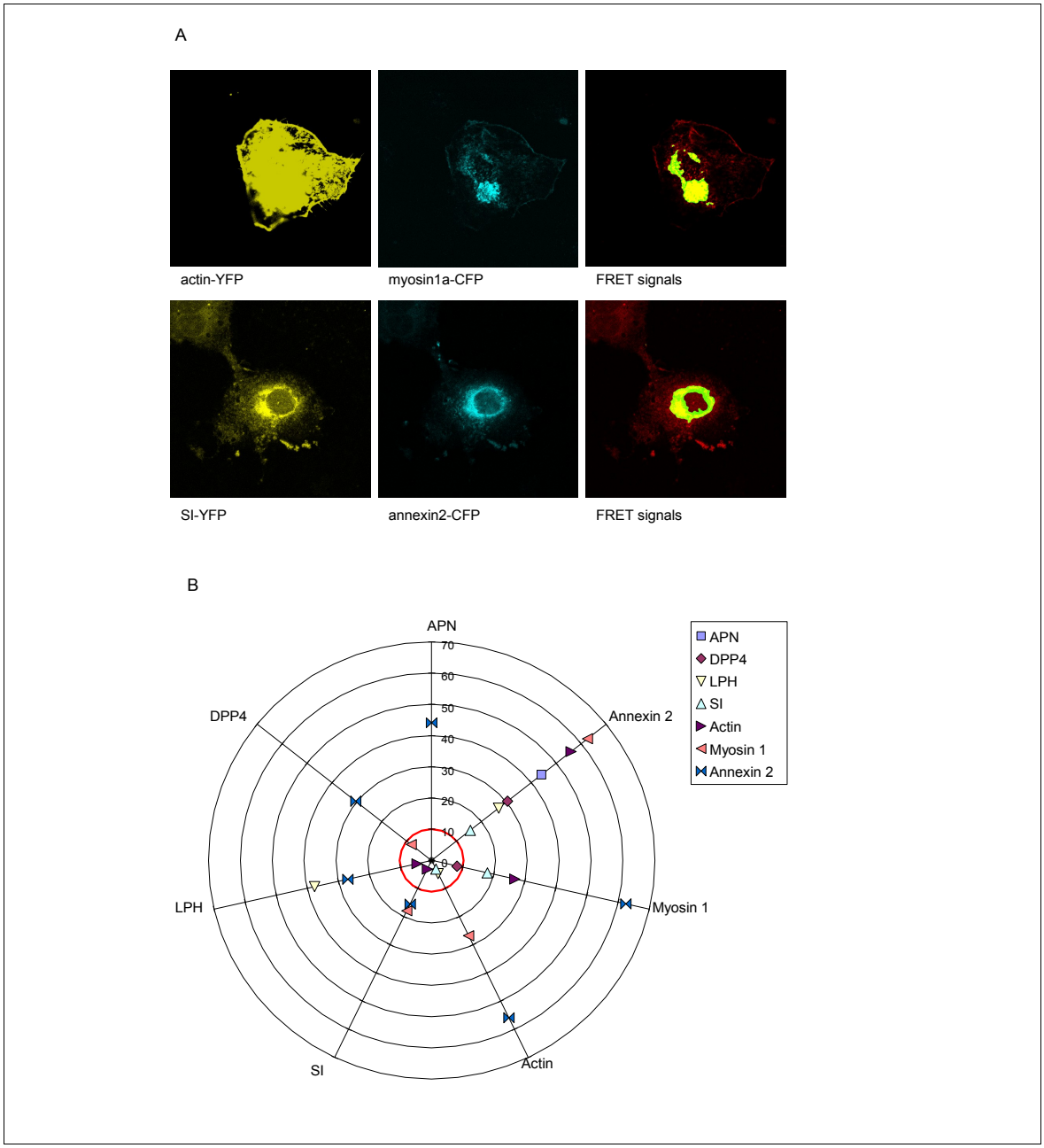

Fig. 18: Interaction detection with FRET
A)Upper panel: FRET measurement of cytosceletal (actin-YFP) and associated proteins (myosin1a – CFP). Lower panel: FRET measurement of membrane (SI-YFP) and cytoplasmic (annexin2-CFP) proteins. The 3rd image highlights the FRET-signals on th cellular background.
B) Polar representation of measured FRET signals in percent of donor areas. The measured proteins are the axes of the polar system and their partners are represented as symbols on the axes. The red circle on the 10% ring denotes the threshold for an interaction.

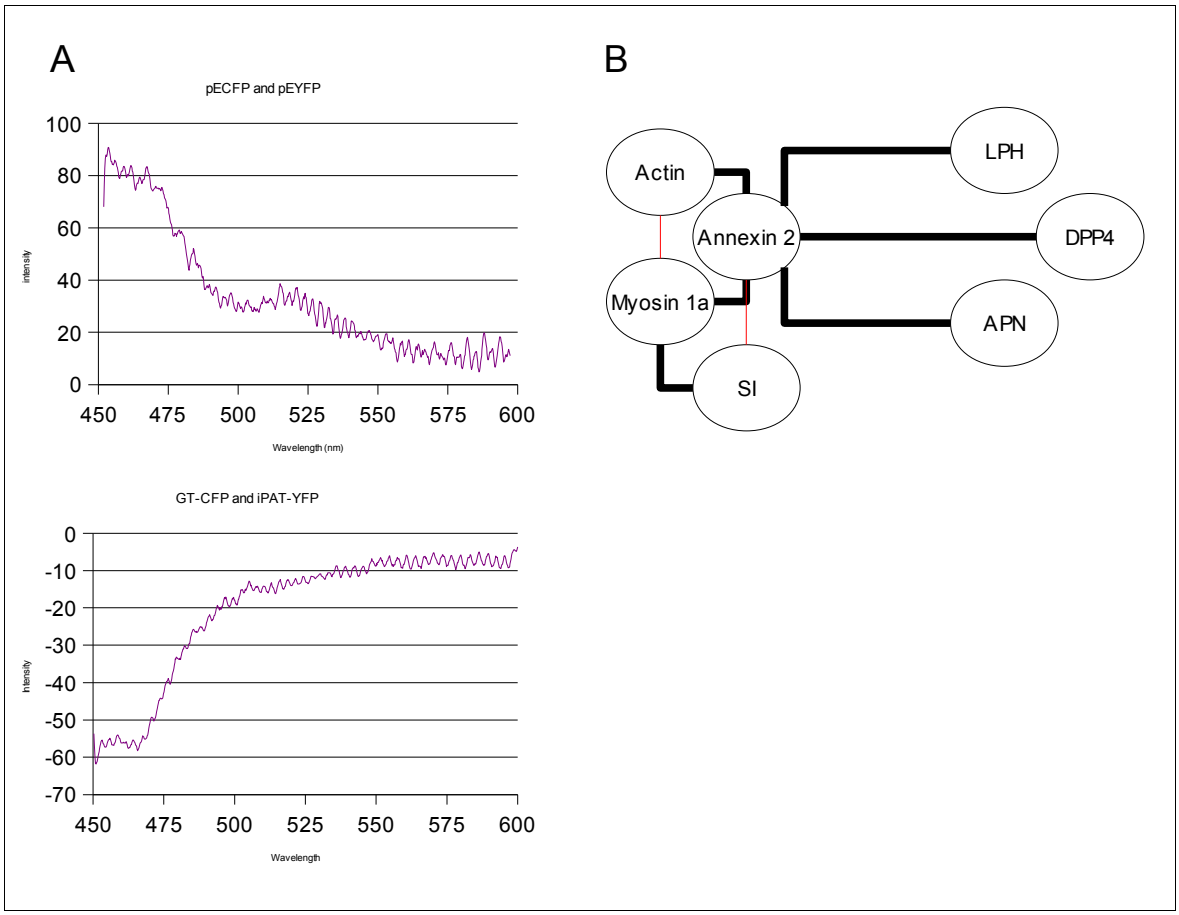

Figure 19: FRET data. A) FRET data achieved by fluorimetric measurements. The upper graph shows the negative control through the application harvested pECFP and pEYFP out of transiently transfected Cos-1 cells. The lower graph was produced using pEYFP – iPAT and pECFP – glycosyltransferase (GT) transiently transfected in Cos-1 cells and subsequently harvested.
B) Graph of a possible transport complex of the SI as it could be derived out of FRET data.

3.10 iPAT Deficient Cells Expose a Different Composition of Glycolipids

To test whether the contradicting results of the TER measurements (fig. 10) and the seemingly decomposition of lipid rafts referring to the distribution of raft associated proteins like SI (fig. 16) could be explained by the appearance of glycolipids (Wrackmeyer et al., 2006a), an TLC was performed with subsequent orcinol staining. Best results were obtained using tween derived lipid rafts (fig. 20 A).

Although four congruent orcinol signals could be spotted (fig. 20 A), at least two bands could be identified in the siiPAT derived pattern, that could not be detected in the wild type. One less hydrophobic signal in the lower section of the chromatogram on the left side in figure 18 A and one close to the middle in the upper half of the left lane. Especially the comparatively hydrophilic band in the lower part seemed to be a candidate for a high glycosylation and in that case a binding site for lectins. It could be expected to find a highly glycosylated lipid or better a lipid bearing a strong glycostructure in this band.

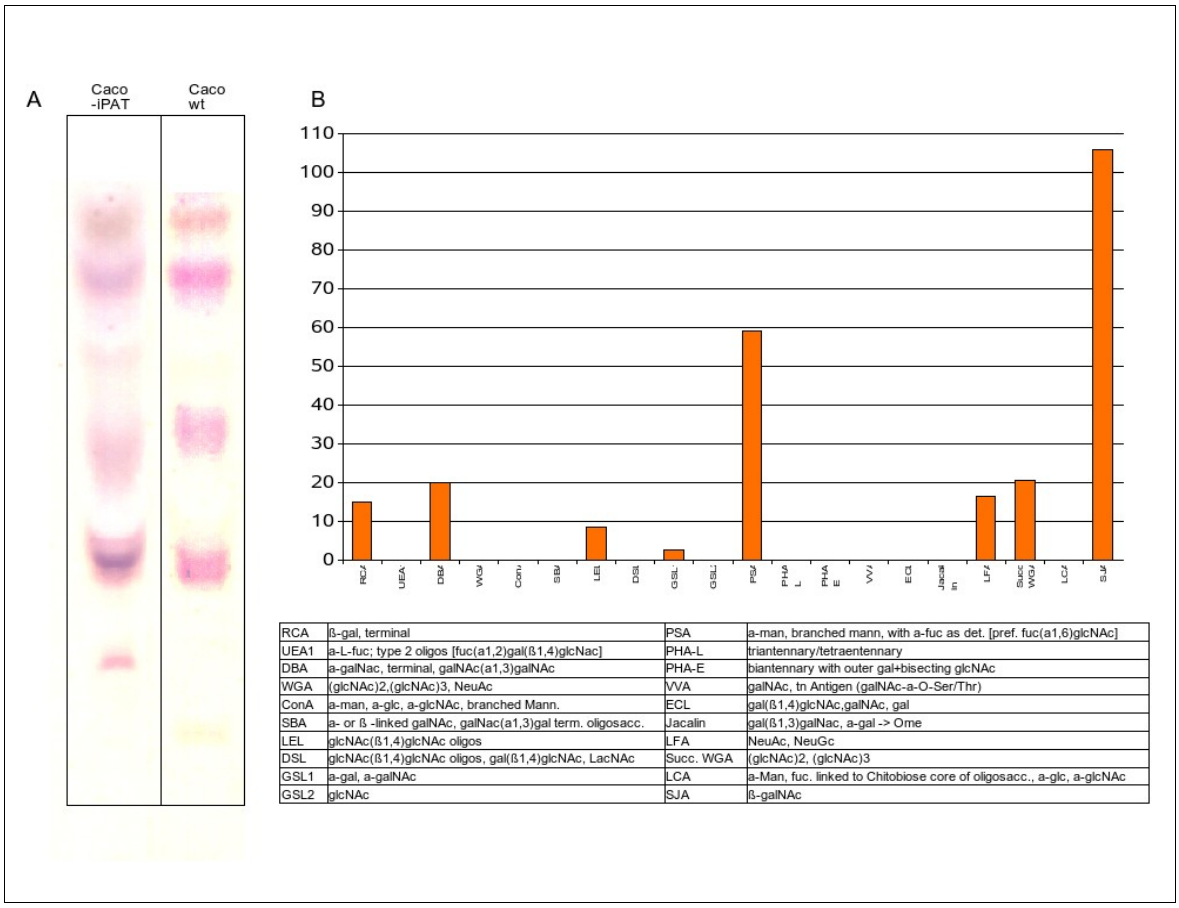

RCA	ß-gal, terminal	PSA	a-man, branched mann, with a-fuc as det. [pref. fuc(a1,6)glcNAc]
UEA1	a-L-fuc; type 2 oligos [fuc(a1,2)gal(ß1,4)glcNac]	PHA-L	triantennary/tetraentennary
DBA	a-galNac, terminal, galNAc(a1,3)galNAc	PHA-E	biantennary with outer gal+bisecting glcNAc
WGA	(glcNAc)2,(glcNAc)3, NeuAc	VVA	galNAc, tn Antigen (galNAc-a-O-Ser/Thr)
ConA	a-man, a-glc, a-glcNAc, branched Mann.	ECL	gal(ß1,4)glcNAc,galNAc, gal
SBA	a- or ß -linked galNAc, galNac(a1,3)gal term. oligosacc.	Jacalin	gal(ß1,3)galNac, a-gal -> Ome
LEL	glcNAc(ß1,4)glcNAc oligos	LFA	NeuAc, NeuGc
DSL	glcNAc(ß1,4)glcNAc oligos, gal(ß1,4)glcNAc, LacNAc	Succ. WGA	(glcNAc)2, (glcNAc)3
GSL1	a-gal, a-galNAc	LCA	a-Man, fuc. linked to Chitobiose core of oligosacc., a-glc, a-glcNAc
GSL2	glcNAc	SJA	ß-galNAc

Figure 20: TLC representation of glycolipids isolated from Tween-20 rafts of Caco siiPAT and Caco-2 wild type cells (A) and lectin binding assay of isolated glycolipid (B).
A) Result of a TLC followed by orcinol staining. At least the lowest glycolipid signal in the siiPAT clone (left lane) does not appear in a detectable amount in the wild type (right lane).
B) Result of a lectin binding assay on the isolated glycolipid off the siiPAT TLC from A. The table in the lower half of B explains the binding affinities of tested lectins.
Abbreviations: ConA = Conconavalin A, DBA = Dolichos biflorus agglutinin, DSL = Datura stramonium lectin, GSL I = Griffonia simplicifolia lectin I, GSL II = Griffonia simplicifolia lectin II, ECL = Erythrina cristagalli lectin, LCA = Lens culinaris agglutinin, LEL = Lycopersicon esculentum lectin, LFA = Limax flavus agglutinin, PHA-E = Phaseoulus vulgaris Erythroagglutinin, PHA-L = Phaseolus vulgaris Leucoagglutinin, PSA = Pisum sativum agglutinin, RCA = Ricinus communis agglutinin, SBA = soybean agglutinin, SJA = Saphora japonica agglutinin, Succ. WGA = succinyl WGA, UEA1 = Ulex europaeus hemaglutinin I, VVA = Vicia villosa agglutinin, WGA = Wheat germ agglutinin

To investigate the possibility of a lectin binding of this glycolipid an isolating this lane out of a TLC – plate with a subsequent solution in methanol was accomplished. The transfer on a methanol resistant 96 well plate followed by drying produced a layer of this glycolipid that was accessible for further investigation.

Using a kit for the detection of lectin binding, a number of assorted lectins could be identified binding to this isolated glycolipid (fig. 20 B). In this lectin binding assay a strong evidence for the existence of ß-GalNAC residues could be deduced out of the *Sophora japonica* agglututinin (SJA) binding. Also a α-mannose contingent has to be expected considering the strong signal out of the *Pisum sativum* agglutinin (PSA) binding. Weaker signals could be identified for GlcNAC (succinyl WGA [succ. WGA]), a-GalNAC (*Dolichos biflorus* agglutinin [DBA]), NeuAC (*Limax flavus* agglutinin [LFA]) and ß-Gal (*Ricinus communis* agglutinin [RCA]).

4.Discussion

4.1 2D-Gelectrophoresis is a Valid Instrument for DRM Analysis

Detergent resistant membranes (DRMs) have been identified to be of importance for a number of cellular processes before (for a review see Grzybek et al., 2005, Orlowski et al., 2007 or Hanzal-Bayer & Hancock, 2007). But considering the fact, that there exist numerous kinds of detergents with different properties (Arnold & Linke , 2007, Seddon et al., 2004, Curnow P, Booth PJ. Biochim Biophys Acta. 2004 Nov 3), a deviating characterisation of DRMs depending on the regarding detergent is to be expected. In fact interdependencies of types of DRMs could be associated to intracellular localization (Castelletti et al., 2008) or cellular proteins typically found in those membrane fractions (Seddon et al., 2004). In this light the investigation of the proteomics of those different DRMs as an initial trial to understand the meaning of defined membrane sections seemed to be necessary. Using only a limited number of detergents (Triton-X100, Tween-20, Lubrol and Brij) the results were encouraging (see fig. 1).

The discrimination between highly variable and highly invariable spots or proteins is partly due to the size of the spots. The higher number of variable spots is in parts caused by the smaller size of those: the smaller a spot the lower the probability of overlapping spots (Arad & Gotsman, 1999). Nevertheless, focusing on invariable spots a high degree of security could be reached. With a number of only five invarible spots a reliable result was achieved. Interpreting the spots in terms of their proteinous identity required the observation of a number of preconditions: to constrain the possible number of results a database search has to be focused on clade of *mammalia*, if possible on the species *homo sapiens*. The

second important constraint was the rejection of proteins with a predicted high number of secondary modifications. All those constraints affect the power of a software based identification of proteins out ot a 2D-gel but the results reached with the aid of those techniques offered the opportunity of a fast choice for an protein to investigate further.

4.2 Palmitoyltransferases are Important Players in the Cell

The decision for the palmitoyltransferase ZDHHC3 was the result of the careful observation of the mentioned constraints with the additional advantage of a protein with a high affinity for the membrane (Mitchell et al., 2006). The usage of protein sequence analysing software that especially searched for transmembranous structures like TMRPres2D (Spyropoulos et al., 2004) a membrane association can be expected with a high degree of security.

Palmitoyltransferases or protein-acyl-transferases (PATs) are a group of transmembrane proteins, that owe the ability to bind palmitate and other long chain fatty acids and transfer them to other proteins at cysteine residues, a process which is denominated S-acylation (reviewed by Dietrich and Ungermann, 2004; Smotrys and Linder, 2004; Basu, 2004). The significance of PATs have long been controversial because of missing identification of a consensus sequence for targeting palmitate and even autoacylation may takes place *in vitro* at the same cysteines could be observed as *in vivo* (Duncan and Gilman, 1996; Dunphy et al., 2000). But at least in yeast finally essential enzymatic S-acylation for targeting a number of proteins to the plasma membrane could be identified (Babu et al., 2004). S-acylation is not a durable protein modification like glycosylation but very dynamic. Its half-life often only is a fraction of the proteins half-life (Schweizer et al., 1996, Stoeckli and Rohrer, 2004). Attached palmitates or other long chain fatty

acids are removed by acyl-protein thioesterases (APTs) from proteins (Smotrys and Linder, 2004) providing a fine tuning system for membrane association or translocation to defined membrane sections like lipid rafts of proteins (Chakrabandhu et al., 2007; Lam et al., 2006). One important aspect of this kind of fine tuning is the localization and activity control of Ras proteins (Hancock et al., 1989) and regulatory G-protein alpha subunits by s-acylation (Wedegaertner et al., 1993; Kleuss and Krause, 2003). A common motif for many PATs is the zinkfinger DHHC motif which was described Putilina et al., 1999 and up to now 23 genes with such an motif could be identified in the mouse and human databases (Fernandez-Hernando et al., 2006).

With iPAT expressed in Caco-2 cells we found out of the group of the ZDHHC proteins a comparatively highly (see Fig. 1) expressed member in intestinal cells. For the first time the *Homo sapiens* protein was explicitly mentioned in the context of a gene expression profile in cancer cells (Choi et al., 2007). Under the name GODZ this protein has been identified previously in the mouse forebrain (Uemura et al., 2002). The confocal data of the CFP-tagged iPAT provide a good insight of this localization (see fig. 4). The Golgi association obvious when taking into account the Golgi disintegration during apoptosis (see fig. 4 C and D, results and Chandran & Machamer, 2008).

4.3 The Function of the iPAT

The palmitoylation targets of the iPAT are generally unknown apart from a few neuronal proteins. A S-acylation target of iPAT is the endothelial nitric oxide synthase but this function can also performed by DHHC-2, -7, -8, and -21 (Fernandez-Hernando et al., 2006).

Also the gamma 2 subunit of the GABA(A) receptor seems to be a probable target

but is also palmitoylated be the DHHC-7 palmitoyltransferase, which is more common in the neurons (Keller et al., 2004). Another neuronal receptor, the AMPA receptor seems to be effected either by the iPAT or by DHHC-7 (Hayashi et al., 2005).

4.3.1 Implications on the Morphology

The alterations of cell growth and morphology after siRNA treatment gave a hint that other functions may be affected. Implications of health and disease in the context of palmitoyltransferases have been observed. Especially in the neural system a number of disease associated changes in palmitoyltransferases could be shown. The loss of function in the ZDHHC8 leads to the neurodevelopmental deficits in mice (Mukai et al., 2008). In prostate cancer palmitoylation events seem to stabilize catenin in the plasmamembrane (Fiorentino et al., 2008). The analysis of cell size, circularity, and transepithial resistance (TER) provided an interpretion of the cell growth, measured by culture dish coverage, that implies an unchanged or even increased netto growth rate (figs. 7, 8, 10). There are cues that ras proteins are involved in control of cell proliferation, transformation, and morpholoy (Matallanas et al., 2006, Li et al., 2007a, Li et al., 2007b).

Another possibility for altered cell growth may be s-acylation of tubulin (Hiol et al., 2003). Interestingly the ultrastuctures from the electromicrographs revealed alterations that point to an influence of the downregulation of iPAT on the cytoskeleton and membranous intracellular structures (see fig. 9). In figure 15 an examination of f-actin reveal a difference between the both types Caco-2 cell lines. The profile of the Caco-2 wild type f-actin distribution provide a more ordered image than its iPAT reduced counterpart. A view that is comparable to the data from the electronmicrographs. Those date fit to a colitis like effects. The occurance of small vesicular structures during induced colitis in mice (Bou-Fersen et al., 2008) is quite similar to the observed comparative large vesicular structures found

in iPAT down regulated Caco-2 cells. Therefore a closer look at the physiological effects of the down regulation of iPAT in Caco-2 cells was necessary to provide information of the iPAT function in Caco-2 cells.
The increase in the TER cannot be explained by those effects. An increase of the TER requires a change in the membrane structure. Comparing the lipid composition (see fig. 12) of Caco-2 wild type and iPAT deficient Caco-2 cells did not help to explain the TER data, contrarily, a decrease of the isolating hydrophobic lipids could be measured. And on the other side an accumulation of less hydrophobic lipids with unsaturated fatty acids could be observed.

As the ultrastructural electronmicrographs revealed the “quality” of the villi is strongly affected in iPAT deficient Caco-2 cells (fig. 9 A and B). This again resembles the phenotype of Colitis (Li et al., 2007a, Bou-Fersen et al., 2008).

With a changed morphology of the brushborder membrane, a altered uptake of nutrients is to be expected. One of the best characterized nutrient uptake systems due to its relatively easy accessibility is glucose (Philpott et al., 1992).
Control of the glucose uptake by palmitoylation dependent regulatory proteins can be deduced out of the literature. Heat shock protein 70 (hsp70) up-regulates the sodium-dependent glucose transporter (SGLT1) (Ikari et al., 2002) and is directed to the membrane by interaction with a cysteine string protein α (csp_{α}), a group of proteins that are generally s-acylated (Boal et al., 2007).

4.3.2 Implications on the Physiology

Our data show also in this context putative contradictory results: if iPAT was involved in the s-acylation of csp_{α} and hence the positive control of glucose uptake, a stable expression of siRNA against iPAT should reduce the glucose uptake activity. A reduction in fact can be noted when a general inhibitor of s-acylation, 2-bromopalmitate, is applied (see fig. 11). The observed raise of glucose

uptake in the iPAT deficient Caco-2 cells can only be explained by redistributed palmitate. Palmitate has to be considered as an intracellular static pool with low concentration tolerances due to its high hydrophobicity. It only can be tolerated in small concentrations before producing micelles (Levin et al., 2009).

A comparison of the quantification of cellular fatty acid composition between Caco-2 wild type cells and iPAT deficient Caco-2 cells approves this (see fig. 13).

A regulation of intracellular palmitate-CoA concentration, the substrate of palmitoyltransferases, takes generally place by cytoplasmic acyl-CoA binding proteins (ACBPs) (Faergeman and Knudsen, 1997). Keeping in mind that iPAT is highly expressed in Caco-2 wild type cells, the loss of a majority of iPAT has to produce an intracellular excess of palmitate-CoA, that cannot be caught by ACBPs.

4.4 Regulation of the Palmitate Concentration

Downstream of the fatty acid synthesis, which stops at C16:0-CoA (palmitate-CoA) the modifications of the fatty acids take place. Those are prolongation, desaturation, and lipid biosynthesis (Zakim & Herman, 1969). If iPAT controls the intracellular level of palmitate-CoA, the level of processed palmitate should raise also if iPAT is reduced. We could show that this is in fact the case (see figs. 13).

An increase in the unsatturated long chain fatty acids compared to the situation in untreated cells approves the higher availability of palmitate for further processing. As mentioned above the lipid composition also seems to have shifted toward hydrophilic lipids. This can be explained as a result of the enhanced intracellular production of long chained unsaturated fatty acids.

The fact that an oversupply of a highly hydrophobic fatty acid like palmitate finally

lead to a reduction of hydrophobic elements in the membrane appears to be confusing. The reason for the shift towards in many cases multiple unsatturated fatty acids can be found in the simultaneous enforced influx of glucose. Since glucose has been shown to be an inductor of stearoyl-CoA desaturase (Jones et al., 1998) an increase of unsaturated long chain fatty acids has to be the result. Following the elongation of surplus palmitate the substrate for stearoyl-CoA desaturases does exist in higher amounts in the iPAT deficient Caco-2 than in wild type Caco-2 cells.

4.5 Model for Colitis

The starting point of this thesis had been the analysis of DRMs and their associated proteins. Changing the lipid composition of those structures should have consequences for the regarding proteins.

In this study the sucrase-isomaltase (SI) was used as a raft associated membrane bound protein (Alfalah et al., 1999) to observe effects of reduced iPAT on such proteins. Because of the significant changes in the lipids, which resembles a resolution of the DRMs, marked changes in the distribution of the SI were expected. Our results show convincing changes in the DRM association of the SI without a complete block of internalisation in DRMs, what implies a transport and maturation mechanism independent of palmitoylation and intact DRMs (fig. 16). Proteins, like DPP4, that are independent of DRMs anchored in the membrane are not affected. Nevertheless, the disruption of DRM association of the SI connected with associated proteins like Annexin 2 or typical raft proteins like Flotilin mirrors an image of colitis situations (Li et al., 2008). A significant difference in the division of SI in the brush border membrane contingent with a high enrichment in the iPAT reduced cells compared to the wild type cells does not contradict those data. This may reflect a palmitoylation dependent mechanism for the retention of the SI. Which kind of regulation may take place at this particular step remain to be

elucidated.

Feeding experiments with polyunsatturated fatty acids (PUFAs) in induced colitis models (Li et al., 2008) strongly point to the importance of the fatty acid metabolism in barrier function and maintenance of the brush border membrane. The results of those experiments strongly resemble the effect of the down regulation of the iPAT: although acute physiological effects diminished, a reassociation of proteins with DRMs did not occur.

It is unlikely, that the iPAT take influence directly on the SI and database searches as visualized in figure 17 could not provide any hints on an interaction. The closest indirect associated protein out of the database analysis was annexin. Although the technique of FRET offered an opportunity for testing a number of interactions none of the used model proteins did produce any positive result in interacting with iPAT. Nevertheless the analysis of the FRET data provided the opportunity to produce a sketch of the transport system in which the SI and LPH are involved in(fig 19 B). The data support an closer association of the SI to the actin cytoskeleton than to the tubulin. On the other hand, the LPH seems be able to use both systems in the same amount with a lower affinity to actin. This fits to the data provided by Jacob et al. (2003). Interestingly a positive signal with the iPAT was produced by the signal sequence of the glycosyltransferase.

All mentioned data and explanations are not able to explain the increase in the TER. The missing factor can be found in the glycolipids. The analysis of the glycolipid composition established a additional hydrophilic glycolipid in the iPAT reduced Caco-2 cell line. Glycolipids are able to bind lectin like structures, a well known fact in the context of the identification of blood groups (Haslam et al., 2008). Recently Wrackmeyer et al. (Wrackmeyer et al., 2006a) could show that a lectin, intelectin, to connect a number of Glycolipids and produce a comparable robust network. The results in figure 20 show that the isolated glycolipid is able to bind lectins. This proposes that the increase in the TER is in its majority the result of interconnected lectins and glycolipids (fig. 21).

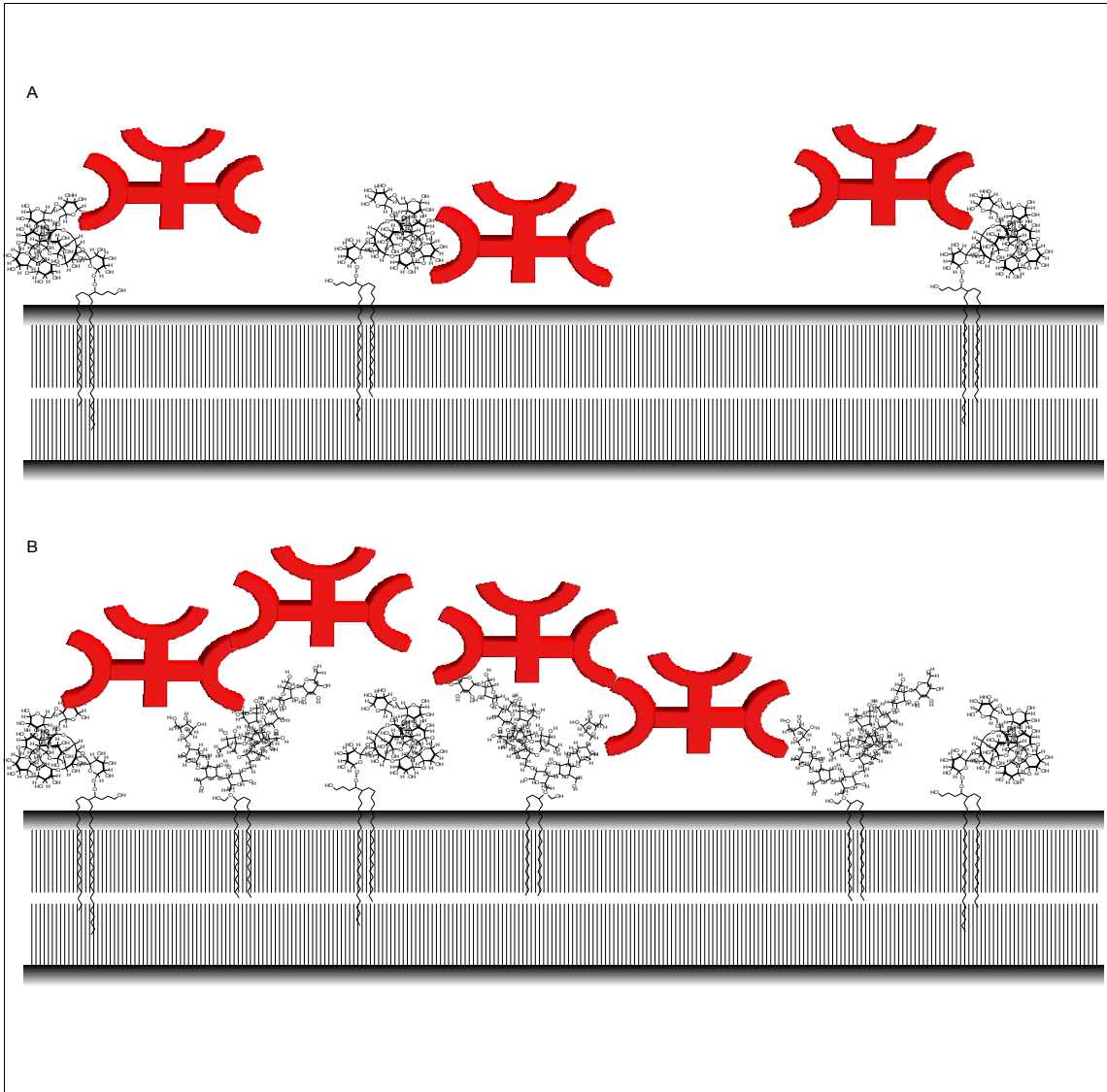

Figure 21: Lectin binding of glycolipids. Visualization of the Influence of glyclipids on the stability of a membrane seen in the context of lectin binding with or without an additional glycolipid.
A) Under normal, wild type, conditions the number of high glycosylated lipids is low. Glycolipid-lectin interactions are limited.
B) An additional hydrophobic glycolipid enables a larger number of lectins to bind to the surface. This causes a more rigid packaging of the lectin-glycolipid network.

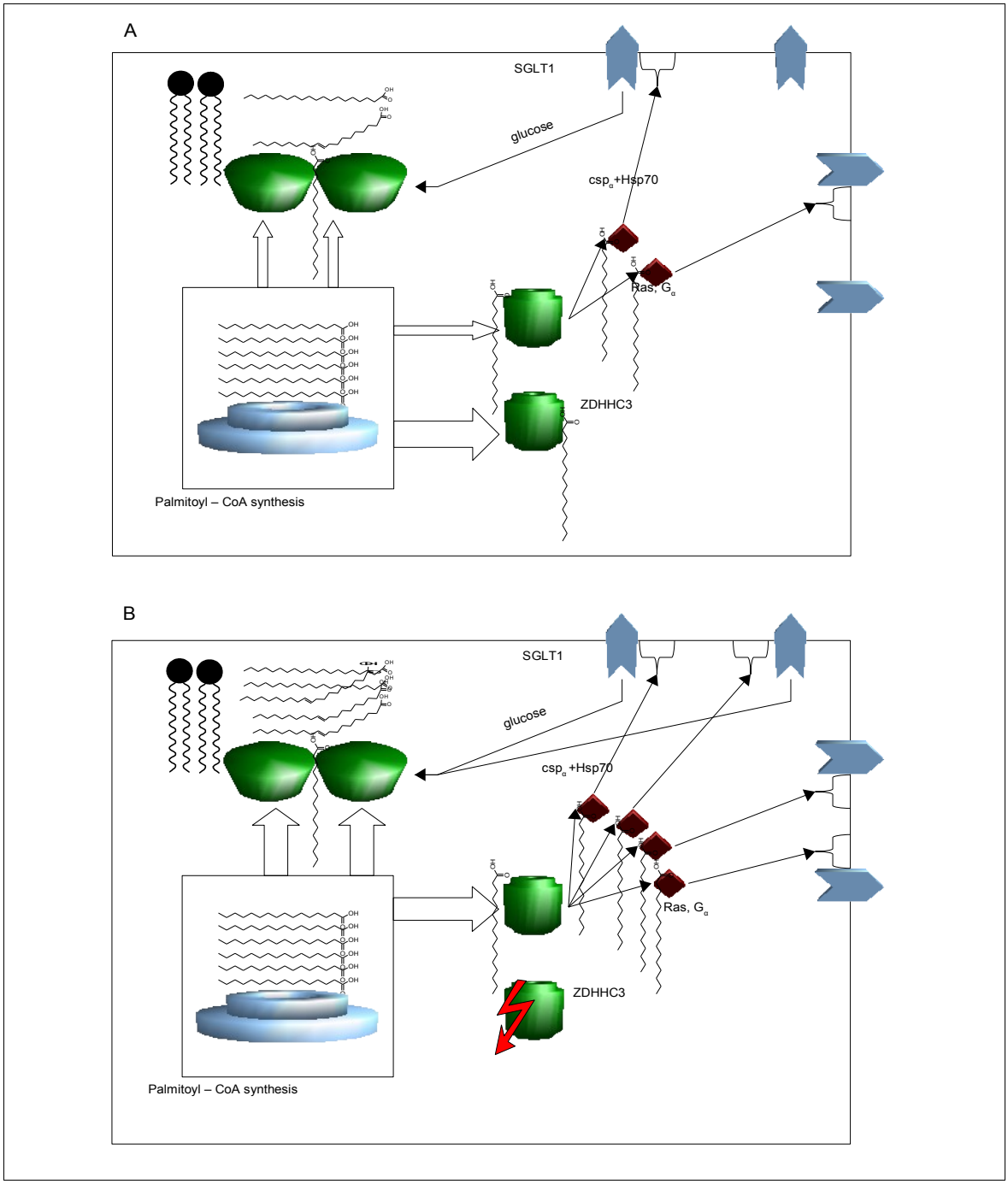

Figure 22: Storage function of the iPAT. This model proposes a storage function of the iPAT indicated by the usage of siRNA.
A) Normal function of iPAT in Caco-2 cells. The iPAT takes over palmitate out of the neosynthesis of fatty acids by the FAS complex.
B) Introduction of siRNA against iPAT leads to a surplus of palmitate in the cells, that has to be utilized immediately.

Therefore a model can be proposed (see fig. 22), in which the palmitoyltransferase iPAT not only mediate the transfer of palmitate or other long chain fatty acids (Hallak et al., 1994; Dietrich and Ungermann, 2004) to other proteins but also balance concentration of intracellular palmitate-CoA level, thus functioning as a fine tuning instrument in multiple cellular processes. In our case this could be observed in the increase of long chain fatty acids, the uptake of glucose, and the changed cell morphology. Due to the high expression rate, iPAT provides a field of activity comparable to ACBPs on a membrane bound level beside its own palmitoylation targets.

4.6 Perspective

The observation of this sensitive tuning system presented here offers the an opportunity to influence intracellular systems by means of a comparable simple molecule, the palmitate. Considering the presented effects, the combination of enhanced glucose uptake and the retention of SI at the brush border membrane, implications for diseases like general deficiencies in the digestion of sucrose or diabetis are possible. Targeting the iPAT may in future offer the possibility for fine tuning and recovering of intestinal diseases like colitis. Moreover the role of glycolipids in the establishment of DRMs remain to be elucidated providing a possible interplay with nontransmembranous like lectins proteins to stabilize the plasmamembrane.

5.Literature

Abramoff et al., 2004: Abramoff, M.D., Magelhaes, P.J., Ram, S.J., Image Processing with ImageJ, Biophotonics International,11,36-42

Alfalah et al., 1999: M. Alfalah and R. Jacob and U. Preuss and K.P. Zimmer and H. Naim and H.Y. Naim, O-linked glycans mediate apical sorting of human intestinal sucrase-isomaltase through association with lipid rafts., Curr Biol,9,593-6

Alfalah et al., 2005: Marwan Alfalah and Gabi Wetzel and Ina Fischer and Roger Busche and Erwin E Sterchi and Klaus-Peter Zimmer and Hans-Peter Sallmann and Hassan Y Naim, A Novel Type of Detergent-resistant Membranes May Contribute to an Early Protein Sorting Event in Epithelial Cells., J Biol Chem,280,42636-43

Arad & Gotsman, 1999: Arad N, Gotsman C., Enhancement by image-dependent warping., IEEE Trans Image Process,8(8),1063-74

Arcaro et al., 2006: Alexandre Arcaro and Muriel Aubert and Maria E Espinosa Del Hierro and Umme K Khanzada and Smaragda Angelidou and Teresa D Tetley and Anne G Bittermann and Margaret C Frame and Michael J Seckl, Critical role for lipid raft-associated Src kinases in activation of PI3K-Akt signalling., Cell Signal,

Arnold & Linke, 2007: Arnold T, Linke D. , Phase separation in the isolation and purification of membrane proteins., Biotechniques,43(4),427-30, 432, 434

Babu et al., 2004: Praveen Babu and Robert J Deschenes and Lucy C Robinson, Akr1p-dependent palmitoylation of Yck2p yeast casein kinase 1 is necessary and

sufficient for plasma membrane targeting., J Biol Chem,279,27138--27147
Basu, 2004: Joyoti Basu, Protein palmitoylation and dynamic modulation of protein function, CURRENT SCIENCE,87,212-217

Boal et al., 2007: Frédéric Boal and Séverine Le Pevelen and Celina Cziepluch and Pier Scotti and Jochen Lang, Cysteine-string protein isoform beta (Cspbeta) is targeted to the trans-Golgi network as a non-palmitoylated CSP in clonal beta-cells., Biochim Biophys Acta,1773,109-119

Bou-Fersen et al., 2008: Bou-Fersen AM, Anim JT, Khan I., Experimental colitis is associated with ultrastructural changes in inflamed and uninflamed regions of the gastrointestinal tract., Med Princ Pract,17(3),190-6

Brett et al., 1971: D. Brett and D. Howling and L. J. Morris and A. T. James, Specificity of the fatty acid desaturases. The conversion of saturated to monoenoic acids., Arch Biochem Biophys,143,535-547

Bromley et al., 2001: Bromley SK, Burack WR, Johnson KG, Somersalo K, Sims TN, Sumen C, Davis MM, Shaw AS, Allen PM, Dustin ML., The immunological synapse., Annu Rev Immunol.,19,375-96

Castelletti et al., 2008: Castelletti D, Alfalah M, Heine M, Hein Z, Schmitte R, Fracasso G, Colombatti M, Naim HY. , Different glycoforms of prostate-specific membrane antigen are intracellularly transported through their association with distinct detergent-resistant membranes., Biochem J.,409(1),149-57

Chakrabandhu et al., 2007: Krittalak Chakrabandhu and Zoltán Hérincs and Sébastien Huault and Britta Dost and Ling Peng and Fabien Conchonaud and Didier Marguet and Hai-Tao He and Anne-Odile Hueber, Palmitoylation is required for efficient Fas cell death signaling., EMBO J,26,209-220

Chandran & Machamer, 2008: Chandran S, Machamer CE., Acute perturbations in Golgi organization impact de novo sphingomyelin synthesis., Traffic,9(11),1894-904

Choi et al., 2007: Choi YW, Bae SM, Kim YW, Lee HN, Kim YW, Park TC, Ro DY, Shin JC, Shin SJ, Seo JS, Ahn WS., Gene expression profiles in squamous cell cervical carcinoma using array-based comparative genomic hybridization analysis., Int J Gynecol Cancer,17(3),687-96

Delacour et al., 2006: Delphine Delacour and Catharina I Cramm-Behrens and Hervé Drobecq and Andre Le Bivic and Hassan Y Naim and Ralf Jacob, Requirement for galectin-3 in apical protein sorting., Curr Biol,16,408-14

Dietrich and Ungermann, 2004: Lars E P Dietrich and Christian Ungermann, On the mechanism of protein palmitoylation., EMBO Rep,5,1053-1057

Duncan and Gilman, 1996: J. A. Duncan and A. G. Gilman, Autoacylation of G protein alpha subunits., J Biol Chem,271,23594-23600

Dunphy et al., 2000: J. T. Dunphy and H. Schroeder and R. Leventis and W. K. Greentree and J. K. Knudsen and J. R. Silvius and M. E. Linder, Differential effects of acyl-CoA binding protein on enzymatic and non-enzymatic thioacylation of protein and peptide substrates., Biochim Biophys Acta,1485,185-198

Faergeman and Knudsen, 1997: N. J. Faergeman and J. Knudsen, Role of long-chain fatty acyl-CoA esters in the regulation of metabolism and in cell signalling., Biochem J,323 (Pt 1),1-12

Fernandez-Hernando et al., 2006: Carlos Fernández-Hernando and Masaki

Fukata and Pascal N Bernatchez and Yuko Fukata and Michelle I Lin and David S Bredt and William C Sessa, Identification of Golgi-localized acyl transferases that palmitoylate and regulate endothelial nitric oxide synthase., J Cell Biol,174,369-377

Fiorentino et al., 2008: Fiorentino M, Zadra G, Palescandolo E, Fedele G, Bailey D, Fiore C, Nguyen PL, Migita T, Zamponi R, Di Vizio D, Priolo C, Sharma C, Xie W, Hemler ME, Mucci L, Giovannucci E, Finn S, Loda M., Overexpression of fatty acid synthase is associated with palmitoylation of Wnt1 and cytoplasmic stabilization of beta-catenin in prostate cancer., Lab Invest.,88(12),1340-8

Fischer et al., 2006: Karin Fischer and Simon Voelkl and Jana Berger and Reinhard Andreesen and Thomas Pomorski and Andreas Mackensen, Antigen recognition induces phosphatidylserine exposure on the cell surface of human CD8+ T cells., Blood,108,4094-4101

Fitzner et al., 2006: Dirk Fitzner and Anja Schneider and Angelika Kippert and Wiebke Möbius and Katrin I Willig and Stefan W Hell and Gertrude Bunt and Katharina Gaus and Mikael Simons, Myelin basic protein-dependent plasma membrane reorganization in the formation of myelin., EMBO J,25,5037--5048

Fulco, 1974: A. J. Fulco, Metabolic alterations of fatty acids., Annu Rev Biochem,43,215-241

Greaves and Chamberlain, 2007: Jennifer Greaves and Luke H Chamberlain, Palmitoylation-dependent protein sorting., J Cell Biol,176,249-254

Grzybek et al., 2005: Grzybek M, Kozubek A, Dubielecka P, Sikorski AF., Rafts-the current picture, Folia Histochem Cytobiol.,43(1),3-10

Hallak et al., 1994: H. Hallak and L. Muszbek and M. Laposata and E. Belmonte

and L. F. Brass and D. R. Manning, Covalent binding of arachidonate to G protein alpha subunits of human platelets., J Biol Chem,269,4713-4716

Hanada, 2003: Kentaro Hanada, Serine palmitoyltransferase, a key enzyme of sphingolipid metabolism., Biochim Biophys Acta,1632,16-30

Hancock et al., 1989: J. F. Hancock and A. I. Magee and J. E. Childs and C. J. Marshall, All ras proteins are polyisoprenylated but only some are palmitoylated., Cell,57,1167-1177

Hanzal-Bayer & Hancock, 2007: Hanzal-Bayer MF, Hancock JF. , Lipid rafts and membrane traffic., FEBS Lett. ,581(11),2098-104

Haslam et al., 2008: Haslam SM, Julien S, Burchell JM, Monk CR, Ceroni A, Garden OA, Dell A., Characterizing the glycome of the mammalian immune system., Immunol Cell Biol.,86(7),564-73

Hayashi et al., 2005: Hayashi T, Rumbaugh G, Huganir RL, Differential regulation of AMPA receptor subunit trafficking by palmitoylation of two distinct sites., Neuron,47(5),709-23

Hiol et al., 2003: Abel Hiol and Joan M Caron and Charles D Smith and Teresa L Z Jones, Characterization and partial purification of protein fatty acyltransferase activity from rat liver., Biochim Biophys Acta,1635,10-19

Hooper and Bashir, 1991: N. M. Hooper and A. Bashir, Glycosyl-phosphatidylinositol-anchored membrane proteins can be distinguished from transmembrane polypeptide-anchored proteins by differential solubilization and temperature-induced phase separation in Triton X-114., Biochem J,280 (Pt 3),745-751

Ikari et al., 2002: Akira Ikari and Mika Nakano and Kazuya Kawano and Yasunobu Suketa, Up-regulation of sodium-dependent glucose transporter by interaction with heat shock protein 70., J Biol Chem,277,33338-33343

Jacob et al., 2003: Ralf Jacob and Martin Heine and Marwan Alfalah Hassan Y Naim, Distinct cytoskeletal tracks direct individual vesicle populations to the apical membrane of epithelial cells., Curr Biol,13,607-12

Jacob et al., 2004: Ralf Jacob and Martin Heine and Jürgen Eikemeyer and Nadine Frerker and Klaus-Peter Zimmer and Ursula Rescher and Volker Gerke and Hassan Y Naim, Annexin II is required for apical transport in polarized epithelial cells., J Biol Chem,279,3680-4

Jones et al., 1979: Jones LM, Cockcroft S, Michell RH., Stimulation of phosphatidylinositol turnover in various tissues by cholinergic and adrenergic agonists, by histamine and by caerulein., Biochem J.,182(3),669-76

Jones et al., 1998: B. H. Jones and M. K. Standridge and K. J. Claycombe and P. J. Smith and N. Moustaïd-Moussa, Glucose induces expression of stearoyl-CoA desaturase in 3T3-L1 adipocytes., Biochem J,335 (Pt 2),405-408

Keller et al., 2004: Cheryl A Keller and Xu Yuan and Patrizia Panzanelli and Michelle L Martin and Melissa Alldred and Marco Sassoè-Pognetto and Bernhard Lüscher, The gamma2 subunit of GABA(A) receptors is a substrate for palmitoylation by GODZ., J Neurosci,24,5881-5891

Kim et al., 1989: K. H. Kim and F. López-Casillas and D. H. Bai and X. Luo and M. E. Pape, Role of reversible phosphorylation of acetyl-CoA carboxylase in long-chain fatty acid synthesis., FASEB J,3,2250-2256

Kleuss and Krause, 2003: Christiane Kleuss and Eberhard Krause, Galpha(s) is palmitoylated at the N-terminal glycine., EMBO J,22,826-832

Koscielak, 1963: Koscielak J. , BLOOD GROUP A SPECIFIC GLYCOLIPIDS FROM HUMAN ERYTHROCYTES., Biochim Biophys Acta.,78,313-28

Lam et al., 2006: Lam, Karen K Y and Davey, Michael and Sun, Beimeng and Roth, Amy F and Davis, Nicholas G and Conibear, Elizabeth, Palmitoylation by the DHHC protein Pfa4 regulates the ER exit of Chs3., J Cell Biol,174,19-25

Levin et al., 2009: Levin LB, Nachliel E, Gutman M, Tsfadia Y., Molecular dynamics study of the interaction between fatty acid binding proteins with palmitate mini-micelles., Mol Cell Biochem.,Epub ahead of Print

Li et al., 2007a: Hong Li and Hou-Fa Cao and Yuan Li and Mei-Ling Zhu and Jun Wan, Changes in gene-expression profiles of colon carcinoma cells induced by wild type K-ras2., World J Gastroenterol,13,4620-4625

Li et al., 2007b: Hong Li and Hou-Fa Cao and Jun Wan and Yuan Li and Mei-Ling Zhu and Po Zhao, Growth inhibitory effect of wild-type Kras2 gene on a colonic adenocarcinoma cell line., World J Gastroenterol,13,934-938

Li et al., 2008: Qiurong Li and Qiang Zhang and Min Zhang and Chenyang Wang and Zhenxin Zhu and Ning Li and Jieshou Li, Effect of n-3 polyunsaturated fatty acids on membrane microdomain localization of tight junction proteins in experimental colitis., FEBS J,275,411-420

Liang et al., 2007: Shuang Liang and Min Wang and Richard I Tapping and Vitaly Stepensky and Hesham F Nawar and Martha Triantafilou and Kathy Triantafilou

and Terry D Connell and George Hajishengallis, Ganglioside GD1a is an essential coreceptor for toll-like receptor 2 signaling in response to the B subunit of type IIB enterotoxin., J Biol Chem,282,7532-7542

Matallanas et al., 2006: David Matallanas and Victoria Sanz-Moreno and Imanol Arozarena and Fernando Calvo and Lorena Agudo-Ibáñez and Eugenio Santos and María T Berciano and Piero Crespo, Distinct utilization of effectors and biological outcomes resulting from site-specific Ras activation: Ras functions in lipid rafts and Golgi complex are dispensable for proliferation and transformation., Mol Cell Biol,26,100-116

Merrill et al., 2008: Merrill AH Jr, Stokes TH, Momin A, Park H, Portz BJ, Kelly S, Wang E, Sullards MC, Wang MD., Sphingolipidomics: a valuable tool for understanding the roles of sphingolipids in biology and disease., J Lipid Res.,Epub ahead of print

Mitchell et al., 2006: David A Mitchell and Anant Vasudevan and Maurine E Linder and Robert J Deschenes, Protein palmitoylation by a family of DHHC protein S-acyltransferases., J Lipid Res,47,1118-1127

Mukai et al., 2008: Mukai J, Dhilla A, Drew LJ, Stark KL, Cao L, MacDermott AB, Karayiorgou M, Gogos JA, Palmitoylation-dependent neurodevelopmental deficits in a mouse model of 22q11 microdeletion., Nat Neurosci.,11(11),1302-10

Naim et al., 1988a: H. Y. Naim and E. E. Sterchi and M. J. Lentze, Structure, biosynthesis, and glycosylation of human small intestinal maltase-glucoamylase., J Biol Chem,263,19709-17

Oriolo et al., 2007: Oriolo AS, Wald FA, Canessa G, Salas PJ., GCP6 binds to intermediate filaments: a novel function of keratins in the organization of

microtubules in epithelial cells., Mol Biol Cell.,18(3),781-94

Orlowski et al., 2007: Orlowski S, Come'ra C, Terce' F, Collet X., Lipid rafts: dream or reality for cholesterol transporters?, Eur Biophys J.,36(8),869-85

Palmer et al. 2007: Christopher P Palmer and Robert Mahen and Eva Schnell and Mustafa B A Djamgoz and Ebru Aydar, Sigma-1 receptors bind cholesterol and remodel lipid rafts in breast cancer cell lines., Cancer Res,67,11166-11175

Pechlivanis and Kuhlmann, 2006: Markos Pechlivanis and Juergen Kuhlmann, Hydrophobic modifications of Ras proteins by isoprenoid groups and fatty acids--More than just membrane anchoring., Biochim Biophys Acta,1764,1914-1931

Peretti et al., 2005: N. Peretti and V. Marcil and E. Drouin and E. Levy, Mechanisms of lipid malabsorption in Cystic Fibrosis: the impact of essential fatty acids deficiency., Nutr Metab (Lond),2,11

Petit et al., 2006: Chad M Petit and Vladimir N Chouljenko and Arun Iyer and Robin Colgrove and Michael Farzan and David M Knipe and K. G. Kousoulas, Palmitoylation of the cysteine-rich endodomain of the SARS-coronavirus spike glycoprotein is important for spike-mediated cell fusion., Virology,360,264-274

Philpott et al., 1992: Philpott DJ, Butzner JD, Meddings JB., Regulation of intestinal glucose transport., Can J Physiol Pharmacol.,70(9),1201-7

Pol et al., 2005: Albert Pol and Sally Martin and Manuel A Fernández and Mercedes Ingelmo-Torres and Charles Ferguson and Carlos Enrich and Robert G Parton, Cholesterol and fatty acids regulate dynamic caveolin trafficking through the Golgi complex and between the cell surface and lipid bodies., Mol Biol Cell,16,2091-2105

Polishchuk et al., 2004: Roman Polishchuk and Alessio Di Pentima and Jennifer Lippincott-Schwartz, Delivery of raft-associated, GPI-anchored proteins to the apical surface of polarized MDCK cells by a transcytotic pathway., Nat Cell Biol,6,297-307

Putilina et al., 1999: T. Putilina and P. Wong and S. Gentleman, The DHHC domain: a new highly conserved cysteine-rich motif., Mol Cell Biochem,195,219-226

Rasband 1997-2008: Rasband, W.S, , U. S. National Institutes of Health, Bethesda, Maryland, USA,http://rsb.info.nih.gov/ij/

Raymond et al., 2007: F. Lucy Raymond and Patrick S Tarpey and Sarah Edkins and Calli Tofts and Sarah O'Meara and Jon Teague and Adam Butler and Claire Stevens and Syd Barthorpe and Gemma Buck and Jennifer Cole and Ed Dicks and Kristian Gray and Kelly Halliday and Katy Hills and Jonathon Hinton and David Jones and Andrew Menzies and Janet Perry and Keiran Raine and Rebecca Shepherd and Alexandra Small and Jennifer Varian and Sara Widaa and Uma Mallya and Jenny Moon and Ying Luo and Marie Shaw and Jackie Boyle and Bronwyn Kerr and Gillian Turner and Oliver Quarrell and Trevor Cole and Douglas F Easton and Richard Wooster and Martin Bobrow and Charles E Schwartz and Jozef Gecz and Michael R Stratton and P. Andrew Futreal, Mutations in ZDHHC9, which encodes a palmitoyltransferase of NRAS and HRAS, cause X-linked mental retardation associated with a Marfanoid habitus., Am J Hum Genet,80,982-987

Saotome et al., 2004: Saotome I, Curto M, McClatchey AI., Ezrin is essential for epithelial organization and villus morphogenesis in the developing intestine., Dev Cell.,6(6),855-64

Schuck et al., 2003: Sebastian Schuck and Masanori Honsho and Kim Ekroos and Andrej Shevchenko and Kai Simons, Resistance of cell membranes to different detergents., Proc Natl Acad Sci U S A,100,5795-5800

Schweizer et al., 1996: A. Schweizer and S. Kornfeld and J. Rohrer, Cysteine34 of the cytoplasmic tail of the cation-dependent mannose 6-phosphate receptor is reversibly palmitoylated and required for normal trafficking and lysosomal enzyme sorting., J Cell Biol,132,577-584

Seddon et al., 2004: Seddon AM, Curnow P, Booth PJ. , Membrane proteins, lipids and detergents: not just a soap opera., Biochim Biophys Acta.,1666(1-2),105-17

Sengupta et al., 2007: Sengupta P, Baird B, Holowka D. , Lipid rafts, fluid/fluid phase separation, and their relevance to plasma membrane structure and function., Semin Cell Dev Biol,18(5),583-90

Simons and Ikonen, 1997: K. Simons and E. Ikonen, Functional rafts in cell membranes., Nature,387,569-72

Smotrys and Linder, 2004: Jessica E Smotrys and Maurine E Linder, Palmitoylation of intracellular signaling proteins: regulation and function., Annu Rev Biochem,73,559-587

Stoeckli and Rohrer, 2004: Jacqueline Stöckli and Jack Rohrer, The palmitoyltransferase of the cation-dependent mannose 6-phosphate receptor cycles between the plasma membrane and endosomes., Mol Biol Cell,15,2617-26

Tsai et al., 1998: S. C. Tsai and R. Adamik and J. X. Hong and J. Moss and M. Vaughan and H. Kanoh and J. H. Exton, Effects of arfaptin 1 on guanine nucleotide-dependent activation of phospholipase D and cholera toxin by ADP-

ribosylation factor., J Biol Chem,273,20697-701

Uemura et al., 2002: Uemura T, Mori H, Mishina M., Isolation and characterization of Golgi apparatus-specific GODZ with the DHHC zinc finger domain., Biochem Biophys Res Commun.,296(2),492-6

Vilhardt and van Deurs, 2004: Frederik Vilhardt and Bo van Deurs, The phagocyte NADPH oxidase depends on cholesterol-enriched membrane microdomains for assembly, EMBO J.,23,739-748

Wedegaertner et al., 1993: P. B. Wedegaertner and D. H. Chu and P. T. Wilson and M. J. Levis and H. R. Bourne, Palmitoylation is required for signaling functions and membrane attachment of Gq alpha and Gs alpha., J Biol Chem,268,25001-25008

Wrackmeyer et al., 2006a: Uta Wrackmeyer and Gert Hansen and Tsukasa Seya and E. Danielsen, Intelectin: A Novel Lipid Raft-Associated Protein in the Enterocyte Brush Border., Biochemistry,45,9188-9197

Yard et al., 2007: Beverley A Yard and Lester G Carter and Kenneth A Johnson and Ian M Overton and Mark Dorward and Huanting Liu and Stephen A McMahon and Muse Oke and Daphné Puech and Geoffrey J Barton and James H Naismith and Dominic J Campopiano, The structure of serine palmitoyltransferase; gateway to sphingolipid biosynthesis., J Mol Biol,370,870-886

Zakim & Herman, 1969: Zakim D, Herman RH., Regulation of fatty acid synthesis., Am J Clin Nutr.,22(2),200-13

Abbreviations

AMPA	=	α-Amino-3-hydroxy-5-methyl-4-isoxazol-propionic acid
APT	=	acyl-protein thioesterase
ARF	=	ADP ribosylation factor
CFP	=	Cyan fluorescence protein
CHS-3	=	Chitin synthase 3
CoA	=	Co-enzyme A
COPB	=	Beta coat protein
DPP4	=	dipeptidyl peptidase
DRM	=	Detergent resistant membrane
ER	=	Endoplasmic retiulum
FAS	=	fatty acid synthase complex
FRET	=	Fluorescence resonance energy transfer
gage1	=	G antigen 1
GODZ	=	Golgi apparatus–specific protein with the DHHC zinc finger domain
GPI	=	glycosyl phosphatidylinositol
GT	=	glycosyltransferase
HSN1	=	hereditary sensory neuropathy type I
HSP70	=	Heatshock protein 70
iPAT	=	intestinal PAT ()
KDS	=	3-ketodihydrosphingosine
MYL 6	=	Myosin light polypeptide
NADPH	=	Nicotinamidediphosphate + H^+
PAGE	=	Poly acrylamide gel electrophoresis
PAT	=	Proteine acyl transferase
PBS	=	Phosphate buffered saline
PCR	=	Polymerase chain reaction
PI3K	=	Phosphinositole 3 phosphate kinase

PUFA	=	Poly unsaturated fatty acids
RT-PCR	=	Reverse transcriptase PCR
SARS	=	Severe acute respiratory syndrome
SGLT1	=	sodium-dependent glucose transporter
SI	=	sucrosase-isomaltase
SPT	=	serine palmitoyltransferase
SYT 3	=	Synaptotagmin 3
SYTL 4	=	Synaptotagmin like protein 4
TER	=	Transepithelial resistance
TLC	=	Thin layer chromatography
TPPC	=	Trafficking protein particle complex
YFP	=	Yellow fluorescence protein

Appendix

BLAST Alignment ZDHHC3

Alignment of the human ZDHHC3 protein (iPAT) using NCBI-Blast. Only the top 10 matching sequences are shown.

```
NP 057682 ZDHHC3 [Homo sapiens]          1    MMLIPTHHFRNIERKPEYLQPEKCVPPPYPGPVGTMWFIRDGCGIACAIVTWFLVLYAEF  60
ZDHHC3 isoform 7 [Pan troglodytes]       1    ............................................................  60
ZDHHC3 isoform 2 [Macaca mulatta]        1    .........D..................................................  60
ZDHHC3 (pred) [Canis familaris]          1    .........D.................H.S..............................  60
ZDHHC3 (pred) [Equus caballus]           1    .........D.............I...H.S..............................  60
ZDHHC3 (pred) isoform 2 [Canis fam.]     1    .........D.................H.S..............................  60
ZDHHC3 (pred) isoform 1 [Equus cab.]     1    .........D.............I...H.S..............................  60
ZDHHC3 [Rattus norvegicus]               1    .........D.............A...F..............................  60
ZDHHC3 [Bos taurus]                      1    .....A....D.............I...H.R.A..........................  60
ZDHHC3 (pred) isoform 5 [Canis fam.]     1    .........D.................H.S..............................  60
ZDHHC3 (pred) isoform 5 [Pan trog.]      1    ............................................................  60
ZDHHC3 (pred) isoform 3 [Macaca mul.]    1    .........D..................................................  60
ZDHHC3 [Mus musculus]                    1    .........D.............A...F...A.A..........................  60
BAC37939 unnamed prot. [Mus mus.]        1    .........D.............A...F...A.A..........................  60
ZDHHC3 isoform 3 [Pan trog.]             1     ...........................................................  59
ZDHHC3 (pred) isoform 1 [Macaca mul.]    1     .........D.................................................  59
ZDHHC3 (pred) isoform 4 [Pan trog.]      1     ...........................................................  59
ZDHHC3 (pred) isoform 2 [Pan trog.]      1     ...........................................................  59
ZDHHC3 (pred) isoform 3 [Canis fam.]     1    .........D.................H.S..............................  60
ZDHHC3 (pred) isoform 1 [Pan trog.]      1     ...........................................................  59

NP 057682 ZDHHC3 [Homo sapiens]         61   VVLFVMLIPSRDYVYSIINGIVFNLLAFLALASHCRAMLTDP------------------  102
ZDHHC3 isoform 7 [Pan troglodytes]       61   ..........................................------------------  102
ZDHHC3 isoform 2 [Macaca mulatta]        61   ..........................................------------------  102
ZDHHC3 (pred) [Canis familaris]          61   ..........................................------------------  102
ZDHHC3 (pred) [Equus caballus]           61   ..........................................------------------  102
ZDHHC3 (pred) isoform 2 [Canis fam.]     61   ..........................................------------------  102
ZDHHC3 (pred) isoform 1 [Equus cab.]     61   ..........................................------------------  102
ZDHHC3 [Rattus norvegicus]               61   .............A............................------------------  102
ZDHHC3 [Bos taurus]                      61   ................V...L.....................------------------  102
ZDHHC3 (pred) isoform 5 [Canis fam.]     61   ..........................................RRPAPCNKSLCSCKRSID  120
ZDHHC3 (pred) isoform 5 [Pan trog.]      61   ..........................................------------------  102
ZDHHC3 (pred) isoform 3 [Macaca mul.]    61   ..........................................------------------  102
ZDHHC3 [Mus musculus]                    61   .......V.....A.............................------------------  102
BAC37939 unnamed prot. [Mus mus.]        61   .......V.....A.............................------------------  102
ZDHHC3 isoform 3 [Pan trog.]             60   ..........................................VRTCTEMAFTLLGRGASF  119
ZDHHC3 (pred) isoform 1 [Macaca mul.]    60   ..........................................VSMKQCQTSSCPSKTGCD  119
ZDHHC3 (pred) isoform 4 [Pan trog.]      60   ..........................................VKSGHCRIGECTFQTTWD  119
ZDHHC3 (pred) isoform 2 [Pan trog.]      60   ..........................................------------------  101
ZDHHC3 (pred) isoform 3 [Canis fam.]     61   ..........................................V-----------------  103
ZDHHC3 (pred) isoform 1 [Pan trog.]      60   ..........................................------------------  101

NP 057682 ZDHHC3 [Homo sapiens]         103  -------------------GAVPKGNATKEF-IESLQLKPGQVVYKCPKC----CSIKPD  138
ZDHHC3 isoform 7 [Pan troglodytes]       103  -------------------.....-.....-.....----.....  138
ZDHHC3 isoform 2 [Macaca mulatta]        103  -------------------.....-.....-.....----.....  138
ZDHHC3 (pred) [Canis familaris]          103  -------------------.....-.....-.....----.....  138
ZDHHC3 (pred) [Equus caballus]           103  -------------------.....-.....-.....----.....  138
ZDHHC3 (pred) isoform 2 [Canis fam.]     103  -------------------.....-.....-.....----.....  138
ZDHHC3 (pred) isoform 1 [Equus cab.]     103  -------------------.....-.....-.....----.....  138
ZDHHC3 [Rattus norvegicus]               103  -------------------.....-.....-.....----.....  138
ZDHHC3 [Bos taurus]                      103  -------------------.....-.....-.....----.....  138
ZDHHC3 (pred) isoform 5 [Canis fam.]     121  PTSGSLCNEGIESIFSLLL.....-.....-.....----.....  175
ZDHHC3 (pred) isoform 5 [Pan trog.]      103  -------------------.....-.....-.....----.....  138
ZDHHC3 (pred) isoform 3 [Macaca mul.]    103  -------------------.....-.....-.....----.....  138
ZDHHC3 [Mus musculus]                    103  -------------------.....-.....-.....----.....  138
BAC37939 unnamed prot. [Mus mus.]        103  -------------------.....-.....-.....----.....  138
ZDHHC3 isoform 3 [Pan trog.]             120  PEKLDKPVSGRSKCLL---.....-.....-.....----.....  171
ZDHHC3 (pred) isoform 1 [Macaca mul.]    120  LICINGERLEGVTSIVL--.....-.....-.....----.....  172
ZDHHC3 (pred) isoform 4 [Pan trog.]      120  PTPVKVLGQGNNSVSQILA.....-.....-.....----.....  174
ZDHHC3 (pred) isoform 2 [Pan trog.]      102  -------------------.....-.....-.....----.....  137
ZDHHC3 (pred) isoform 3 [Canis fam.]     104  -------------------SEA.V.SGV..IGL.GAI..SLFKSLNSNI.LDRW.TSV.N  144
ZDHHC3 (pred) isoform 1 [Pan trog.]      102  -------------------.....-.....-.....----.....  137
```

```
NP 057682 ZDHHC3 [Homo sapiens]        139  RAHHC-------SVCKRCIRKMDHHCPWVNNCVGENNQKYFVLFTMYIALISLHALIMVG  191
ZDHHC3 isoform 7 [Pan troglodytes]     139  ..........-.....................................................  191
ZDHHC3 isoform 2 [Macaca mulatta]      139  ..........-.....................................................  191
ZDHHC3 (pred) [Canis familaris]        139  ..........-.....................................................  191
ZDHHC3 (pred) [Equus caballus]         139  ..........-.....................................................  191
ZDHHC3 (pred) isoform 2 [Canis fam.]   139  ..........-.....................................................  191
ZDHHC3 (pred) isoform 1 [Equus cab.]   139  ..........-.....................................................  191
ZDHHC3 [Rattus norvegicus]             139  ..........-.....................................................  191
ZDHHC3 [Bos taurus]                    139  ..........-.....................................................  191
ZDHHC3 (pred) isoform 5 [Canis fam.]   176  ..........-.....................................................  228
ZDHHC3 (pred) isoform 5 [Pan trog.]    139  ..........-.....................................................  191
ZDHHC3 (pred) isoform 3 [Macaca mul.]  139  ..........-.....................................................  191
ZDHHC3 [Mus musculus]                  139  ..........-.....................................................  191
BAC37939 unnamed prot. [Mus mus.]      139  ..........-.....................................................  191
ZDHHC3 isoform 3 [Pan trog.]           172  ..........-.....................................................  224
ZDHHC3 (pred) isoform 1 [Macaca mul.]  173  ..........-.....................................................  225
ZDHHC3 (pred) isoform 4 [Pan trog.]    175  ..........-.....................................................  227
ZDHHC3 (pred) isoform 2 [Pan trog.]    138  ..........-.....................................................  190
ZDHHC3 (pred) isoform 3 [Canis fam.]   145  A.ASSLTDLVVGV.....................................................  204
ZDHHC3 (pred) isoform 1 [Pan trog.]    138  ..........-.....................................................  190


NP 057682 ZDHHC3 [Homo sapiens]        192  FHFLHCFEEDWTTYGLNREEMAETGISLHEKMQPLNFSSTECSSFSPPTTVILLILLCFE  251
ZDHHC3 isoform 7 [Pan troglodytes]     192  ..................................V.............................  251
ZDHHC3 isoform 2 [Macaca mulatta]      192  ......................A...........V.............................  251
ZDHHC3 (pred) [Canis familaris]        192  ................T..GT..ARL.....K...KV.............................  251
ZDHHC3 (pred) [Equus caballus]         192  ............S.R.T.K.T..AR...Q..KP..KV.............................  251
ZDHHC3 (pred) isoform 2 [Canis fam.]   192  ..........----------------------------.K.....................  223
ZDHHC3 (pred) isoform 1 [Equus cab.]   192  ..........----------------------------.K.....................  223
ZDHHC3 [Rattus norvegicus]             192  ..........----------------------------.K.....................  223
ZDHHC3 [Bos taurus]                    192  ..........----------------------------.K.....................  223
ZDHHC3 (pred) isoform 5 [Canis fam.]   229  ..........----------------------------.K.....................  260
ZDHHC3 (pred) isoform 5 [Pan trog.]    192  ..........----------------------------.K.....................  223
ZDHHC3 (pred) isoform 3 [Macaca mul.]  192  ..........----------------------------.K.....................  223
ZDHHC3 [Mus musculus]                  192  ..........----------------------------.K.....................  223
BAC37939 unnamed prot. [Mus mus.]      192  ..........----------------------------.K.....................  223
ZDHHC3 isoform 3 [Pan trog.]           225  ..........----------------------------.K.....................  256
ZDHHC3 (pred) isoform 1 [Macaca mul.]  226  ..........----------------------------.K.....................  257
ZDHHC3 (pred) isoform 4 [Pan trog.]    228  ..........----------------------------.K.....................  259
ZDHHC3 (pred) isoform 2 [Pan trog.]    191  ..........----------------------------.K.....................  222
ZDHHC3 (pred) isoform 3 [Canis fam.]   205  ............S--------------------------D.....................  235
ZDHHC3 (pred) isoform 1 [Pan trog.]    191  ..........----------------------------.K.....................  222


NP 057682 ZDHHC3 [Homo sapiens]        252  GLLFLIFTSVMFGTQVHSICTDETGIEQLKKEERRWAKKTKWMNMKAVFGHPFSLGWASP  311
ZDHHC3 isoform 7 [Pan troglodytes]     252  ..........-.....................................................  311
ZDHHC3 isoform 2 [Macaca mulatta]      252  ..........-.....................................................  311
ZDHHC3 (pred) [Canis familaris]        252  ..........-.....................................................  311
ZDHHC3 (pred) [Equus caballus]         252  ..........-.....................................................  311
ZDHHC3 (pred) isoform 2 [Canis fam.]   224  ..........-.....................................................  283
ZDHHC3 (pred) isoform 1 [Equus cab.]   224  ..........-.....................................................  283
ZDHHC3 [Rattus norvegicus]             224  A.........-.....................................................  283
ZDHHC3 [Bos taurus]                    224  ..........-.....................................................  283
ZDHHC3 (pred) isoform 5 [Canis fam.]   261  ..........-.....................................................  320
ZDHHC3 (pred) isoform 5 [Pan trog.]    224  ..........-.....................................................  283
ZDHHC3 (pred) isoform 3 [Macaca mul.]  224  ..........-.....................................................  283
ZDHHC3 [Mus musculus]                  224  A.........-.....................................................  283
BAC37939 unnamed prot. [Mus mus.]      224  A.....................G.....................................  283
ZDHHC3 isoform 3 [Pan trog.]           257  ..........-.....................................................  316
ZDHHC3 (pred) isoform 1 [Macaca mul.]  258  ..........-.....................................................  317
ZDHHC3 (pred) isoform 4 [Pan trog.]    260  ..........-.....................................................  319
ZDHHC3 (pred) isoform 2 [Pan trog.]    223  ..........-.....................R..RKNQPREHTGS.QSV.ET..GD...N.FN.  282
ZDHHC3 (pred) isoform 3 [Canis fam.]   236  ..........-.....................................................  295
ZDHHC3 (pred) isoform 1 [Pan trog.]    223  ..........-.....................AADDHPGR.C.MP.                   260


NP 057682 ZDHHC3 [Homo sapiens]        312  FATPDQGKADPYQYVV  327
ZDHHC3 isoform 7 [Pan troglodytes]     312  ................  327
ZDHHC3 isoform 2 [Macaca mulatta]      312  ................  327
ZDHHC3 (pred) [Canis familaris]        312  ................  327
ZDHHC3 (pred) [Equus caballus]         312  ................  327
ZDHHC3 (pred) isoform 2 [Canis fam.]   284  ................  299
ZDHHC3 (pred) isoform 1 [Equus cab.]   284  ................  299
ZDHHC3 [Rattus norvegicus]             284  ................  299
ZDHHC3 [Bos taurus]                    284  ................  299
ZDHHC3 (pred) isoform 5 [Canis fam.]   321  ................  336
ZDHHC3 (pred) isoform 5 [Pan trog.]    284  ................  299
ZDHHC3 (pred) isoform 3 [Macaca mul.]  284  ................  299
ZDHHC3 [Mus musculus]                  284  ................  299
BAC37939 unnamed prot. [Mus mus.]      284  ................  299
ZDHHC3 isoform 3 [Pan trog.]           317  ................  332
ZDHHC3 (pred) isoform 1 [Macaca mul.]  318  ................  333
ZDHHC3 (pred) isoform 4 [Pan trog.]    320  ................  335
ZDHHC3 (pred) isoform 2 [Pan trog.]    283  .SR.C.............  288
ZDHHC3 (pred) isoform 3 [Canis fam.]   296  ................  311
```

Complete BLAST ZDHHC3 Tree

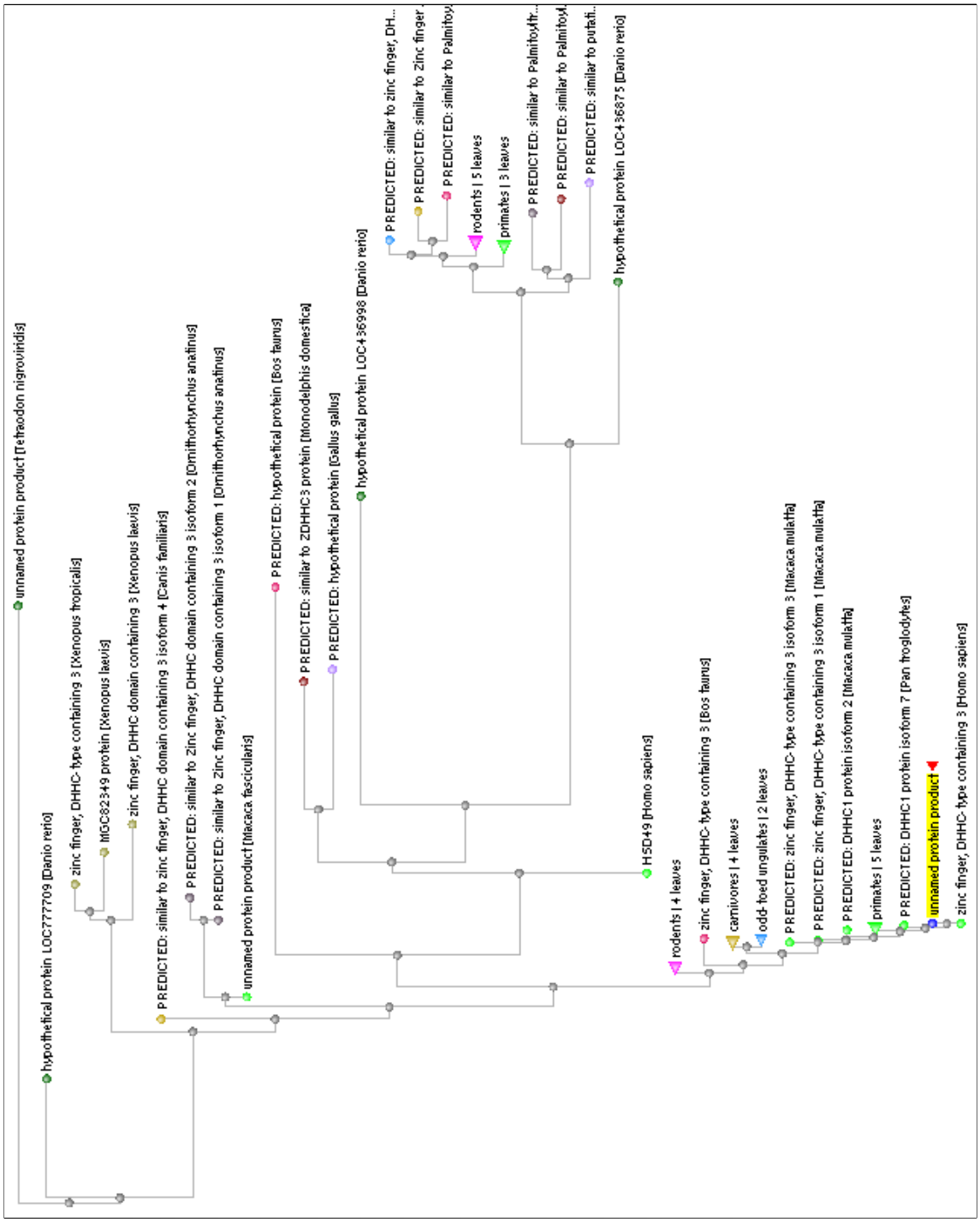

Interaction map for ZDHHC3

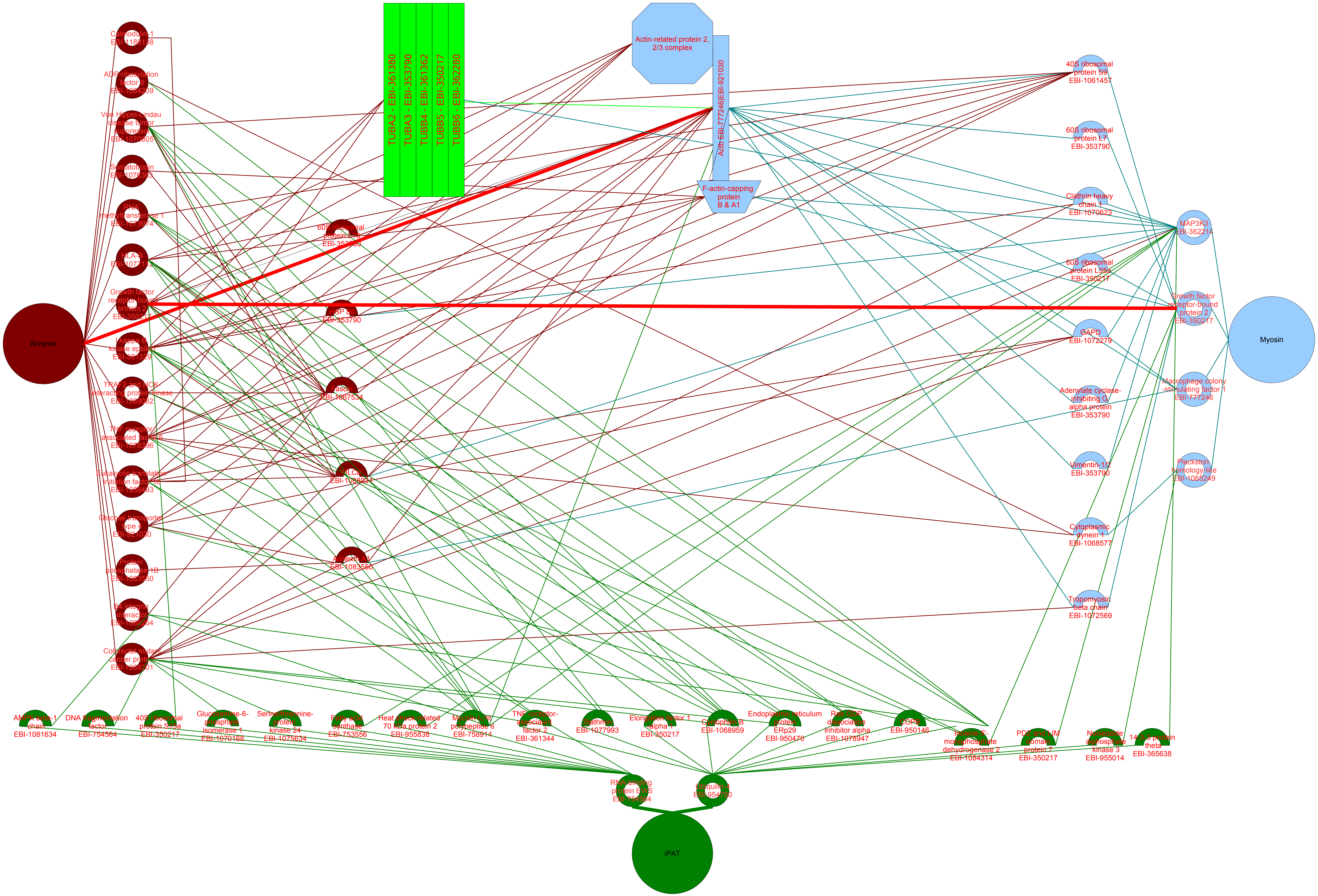

Annexin
iPAT
Myosin
TUBA2 - EBI-361380
TUBA3 - EBI-353790
TUBB4 - EBI-361362
TUBB5 - EBI-350217
TUBB6 - EBI-362280
Actin-related protein 2, 2/3 complex
Actb EBI-777246|EBI-921030
F-actin-capping protein B & A1
40S ribosomal protein S9 EBI-1061457
60S ribosomal protein L7 EBI-353790
Clathrin heavy chain 1 EBI-1070623
60S ribosomal protein L35a EBI-350217
GAPD EBI-1072279
Adenylate cyclase-inhibiting G alpha protein EBI-353790
Vimentin-1/2 EBI-353790
Cytoplasmic dynein 1 EBI-1068577
Tropomyosin beta chain EBI-1072569
MAP3K3 EBI-362214
Growth factor receptor-bound protein 2 EBI-350217
Macrophage colony-stimulating factor 1 EBI-777246
Pleckstrin homology-like EBI-1068249
AMPK beta-1 chain EBI-1081634
DNA fragmentation factor EBI-754564
40S ribosomal protein S15a EBI-350217
Glucosamine-6-phosphate isomerase 1 EBI-1070168
Serine/threonine-protein kinase 24 EBI-1075634
Fatty acid synthase EBI-753556
Heat shock-related 70 kDa protein 2 EBI-955838
Myosin light polypeptide 6 EBI-758914
TNF receptor-associated factor 2 EBI-361344
Stathmin EBI-1077993
Elongation factor 1 alpha 1 EBI-350217
Cyclophilin B EBI-1068959
Endoplasmic reticulum protein ERp29 EBI-950470
Rab GDP dissociation inhibitor alpha EBI-1078947
COPB EBI-950146
Inositol monophosphate dehydrogenase 2 EBI-1084314
PDZ and LIM domain protein 7 EBI-350217
Nucleoside diphosphate kinase 3 EBI-955014
14-3-3 protein theta EBI-365638
RNA-binding protein EWS EBI-754564
Ubiquilin-4 EBI-954750
Calmodulin-1 EBI-1186138
ADP-ribosylation factor 6 EBI-1064209
Von Hippel-Lindau disease tumor suppressor EBI-1070605
Somatotropin EBI-1076303
RNA methyltransferase 1 EBI-1073974
HLA-B
Growth factor receptor-bound protein 2
TRAF2 and NCK-interacting protein kinase EBI-1069062
TNF receptor-associated protein EBI-1078396
Eukaryotic translation initiation factor EBI-1059493
Glucose transporter type
Protein phosphatase 1B EBI-1083560
Colorectal mutant cancer protein EBI-1059701
60S ribosomal protein L10
EBI-353790
EBI-1067534
EBI-1068931
EBI-1083550

Acknowledgment

This thesis has been performed between the years 2003 and 2008 under the supervision of Prof. Dr. H.Y. Naim at the Institute for Physiological Chemistry of the Foundation University of Veterinary Medicine Hannover.

I like to thank Prof. Dr. H.Y. Naim for inspiring encouragments and providing me with material, equipment and premises.

Prof. Dr. M. J. Pröpsting I have to thank for his practical assistence, energy and patience.

I have to thank Prof. Dr. G. Bicker and his group for technical advise and provision of material especially with westernblot and lectin screening.

Especially Sabine Knipp for her personal enthusiasm and privat engagement. Many, many thanks.

The encouragement and assistence from the whole institute of the Physiological Chemistry enabled me to proceed to this manuscript.

Special thanks to Yvonne Reinke for her patient trials to teach me the technique of westernbloting. Gabi Wetzel, Jürgen Eikemeyer, Heike Kanapin thanks for keeping calm and answering even the hardest questions.

Finally thanks to my family who supplied me with energy I did not have.

And former members of the Group who turned out to be friends like Ina Fischer, Markus Kaiser, Deborah Castelletti and Zeynep Hein.

This thesis was in parts financed by the SFB 621.

A r n d t R o h w e d d e r

Daimlerstr. 18 · 30165 Hannover
Tel.: 0511-2208720 · E-Mail: arndt.rohwedder@gmx.de

Lebenslauf

Angaben zur Person

Geburtsdatum und -ort	25.03.69, Bremen
Familienstand	ledig
Staatsangehörigkeit	deutsch

Ausbildung

08.1975 – 06.1979	Grundschule Schule an der Robinsbalje Bremen
08.1979 – 06.1981	Orientierunggstufe Schulzentrum Süd Delmenhorst
08.1981 – 06.1986	Realschule mit Abschluss Mittlere Reife Schulzentrum Süd Delmenhorst
08.1986 – 06.1987	Höhere Handelsschule Berufsbildende Schulen I Delmenhorst
08.1987 – 06.1989	Ausbildung zum Industriekaufmann bei der Vereinigte Möbelwerke Delmenhorst AG
08.1989 – 06.1992	Fachgymnasium Wirtschaft mit Abschluss Allgemeine Hochschulreife Berufsbildende Schulen I Delmenhorst
09.1992 – 09.2001	Studium der Biologie an der Universität Bremen mit Abschluss Diplom;

	Thema der Diplomarbeit :“Beobachtung der Regulation von Zelloberflächen-Protonenkanälen und Adhäsionsrezeptoren durch die Polymerisation von Aktinfilamenten“
01.2004 – 06.2007	Promotionsstudium am Institut für physiologische Chemie der Stiftung tierärzliche Hochschule Hannover, Thema der Dissertation: „The Palmitoyltransferase ZDHHC3 as an Essential DRM Associated Protein of Golgi Compartement“

Beruflicher Werdegang

03.1993 – 03.1994	Wehrdienst bei der Bundeswehr
01.1999 – 04.1999	Universität Bremen, Fachbereich 2, Studentische Hilfskraft, Projekt Kläranlage auf pflanzlicher Basis
05.1999 – 08.2000	Extra Verbrauchermärkte, Aushilfskraft
08.2000 – 04.2002	ZARM (Zentrum für angewandte Raumfahrttechnik und Mikrogravitationstechnik), Studentische Hilfskraft
06.2002 – 07.2002	Max Planck Institut für Marine Mikrobiologie, Bremen, Studentische Hilfskraft
08.2002 – 03.2003	Hautklinik der Uniklinik Mainz, Arbeitsgruppe Mastezelle, „innate immunity“, wissenschaftlicher Mitarbeiter
05.2003 – 12.2003	Max Planck Institut für Marine Mikrobiologie, Bremen, wissenschaftliche Hilfskraft
01.2004 – 03.2007	Institut für physiologische Chemie der Stiftung tierärzliche Hochschule Hannover, wissenschaftlicher Mitarbeiter

Weiterbildungen

09.1997 – 05.2003	Zweitstudium der Informatik an der Universität Bremen

Eidesstattliche Erklärung

Hiermit erkläre ich, dass ich die vorliegende Dissertation mit dem Titel „The Palmitoyltransferase hZDHHC3 as a Lipid Raft Associated Protein in its Cellphysiological Context“ selbständig verfasst und alle benutzten Hilfsmittel sowie eventuell zur Hilfeleistung herangezogenen Institutionen vollständig angegeben habe.

Die Dissertation wurde nicht schon als Diplom- oder ähnliche Prüfungsarbeit verwendet.

Die vorliegende Arbeit wurde am Institut für Physiologische Chemie der Stiftung Tierärztliche Hochschule Hannover angefertigt.

Hannover, 23 Januar 2009

Arndt Rohwedder